การพัฒนาโครงสร้างเส้นใยสามมิติและเส้นใยแบบฟูผ่านกระบวนการอิเล็กโตรสปินร่วมแบบสองขั้ว

นางสาวนริศรา กุลปรีชานันท์

วิทยานิพนธ์นี้เป็นส่วนหนึ่งของการศึกษาตามหลักสูตรปริญญาวิทยาศาสตรดุษฎีบัณฑิต
สาขาวิชาวิทยาศาสตร์นาโนและเทคโนโลยี (สหสาขาวิชา)
บัณฑิตวิทยาลัย จุฬาลงกรณ์มหาวิทยาลัย
ปีการศึกษา 2555
ลิขสิทธิ์ของจุฬาลงกรณ์มหาวิทยาลัย

DEVELOPMENT OF 3D-FIBROUS STRUCTURE AND FLUFFY YARN VIA DUAL-POLARITY CO-ELECTROSPINNING PROCESS

Miss Narissara Kulpreechanan

A Dissertation Submitted in Partial Fulfillment of the Requirements
for the Degree of Doctor of Philosophy Program in Nanoscience and Technology
(Interdisciplinary Program)
Graduate School
Chulalongkorn University
Academic Year 2012

Thesis Title	DEVELOPMENT OF 3D-FIBROUS STRUCTURE AND FLUFFY YARN VIA DUAL-POLARITY CO-ELECTROSPINNING PROCESS
By	Miss Narissara Kulpreechanan
Field of Study	Nanoscience and Technology
Thesis Advisor	Ratthapol Rangkupan, Ph.D.
Thesis Co-advisor	Assistant Professor Tanom Bunaprasert, MD.

Accepted by the Graduate School, Chulalongkorn University in Partial Fulfillment of the Requirements for the Doctoral Degree

.....Dean of the Graduate School

(Associate Professor Amorn Petsom, Ph.D.)

THESIS COMMITTEE

.....Chairman

(Associate Professor Vudhichai Parasuk, Ph.D.)

.....Thesis Advisor

(Ratthapol Rangkupan, Ph.D.)

.....Thesis Co-advisor

(Assistant Professor Tanom Bunaprasert, M.D.)

.....Examiner

(Professor Suwabun Chirachanchai, Ph.D.)

.....Examiner

(Assistant Professor Sukkaneste Tungasmita, Ph.D.)

.....External Examiner

(Nuttaporn Pimpha, Ph.D.)

นริศรา กุลปรีชานันท์ : การพัฒนาโครงสร้างเส้นใยสามมิติและเส้นใยแบบฟูผ่านกระบวนการอิเล็กโตรสปินร่วมแบบสองขั้ว. (DEVELOPMENT OF 3D-FIBROUS STRUCTURE AND FLUFFY YARN VIA DUAL-POLARITY CO-ELECTROSPINNING PROCESS) อ.ที่ปรึกษาวิทยานิพนธ์หลัก : ดร.รัฐพล รังกุพันธุ์,
อ.ที่ปรึกษาวิทยานิพนธ์ร่วม : ผศ.นพ.ถนอม บรรณประเสริฐ, 133 หน้า.

จุดมุ่งหมายของงานวิจัยนี้คือการพัฒนาโครงสร้างเส้นใยสามมิติและเส้นใยแบบฟูผ่านกระบวนการอิเล็กโตรสปินร่วมแบบสองขั้วของพอลิคาร์โปรแลกโทน (poly caprolactone) งานวิจัยนี้แบ่งเป็น 3 ส่วน คือ 1) การศึกษาผลของปัจจัยการผลิตต่อขนาดและลักษณะทางสัณฐานวิทยาของเส้นใยอิเล็กโตรสปัน 2) การพัฒนาโครงสร้างเส้นใยสามมิติและเส้นใยแบบฟูผ่านกระบวนการอิเล็กโตรสปินร่วมแบบสองขั้ว และ 3) ศึกษาผลของขนาดของเส้นใยต่อพฤติกรรมของเซลล์ไฟโบรบลาสของหนู (L929) ในส่วนแรกทำการศึกษาปัจจัยของกระบวนการผลิตที่มีอิทธิพลต่อขนาดและลักษณะทางสัณฐานวิทยาของเส้นใย ได้แก่ ความเข้มข้นของสารละลายพอลิคาโปรแลกโทน, ความต่างศักย์ไฟฟ้า, ระยะห่างระหว่างเข็มและฉากรองรับ และอัตราการไหลของสารละลาย ส่วนที่สองเป็นการพัฒนาโครงสร้างเส้นใยสามมิติและเส้นใยแบบฟูผ่านกระบวนการอิเล็กโตรสปินร่วมแบบสองขั้ว โดยกระบวนการนี้เป็นการใช้ประจุบวกและลบพร้อมกันในกระบวนการอิเล็กโตรสปินนิ่งภายใต้เงื่อนไขที่ปั่นบางประการ ทำให้งานวิจัยนี้ประสบความสำเร็จในการพัฒนาโครงสร้างเส้นใยสามมิติและเส้นใยแบบฟูผ่านกระบวนการอิเล็กโตรสปินร่วมแบบสองขั้ว ซึ่งได้มีการประยุกต์จากกระบวนการปั่นเส้นใยด้วยไฟฟ้าสถิตย์แบบทั่วไปโดยการใช้ประจุบวกและประจุลบระบบการปั่นเส้นใยด้วยไฟฟ้าสถิตย์และเก็บโครงสร้างเส้นใยสามมิติบนฉากรองรับแบบหมุน การเปลี่ยนแปลงของปัจจัยการผลิตทำให้ลักษณะโครงสร้างของเส้นใยแตกต่างไปจากลักษณะปกติทั่วไป นั่นคือสามารถพัฒนาเป็นโครงสร้างสามมิติและทำให้มีความพรุนเพิ่มขึ้น จากการศึกษาโดยกล้องจุลทรรศน์อิเล็กตรอนแบบส่องกราด (SEM) และ เครื่องวัดความเป็นรูพรุน ผลการศึกษาพบว่าในขณะที่เส้นใยที่มีลักษณะเป็นโครงสร้างสามมิติและเส้นใยแบบฟูมีความเป็นรูพรุนสูงกว่าเส้นใยที่ได้จากการผลิตจากกระบวนการอิเล็กโตรสปินแบบทั่วไป ส่วนสุดท้ายของงานวิจัยนี้มีการศึกษาโดยการเตรียมเส้นใยโครงสร้าง 3 มิติและเส้นด้ายฟูนำมาใช้เพื่อศึกษาผลกระทบของขนาดเส้นใยและโครงสร้างของเส้นใยต่อการยึดเกาะและการเพิ่มจำนวนของเซลล์ไฟโบบลาสต์หนู L929 พบว่าการเซลล์สามารถเคลื่อนตัวและยึดเกาะได้ในระหว่างช่องว่างของโครงสร้างสามมิติและเส้นใยแบบฟู แสดงให้เห็นว่าการพัฒนาโครงสร้างสามมิติด้วยกระบวนการใหม่ในงานวิจัยนี้เป็นการออกแบบที่มีศักยภาพและนอกจากนี้สามารถนำไปประยุกต์ในงานด้านอื่นได้

สาขาวิชา วิทยาศาสตร์นาโนและเทคโนโลยี ลายมือชื่อนิสิต .....
ปีการศึกษา 2555 ลายมือชื่อ อ.ที่ปรึกษาวิทยานิพนธ์หลัก .....
ลายมือชื่อ อ.ที่ปรึกษาวิทยานิพนธ์ร่วม .....

5187784220 :MAJOR NANOSCIENCE AND TECHNOLOGY
KEYWORDS:POLYCAPROLACTONE / FIBER SIZE EFFECT / DUAL-POLARITY CO-ELECTROSPINNING PROCESS / 3D-FIBROUS STRUCTURE / FLUFFY YARN

NARISSARA KULPREECHANAN : DEVELOPMENT OF 3D-FIBROUS STRUCTURE AND FLUFFY YARN VIA DUAL-POLARITY CO-ELECTROSPINNING PROCESS.ADVISOR : RATTHAPOL RUNGKUPAN, CO-ADVISOR, Ph.D. : ASST. PROF. TANOM BUNAPRASERT, M.D., 133 pp.

In this research we had developed a novel electrospinning process, a dual polarity co-electrospinning, that could be used to produce 3 dimensional structure.The research was separated into 3 main parts i.e. a) an investigation of processing parameters effect on formation and morphology of poly (caprolactone) (PCL) electrospun fibers, b) a development of dual polarity co-electrospinning process and c) a study on the effect of fiber size and fiber mat structureon cell matrix interaction. In the first part, the effect of PCL solution concentration, applied voltage, collecting distance and solution flow rate on PCL fiber morphology were assessed. In the second part, the dual polarity co-electrospinning process were developed. This technique utilized a positive and negative charge simultaneously. Under certain spinning condition, a 3 dimension structures from PCL electrospun fiber in the 3D-fibrous and fluffy yarn structure were formed. The effect of the applied opposite charge, flow rate, fiber size, ratio of fiber and spinning rate of the collectoron fiber formation were studied. The morphologies and porosity (distribution of porosity and pore size) of a 3D-fibrous and fluffy yarn structure of PCL were determined using scanning electron microscope (SEM) and porosimeter. The 3D-fibrous and fluffy yarn had more porosity compared to fiber mat from the ordinary electrospinning process.In the last part, PCL fiber mats with three different fiber sizes, PCL fiber in the form of 3D-fibrous structure and fluffy yarns were prepared and used to evaluate effects of fiber size and fiber structure on cell adhesion and proliferation using L929 as a model cell. The results showed that both size and structure played a role in prohibiting or accommodating cellular distribution or penetration into the under layer of electrospun fiber mat.

Field of Study : Nanoscience and Technology ..... Student's Signature .....

Academic Year : 2012 ..... Advisor's Signature .....

Co-advisor's Signature .....

ACKNOWLEDGEMENTS

This research has been completely restructured to consist of several persons. First of all, I would like to express my deepest gratitude to my main advisor and co-advisor, Dr. Rattapol Rungkupan and Asst. Prof. Tanom Bunaprasert for providing technical guidance in the design, planning guidelines, continued support and inspiration throughout for the research work and corrections research.

I would like to thank Miss Juthamas Ratanavaraporn and Mrs.Thongchan Phuthong, biotechnology laboratory Chulalongkorn University, for kind attention and suggestion in cell culture as well as facilities.

I would like to thank the Doctor of Philosophy Program in Nanoscience and Technology, Graduate school, Chulalongkorn University for graduate courses, Chulalongkorn University Centenary Academic Development Project (Under the Center of Innovative Nanotechnology, Chulalongkorn University), Thailand Research Fund, the 90th Anniversary of Chulalongkorn University fund (Ratchadaphiseksomphot Endowment Fund) and National Science and Technology Development Agency for their financial support of this work.

I would like to extend grateful thank to all member of Electrospinning Laboratory, Chulalongkorn University, for their kindness, great companion and help making happiness and enjoyment.

Finally, I would like to express my deepest gratefulness to my parents, Mr. Somsak, Mrs. Jintana and my brother, Mr. Jessada who loved, supported, motivated all the way and encouraged me in everything what I do throughout the research to be done well. I thank them with my deepest heart.

CONTENTS

LIST OF TABLES

LIST OF FIGURES

Figure

CHAPTER I

INTRODUCTION

1.1 Introduction of work

Development of science and technology is importance for human life in particular due to the desire of life convenience, the conservation of sustainable energy and environment and the treatment of health crisis which affected both directly and indirectly to the economy and the competitiveness of the country. Nanotechnology is engineering at a very small scale [1]), it requires the production and application of materials and processes in billionths of a meter (10-9 m) to improve the properties of the material. Nanotechnology is functional in many research area for example textile, cosmetic, semiconductor, plastic and especially medical field. Nanotechnology has been applied in tissue engineering. Tissue engineering is the advanced technology for the treatment of illnesses, rebuilding organs, drug and gene delivery system that restore, maintain, and improve the function of damaged tissue and organs through the body [2].

Tissue engineering usually requires 3 main components working which concern with appropriate sequences. These components are cells, signaling molecules and extra-cellular matrix (ECM). ECM functions as a cellular scaffold providing a necessary mechanical stability and cell anchor site [3]. It supports the formation of tissue and mimics relevantly, also promotes cellular migration, attachment, formation of new one. Moreover it performs about growth of tissue that concern to the transport of nutrients and metabolic

wastes. In case cell without ECM, cells would not grow and function properly, it may results the tissue malfunction. Therefore, preparation of suitable artificial tissue scaffold with required properties is much importance in tissue engineering applications.

There are many method could produce tissue engineering. The electrospinning is the widespread method that now a day many researchers pay attention , the system is low cost, and convenient use and then advantage of electrospinning over other method.

Electrospinning, a process that can be used to prepare the nano-fibers of polymeric material and inorganic oxide supported material for various applications such as medical, pharmaceutical, engineering, military, and more. Fiber diameter can be fabricated from 10 nm to more than 1 micrometer by the high electrical voltage. The basic system consists of three major parts: a high-voltage source (high voltage power supply), tube containing a solution with the metal needle (syringe with needle) and a metal substrate (metal collector). The system was amended to add a device for controlling the flow of solution (syringe pump) and the efficiency of the fiber of the invention is to control the size and the amount of fiber has more continuity. In addition, fiber produced from the electrospinning process also features prominently are (1) fibers are very small size in range of a several ten nanometers up to about 1-2 microns, it is often called nanofiber or electrospun nanofiber and (2) a porous nanofiber can be prepared with a minuscule amount of the well-transferring liquid and gas. Nanofibers have a smaller pore size, resulting in unique properties such as mechanical, electrical and biological properties. Therefore, it is a much better response to the highly requirement materials. The advantage of very small size depending on the substance used and inventive, normally, the application was appeared in the various nanofibers. Such widespread application of polymer nanofibers that are

biodegradable, non-toxic and bio-compatible for the filtration system, drug delivery, wound dressing, tissue engineering [4].

1.2 **Problem statement**

The tissue engineering scaffold and cell interaction that found conventional cell culture provides condition with only two dimensions (2D) for growing cells, although suitable for certain tissue such as skin. However, there is limited for 2D application, thus leading to the development of physiological compromised cells of other tissues that required three dimensional (3D) scaffold. For those tissues, i.e. bone, cartilage and most internal organs, the cell culture based models should incorporate both the 3D organization and multicellular of organ while allowing the experimental interventions in the body. This involves the development of ECM mimicking 3D scaffold [5].

Due to the universal application of nanofiber often use fiber with structure in two dimensions is still limited in its applications, such as applications in the field of tissue engineering, the adhesion between cells in the structure of the fiber is not good enough and the implementation is not fully effective. The fabric structure which is suitable for using in the medical field should be highly porous, channels connect the pores facilitate the transfer of various subject matters, control the degradation process, the suitable chemical properties for the cells growthing, good mechanical properties, and the uniform pores size and shape.

Therefore, the objective of this study is to bring about the nano-fibers with a three-dimensional structure of the electrospun nanofiber to enhance applications in tissue engineering. However, that preparation of fibers from a polymer solution in a three-

dimensional structure of the process that much more difficult to electrospinning. There are several ways to develop a 3D tissue engineering scaffold, for example, by particulate leaching, gas foaming , emulsification/freeze drying, thermally induced phase separation, and melt molding process. Each technique has its own advantages and disadvantages.

Beside fabrication method, material types are the one of importance to the needs of tissue engineering. There are many natural and synthetic polymers also ceramics which have high potential as biocompatible and biodegradable materials for scaffolding. Focused on a variety of synthetic biodegradable polymers can be utilized to fabricate tissue engineering matrices such as, poly(caprolactone) (PCL), poly(ethyl alcohol) (PEO), polylactic acid (PLA), polyglycolic acid (PGA), and natural polymer i.e. collagen, hyaluronic acid.

1.3 Research objectives

The main objectives of this research are:

1. Develop fabrication techniques for construction of 3D-structure from electrospun fiber.
2. Investigate the effect of processing parameters on porosity and morphology of the structure.
3. Evaluate cell-matrix interaction of developed scaffolds on cellular activities i.e. cell adhesion, proliferation and migration.

1.4 **Scope of this work**

The main goals of this research are to develop a fabrication technique that would allow us to construct two types of 3D electrospun fiber, 3D structure and fluffy yarn, with a regular distribution of pore size and porosity by dual-polarity co-electrospinning process and to evaluate a potential use of the obtained structure in tissue engineering application. The effect of their respective processing parameters such as fiber size and ratio of each fiber, on the morphology and porosity of the meat would be studied. Selected fiber mats with different pore size and porosity will be studied further, with at least 1 cell line, in cell-matrix interaction assessment to evaluate their potential role as an artificial tissue scaffold.

1.5 Research outcomes

The development of sponge-liked structure from electrospun fiber using co-fabrication techniques and multisizes approach with regularly distribute of pore size and porosity which could have cell attachment enhancement (from nanofiber component) and porosity in the thickness direction to enhance cell penetration (in cell seeding step) and cell migration during tissue regeneration. Likewise, our study would apply a knowledge and know-how to tailor the pore size/porosity of our desire.

CHAPTER II

LITERATURE REVIEW

2.1 Tissue engineering [6]

Tissue engineering, is *"an interdisciplinary field that applies principles of engineering; and the life sciences toward the development of biological substitutes that restore, maintain, and improve the function of damaged tissue and organs"*. The scaffolds mush posses many key characteristic for tissue engineering, including high porosity and surface area, structural strength, and three-dimensional shapes, to be used as materials for tissue engineering. These characteristics are determined by scaffold fabrication technique and biocompatible of the materials of construction. The techniques for scaffold fabrication have been to tailor to create scaffolds with particular characteristic and critical requirement for tissue engineering of a specific organ.

The technique used to manufacture scaffold for tissue engineering is depend on the properties of the polymer and its designated application. Scaffold manufacturing techniques were therefore developing using commercially starting materials, small solid polymer chunks or in any case long fibers. The technique was developed to involve heating the polymer or dissolving them in the suitable organic solvent. The viscous behavior of the polymer above their transition or melting temperature and their solubility in various organic solvents were two of the most important characteristics to consider during process development. There are several techniques for scaffold fabrication. Each technique has its advantages, but none can be considered as an ideal method of scaffold fabrication. In the body, the choice of the fabrication technique or the exploitation of the new one are

organized into three-dimensional structures as functional organs and organ systems, is depending on the critical requirements for the tissue of interest.

In this research focused on techniques of scaffold tissue fabrication via electrospinning process. In addition, three parts of the basic knowledge of tissue engineering scaffold are discussed including

1. Scaffolds for tissue engineering
2. Materials for scaffold
2. Technique for scaffold fabrication

2.1.1 Scaffold for tissue engineering [5, 7]

For impairment and regeneration, porous scaffold is needed in tissue engineering. One objective is that it is the way of developing scaffolds used for forming functional tissue. There are many techniques for creating scaffolds in tissue engineering and techniques of scaffold processing that are a major part of this writing.

Scaffolds are added in tissue engineering playing a role to help creating relevant-tissue model including to support the migration and attachment of cells, new extracellular matrix's formation and tissue ingrowths and to maintain the transport of nutrients and metabolic waste. Scaffolds used for tissue engineering should be as follows:

First, the scaffolds should be in three- dimensional structure with dense pores and interconnected pore network for growing cell/tissue and smoothening transport of nutrients and metabolic waste and to support cellular attachment, migration, inter-cell interaction, cell

multiplication and differentiation. Both essential factors for organ regeneration, porosity and pore size, should be controlled in the processing because the high-density porous scaffold will help generating cells or their migration via the materials. Pore size influences tissue ingrowths and internal surface for cell attachment. In large area, there should be a lot of cells that are enough to replace or restore organ's function.

Second, the biocompatibility of scaffolds to the host's immune system, in which tissues are implanted, is one of important characteristics because it plays a role for choosing suitable materials structure for building scaffolds, though the technique of processing may affect scaffolds' suitability. Moreover, many biocompatible materials, natural and man-made ones, can be used for building scaffolds such as collagen, poly (α-hydroxyester), and poly (anhydride) and so forth. Researchers use poly (α-hydroxyester) as starter to build scaffolds with many techniques. Materials are extensively applied as materials for scaffold creation. They are biocompatible, degradable and certified by Food and Drug Administration (FDA) as for specific clinical application.

Third, It is essential that controllable biodegradation matches tissue growth's rate and simplifies the connection of contrived tissues with host tissues and, in the first stage of post-implantation" support structure for cells and tissues assembled in scaffolds.

Last, mechanical qualities play a role generating hard tissues such as cartilage and bone and helping the match of tissues during implantation. Yet, there are various processing alternatives by creating scaffolds in terms of structure and morphology (shapes and sizes) that are particularly relevant to the tissues. Polymer building can influence the process though its solidity and scaffolds' porosity affect mechanical qualities. The crystallization of

polymer chain may cause extensible strength's enhancement but polymer's molecular weight may decrease during the process of production. That leads to corrosive impact on mechanical characters. It is vital for hard tissue's shape to affect its function. For this, the processing technique plays a role in preparation of twisted- three-dimensional scaffold creation.

The fundamental knowledge of tissue engineering scaffold and cell interaction in terms of cell culture causes only two-dimensional space for seeding cells resulting in physiological development of the cell. Anyhow, three-dimensional tissues are needed and that can be done by multiplying cells onto porous matrices or scaffolds where cells attach and colonize. Major models of cell culture should unite both three-dimensional organization and multi-cellular organs during internal-body interference. For Extracellular Matrix (ECM) – modeling three-dimensional scaffolds-, which can be united with relevant ECM, this means it can support interactive versatility in medical or non-medical use. Therefore, to culture and maintain cells is the way of conventional flat surface that needs ECM modeling three-dimensional environment.

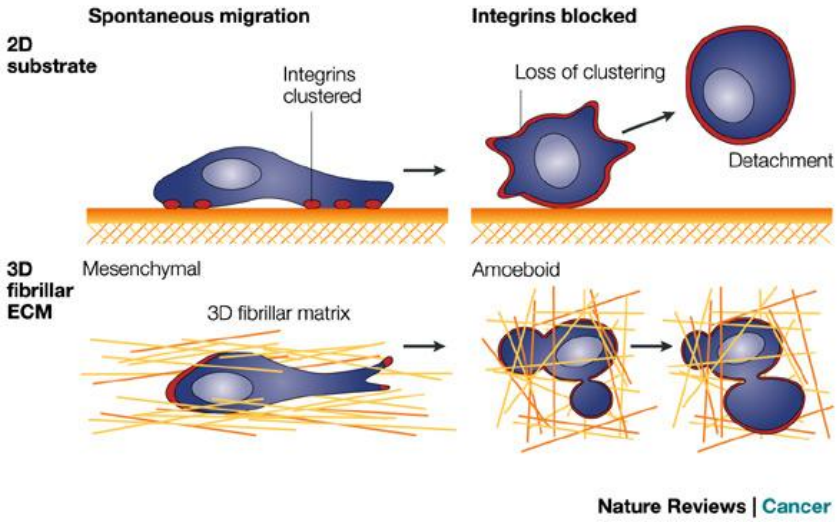

Figure 2.1 A cell migration across to 2D substrate and 3D fibrillar ECM [7].

2.2 Technique for scaffold fabrication [7, 8]

2.2.1 Particulate Leaching [65]

When talking about particulate, it is an extensively-used way of building scaffolds for tissue engineering applications. It is preparing normal-porous structures in limited thickness. Firstly, the polymer will melt into a suitable - state organic solvent. For instance, Polylactic Acid dissolves into Dichrolomethane. Later, the solution is poured into a cast full of paraffin particles as they can be transformed to inorganic salt like Sodium Chloride, Crystal of Succarose, Gelatin or Paraffin. Monosodium Glutamate, Alginate Hydrogel are included. Paragon particle size is directly related to the amount of final structure's porosity. After that, polymer solution and solvent can completely evaporate. Then, the mixture in the mold will be immersed in liquid that suits melting porogen, water in case of Sodium Chloride, Saccarose and Gelatin or Aliphatic solvent like Hexane for Paraffin. When the porogen completely dissolves, porous structure will be available with kind of thickness. Particulate Leaching also causes residues in using organic solvents that must be fully removed as they might probably result in damages to cells on scaffolds.

This technique is advantageous in terms of simplicity and user-friendliness. It also suits with biomaterials and requires no extra equipments. When comparing Salt-leaching Method used to build porous gelatin scaffolds to freeze-drying scaffolds, salt-leaching gelatin scaffolds are easier formed into desirable shapes with equally distributed and interconnected pore structure. The mechanical strength and biodegradation rate are relevant to porosity conformable and are simply modulated by the addition of salt [9]. On the other hand, its disadvantages are different density result in unequal distribution of pore size. It is

hard to complete the interconnectivity and pore interconnection that leads to skinning effects on external surface of scaffolds.

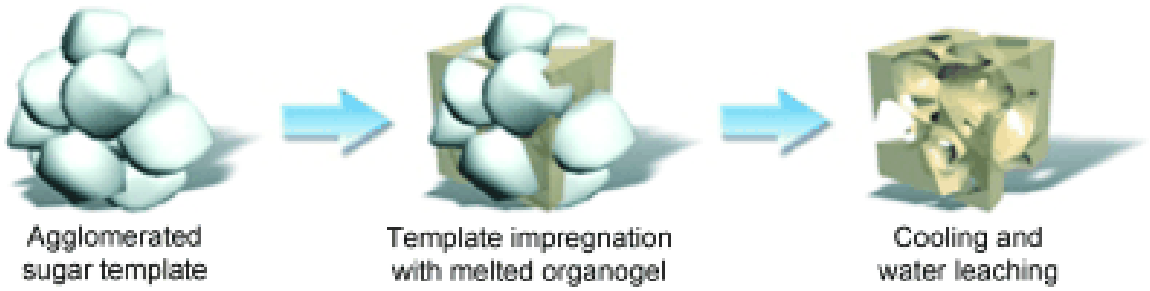

Figure 2.2 Soft Microporous scaffold by salt leaching process

Mcintosh reported about effective elastic properties of hydroxyapatite scaffold/bone composites using representative volume elements (RVE) prepared by particulate leaching techniques [10]. In 2004, the researchers reported to investigate the effect of three-dimensional silk fibroin scaffold preparation porous 3D protein scaffolds with similar sized pores of 900±50 μm on osteogenic responses of human bone marrow stem cells [11].

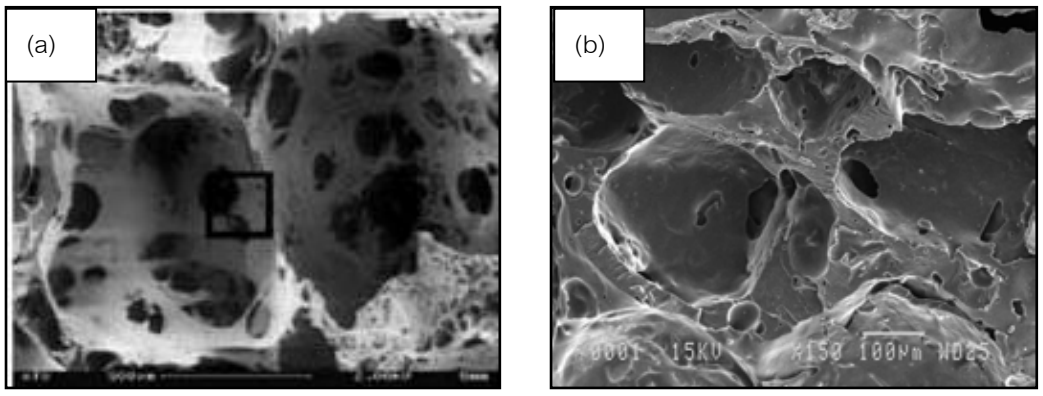

Figure 2.3 (a). SEM of microstructure of pore surfaces in water-based silk scaffolds (b). Poly(lactic-coglycolic acid) porous scaffold for bone tissue engineering produced by melt casting and particulate leaching [11].

Moreover, the preparation of hydroxyapatite nanoparticles (nHA)/poly(ester urethane) composite scaffolds using a salt-leaching-phase inverse process was reported by C.I.R. Boissard et al. In this present, they found that increasing the amount of nHA particles in the composite scaffold decreased the porosity, increased the wall thickness and consequently decreased the pore size. The Young's modulus of the poly(ester urethane) scaffold was improved by 50% by addition of 10 wt.% nHA (from 0.95 ± 0.5 to 1.26 ± 0.4 MPa), while conserving poly(ester urethane) viscoelastic properties and without significant changes in the scaffold macrostructure. Moreover, the process permitted the inclusion of nHA particles not only in the poly(ester urethane) matrix, but also at the surface of the scaffold pores, as shown by scanning electron microscopy. nHA/poly(ester urethane) composite scaffolds have great potential as osteoconductive constructs for bone tissue engineering [12].

The adventages of this technique are simple and user friendly method, suitable with a range of biomaterials and no special equipment is needed. Porous gelatin scaffolds were prepared using a salt-leaching method and these were compared to scaffolds fabricated using a freeze-drying method. The salt-leached gelatin scaffolds were easily formed into desired shapes with a uniformly distributed and interconnected pore structure. The mechanical strength and the biodegradation rate of the scaffolds increased with the porosity, and were easily modulated by the addition of salt[13]. However, disadvantages; density differences result in non uniform pore size distribution. Difficult to achieve full interconnectivity and large pore interconenctions. Skinning effect on outside surfaces of scaffolds.

2.2.2 Gas foaming

Gas Foaming is used to avoid residues caused by organic solvent applied in salt-leaching method that can lead to poisonous hazard in human body and environment. Biodegradable polymers such as poly (lactic-co-glycolic acid) (PLGA) are saturated in Carbon Dioxide (CO2) at high pressure. When bringing back CO2 at atmospheric level, gas solubility in polymer quickly decreases that causes gas bubble or cells' nucleation and growth having 100-500 μm size in polymer solution. Technique that uses gas as porogen is developed to have a better way than using organic solvents and solid porogen. At first, Compression molding that use heat is the way to prepare polymer. Then, the disc is placed in a chamber that exposed to high-pressure CO2 for days. The pressure will become at atmospheric level and during this restoration, pores are formed by Carbondioxide molecules from polymer causing sponge-like structure. Using excessive heat during compression molding is main disadvantage of this technique because it will make pores not to form an interconnected structure. Silica is added in polymer while micro-particulate during the processing. That leads to particulate growing on interconnectivity of pore size and pore dispersal.

A biodegradable polymer, such as poly(lactic-co-glycolic acid) (PLGA) is saturated with carbon dioxide (CO2) at high pressures. The solubility of the gas in the polymer is then decreased rapidly by bringing CO2 pressure back to atmospheric level. This results in nucleation and growth of gas bubbles, or cells, with sizes ranging between 100-500μm in the polymer. To overcome the necessity to use organic solvents and solid porogens a technique using gas as a porogen has been developed.

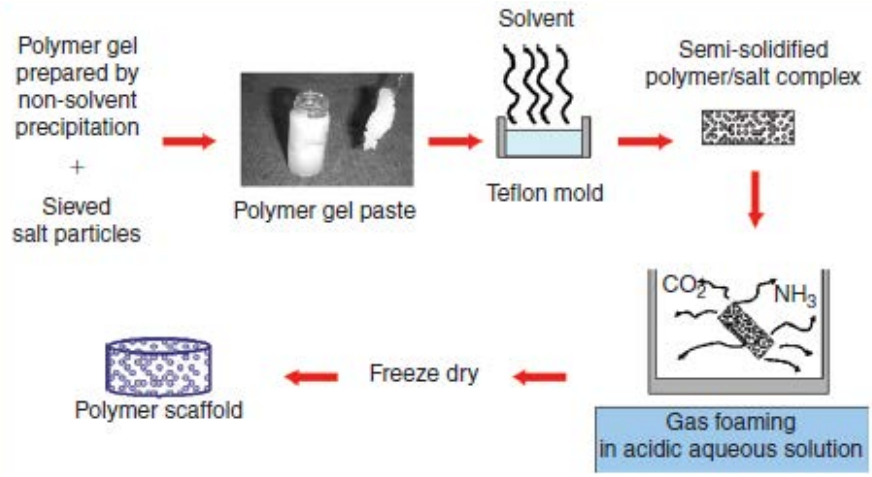

Figure 2.4 Schematic of gas-foamimg and salt-leaching process to fabricate macroporous scaffolds [43].

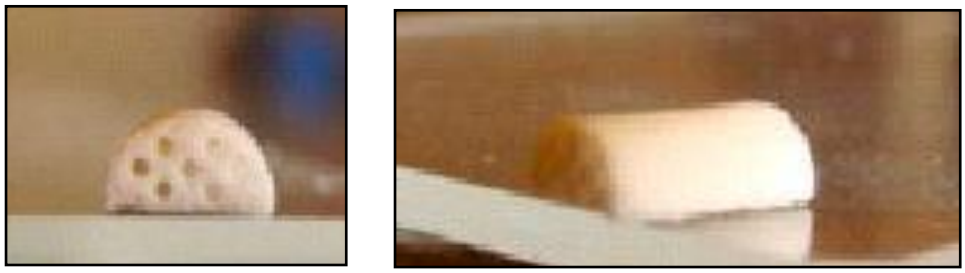

Figure 2.5 250 μm multichannel bridges are fabricated using a gas foaming process microspheres (PLGA) [43].

First polymer are prepared by means of compression molding using a heated mold. The disc are then placed in a chamber where are exposed to high pressure CO_2 for several days. The pressure inside the chamber is gradually restored to asmospheric levels. During this procedure the pore are formed by the carbondioxide molecules that abandon the polymer, resulting in a sponge like structure. The main problems related to such a technique are caused by the excessive heat used during compression molding and by the fact that the pores do not form an interconnected structure. While microparticulate silica was added to the polymer during processing and the effects of this particulate seeding on the

interconnectivity of the pore structure and pore size distribution were investigated by Niki J. Collins et al. Scaffolds comprising polylactide and a range of silica contents (0–50 wt.%) were produced by foaming with supercritical CO_2. In this study, the resulting that incorporation of increasing quantities of silica particles increased the interconnectivity of the scaffold pore structure. The pore size distribution was also reduced through the addition of silica, while total porosity was found to be largely independent of silica content. In addition, the architecture of foamed polymeric scaffolds can be advantageously manipulated through the incorporation of silica microparticles. The findings of this study further establish supercritical fluid foaming as an important tool in scaffold production and show how a previous limitation can be overcome [14].

2.2.3 Emulsification/Freeze-drying

For this technique, using solid porogen like particulate leaching is not needed. The synthetic polymer melts into suitable-state solvent (e.g. Polylactic acid in Dichloromethane) and water is then added in polymer solution, then the mixture becomes emulsion. Before both liquids seclude, the emulsion is put into a mold and using liquid Nitrogen can rapidly freeze it. the frozen emulsion is accordingly freeze-dried and water and the solvent are eliminated. It remains solidified, porous polymeric structure.

Artificial polymers like PLGA can dissolve in frozen acetic acid or benzene. So, the solution is icy and freeze-dried to give porous matrices. Likewise, collagen scaffolds are created by freezing collagen solution and then freeze-drying. They lead to formation of frozen crystals that carry collagen molecules into inserting spaces. After that, they will be

taken away by freeze-drying. Pore sizes can be adjusted according to freezing rate and pH. The faster the freezing rate, the smaller the pores.

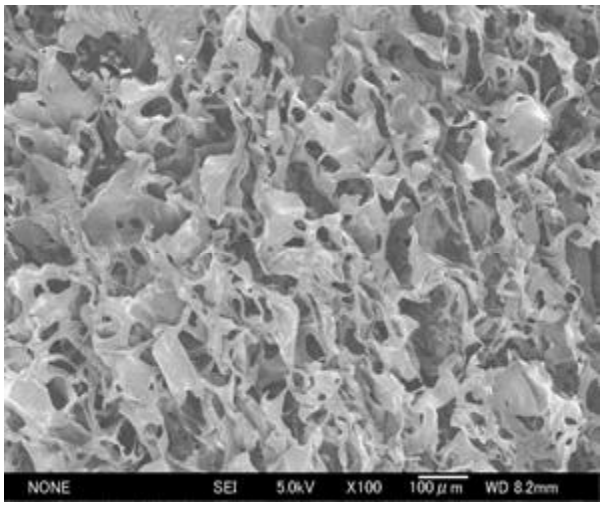

Figure 2.6 Scaffold by freeze-drying technique [44].

Moreover, Chaire et al. studied about effect of collagen concentration and crosslink density on the biological, structural and mechanical properties of collagen-GAG for bone tissue engineering with freez-drying process [15]. While emulsification and freez-drying allows a faster preparation if compared to particulate leaching since it does not require a time consuming leaching step, it still requires the use of solvents, moreover, pore size is relatively small and porosity is often irregular. In addition, Amir et al. discussed the development of a calcium phosphase coating for collagen scaffold, which using by these technique, in order to improve their mechanical properties for bone tissue engineering [16]. Freez-drying by itself is a commonly employed technique for the fabrication of scaffolds. In particular it is used to prepare collagen sponges, collagen is dissolved into acidic solutions of acetic acid or hydrochloric acid that are cast into a mold frozen with liquid nitrogen then lyophilized.

2.2.4 Thermally Induced Phase Separation (TIPS)

Biodegradable synthetic polymer melts in dissolved Phenol or Naphthalene and molecules that are biologically active can be inserted in solutions. After that, the temperature will become lower to create liquid-liquid phrase separation and fast cool to structure second-phrase solid. The sublimation of solvent give porous scaffolds with bioactive molecule congregated in structure.

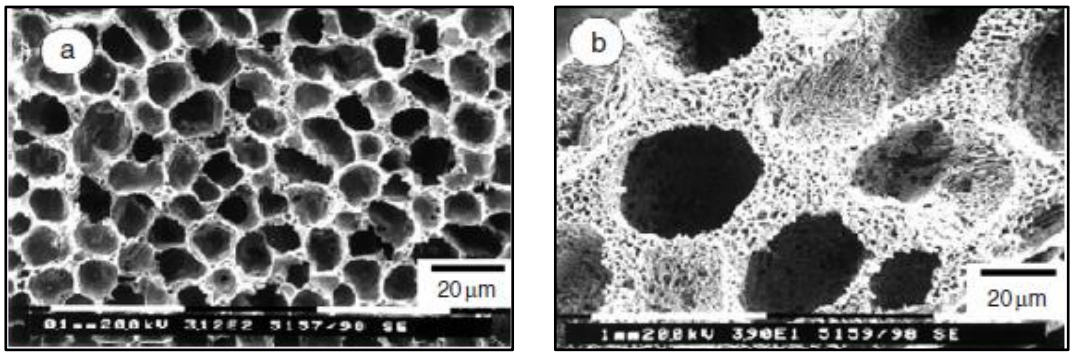

Figure 2.7 Cross sectional SEM images of PLGA scaffolds fabricated by TIPS methods, quenching in liquid nitrogen [44].

Bioomimatic nanofibrous gelatin/apatite composite scaffolds for bone tissue engineering were studied by Xiaohua Lui et al. They prepared the composite scaffolds by TIPS method comparing with a commercial gelatin foam. In comparison, with similar pore size and porosity, the prepared much higher surface area and mechanical strength. In addition, the biomimatic nanofibrous gelatin/apatite scaffolds are excellent for bone tissue engineering [17].

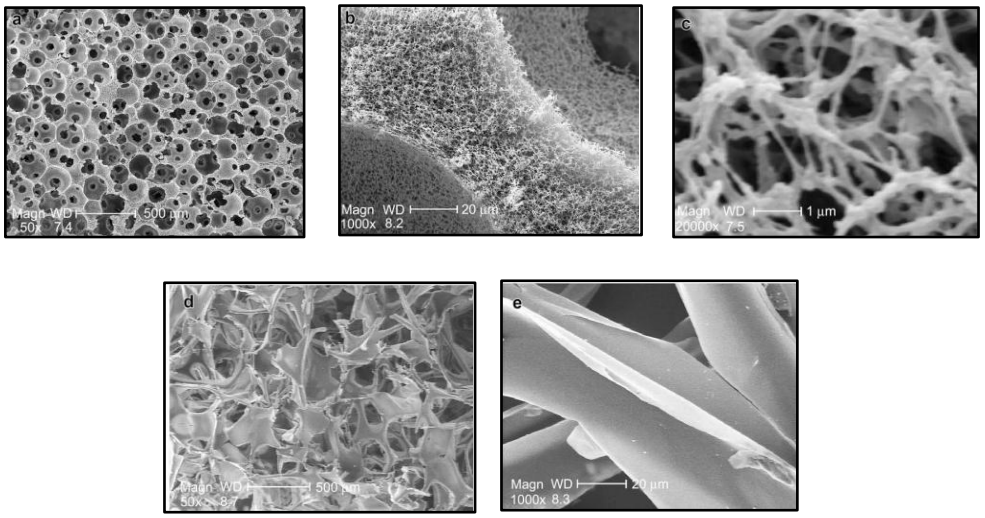

Figure 2.8 Comparision of SEM micrographs of NF-gelatin scaffold and Gelfoam (a) NF-gelatin scaffold (porogen diameter: 150–250 mm), overview; (b) pore-wall structure of NF-gelatin scaffold (higher magnification image of (a)); (c) higher magnification image of (b); (d) Gelfoam, overview; (e) pore-wall structure of Gelfoam [17].

2.2.5 Melt molding

Melt molding is the way of building three-dimension scaffolds that has several disadvantages over membrane layers. PLGA powder and Gelatin Microspheres are added in Teflon mold and then it is given the heat above the glass-transition temperature of PLGA under the pressure of mixture [14]. This process happens to originate PLGA particles' bond. When removing the mold, scaffolds will be dried after putting gelatin in water that it is filtered. The shapes of mold can be predicted by such scaffolds. The procedure of melt molding is adapted to be used to assemble of short fibers like Hydroxyapatite (Hap). To

accomplish the process of Hap fibers' distribution thoroughly in PLGA scaffolds, solvent casting technique should be applied to prepare compound components of Hap fibers, PLGA Matrix and gelatin or salt porogen used in melt molding process.

2.2.6 Electrospinning

Nanofibers in tissue engineering are similar to ECM. Yet, usual polymer processing techniques are hard to build fibers that have a diameter smaller than 10 μmin, that is, they have larger magnitude orders than ECM (50-500 nm). That is why there have been lots of attempts to develop ways of building nanofibers that have closest similarity to ECM geometry. Electrospinning is proven successful to daily produce nanofibrous tissue engineering structures.

It is the way of preparing the non-woven mesh of diverse polymer matrices, electrospinning process. Electrospun nanfibers and fibers correlate for tissue engineering use. They are always related to decisions including choices of materials, fiber orientation, porosity, surface modification and tissue application. For materials' choice, it includes natural and artificial materials. The porosity and pore size of electrospun scaffolds is controllable for individual use. For electrospinning process, it is proven good performance to engineer number of tissue such as vasculature, bone, neuron and ligament. It has been interesting in field of tissue engineering to structure scaffolds.

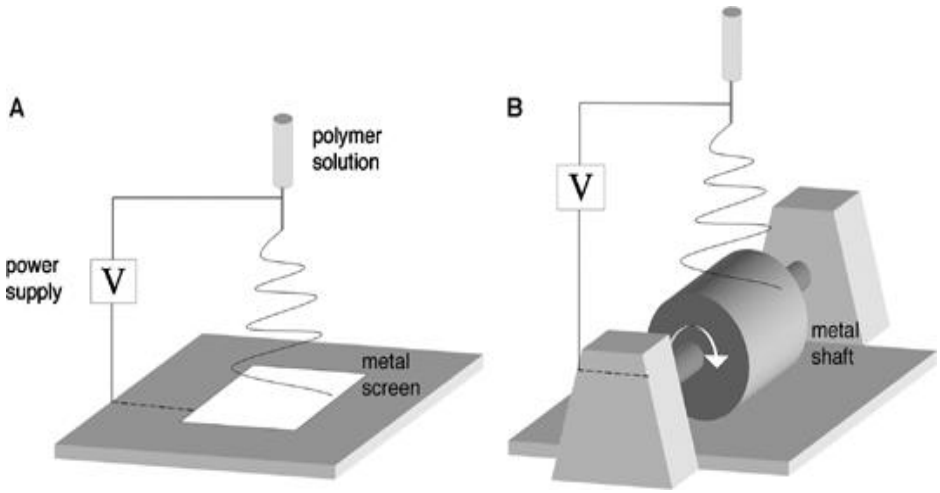

Figure 2.9 The electrospinning [45].

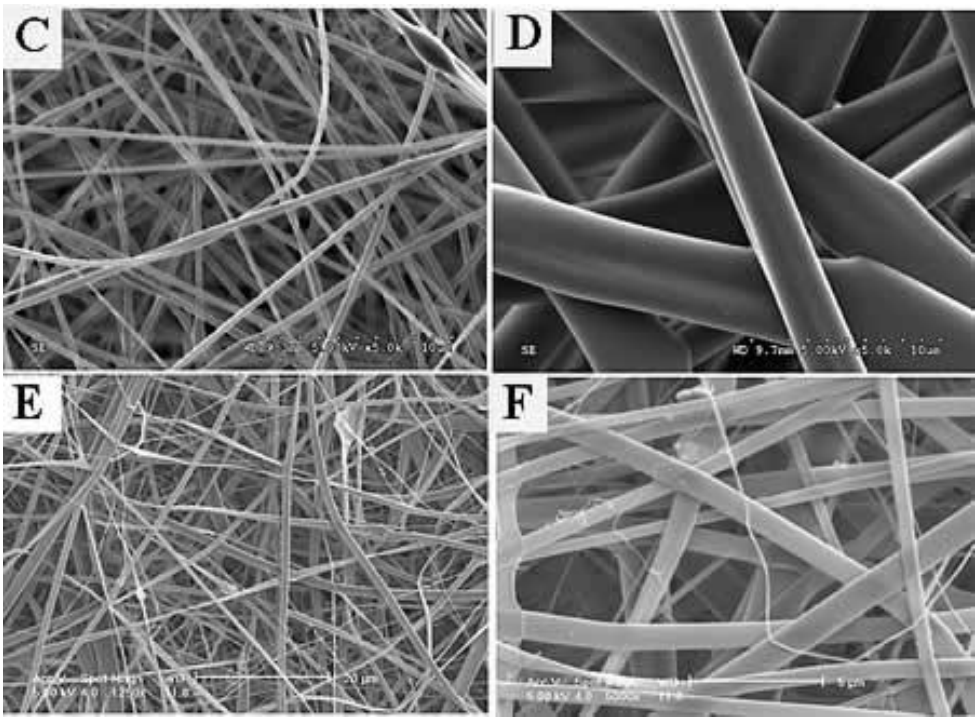

Figure 2.10 Electrospun gelatin scaffolds (C&D), and electrospun collagen scaffolds (E&F) [45].

2.3 Basic of electrospinning

The electrospinning process structures synthetic fibers by using electrostatic forces. It applies high-voltage source to charge polarity into polymer solution that can accelerate an opposite polarity's collector. Fiber Jet is lastly thrown out from Taylor Cone due to excessive electric field strength than liquid's surface tension. It moves through the atmosphere where solvent is able to evaporate, causing deposition of solid polymer fibers on the collector. Fibers products manufactured by using this process regularly have diameter in rang of 2-3 micrometers to 10 nanometers. The capacity to simply build materials at this biological scale occurs in electrospinning for tissue engineering applications. Besides, it has been suggested that this mixture instability is from repulsive interaction between same-polar charge in polymer jet.

Electrospinning is the procedure to produce nanofibers by using materials like protein or polymer, natural and synthetic ones. There are diverse parameters for applications, tissue engineering, controlling physical and chemical properties of nanofibers. Nanofiber production in present by electrospinning for tissue engineering use has been paid attention by both domestic and international researchers. Their studied design and production of nanofiber structure look like two-dimensional fabric. It is the way to improve material's efficacy for tissue engineering such as Vascular grafts, artificial skin, nervous system, muscles, bone structures including internal organs. [18].

Doshi and Reneker had hypothesized that charge density increases as the fiber jet thins, dramatically increasing radial charge repulsion which causes the fiber jet to split into a number of smaller fibers when a critical charge density is met [19]. However, in more

recent studies high speed photography has been used to image the unstable zone of the fiber jet, revealing that a whipping instability causes the single fiber to bend and turn rapidly giving the impression that the fiber is spitting.

The fabrication report of electrospun poly(lactic acid-co-glycolic acid) scaffold was prepared by Sangamesh et al. This study reported the fabrication of poly(lactic acid-co-glycolic acid), PLAGA, matrixes with fiber diameters of 150-225, 200-300, 250-467, 500-900, 600-1200, 2500-3000, and 3250-6000 nm via electrospinning. Furthermore, the porous fiber matrixes have porosity between 38-60% and everage pore diameters between 10-14 mm [20]. In the part of non-woven polyglycolic structures have been tested for tissue engineering applications.

Laleh et al. studied chemical and mechanical properties of PCL/gelatin nanofibrous scaffold by electrospinning process. They found to exhibit the most balance properties and prove to be a promising biomaterials and technique suitable for nerve regeneration [46]. Similarly, Deepika et al reported about prepration of nanofibrous (PCL/gelatin) for neural tissue engineering by electrospinning. The everage fiber diameter of polymer blend ranged from 232 ± 194 to 160 ± 86 nm with high porosity (90%). The resulting in increased hydrophilicity of nanofibrous scaffolds and better mechanical properties. Moreover, they found the results PCL/gelatin nanofibrous scaffolds are suitable for neural tissue engineering [47].

The property of the nanofibrous scaffold can be further improved with innovative development in electrospinning processes, such as two-component electrospinning and in-situ mixing electrospinning. Post modifications of electrospun membranes also provide

effective means to render the electrospun scaffolds with controlled anisotropy and porosity. In this article, Dehai Liang et al. review the materials, techniques and post modification methods to functionalize electrospun nanofibrous scaffolds suitable for biomedical applications [48].

The advantage in this method is inexpensive to produce nanofibers from a wide range of polymers. In addition, excellent cell and tissue compatability for mesenchymal cells. By using ice crystals as a collector, scaffolds with large pores and significant volume may be fabricated. On the other hand, disadvantage of these technique, organic solvents often required, scaffolds with volume, and large pore size or thickness are difficult to manufacture except by using ice crystal technique which has the disadvantage that sublimation required that increases complexity of manufacture. Mechanical properties of electrospun fibers is generally poor.

Electrospinning is the general process of producing nanofibers. The material used to produce substances such as protein or polymer, natural polymer to synthesis polymer. The physical and chemical properties of nanofibers are controlled by various parameters for applications such as tissue engineering applications. The current nanofiber production by electrospinning for use in tissue engineering has been a lot of attention from researchers both local and international. The researcher studied design and production of nanofiber structure would look like a piece of fabric with a two-dimensional structure, which is a process for improving the efficiency of the material for tissue engineering. For example, Vascular grafts, artificial skin, nervous system, muscles, bone structure, as well as organ in the body.

2.4 Effect of parameter on electrospinning process

2.4.1 Solution parameters [53-63]

Solution parameters are important to the structure, morphology and characteristic of the product, which includes concentration, viscosity, solvent, solution temperature, surface tension, conductivity and molecular weight [21].

2.4.1.1 Concentration

The concentration is related to viscosity and surface tension of the solution that it must have enough concentration to generate the connection of polymer chain becoming elongated to be fiber. If the solution has too little viscosity to create the connection, the products will be beads that have circle or ellipse shape on the fiber and the example of bead on the fiber is shown in picture 2.3. However, if the concentration increases, the polymer chain will block the elongation of charge jet that causes the increasing viscosity and the fiber will have wider diameter that is the result of less elongation of charged jet and too high viscosity of the solution, it's hard to control the flowing ratio of the solution. Therefore, it's better to use the polymer solution that has the concentration suiting electrostatic spinning when other parameters are stably controlled [22].

From the report of Sukigara, S. et al [23], the concentration is essential parameter that greatly affects electrostatic spinning. The concentration has direct involvement with viscosity [24] that the range of concentration can signify the quality of

products by using the concentration's mean to diversify the quality of products that is called critical concentration or C* of solution. The critical concentration can fundamentally identify the quality of products, that is, during the concentration is less than critical concentration, the products will have quality of sphere-shape microparticle or less. When increasing the concentration, the sphere particle will be more tapering and shuttle and fiber are formed alternately. When adding continuous concentration, the forming of bead on the fiber will decrease. Polymer is connected and elongated to be polymer chain and the product is pure fiber which occurs when the concentration is more than critical concentration [25].

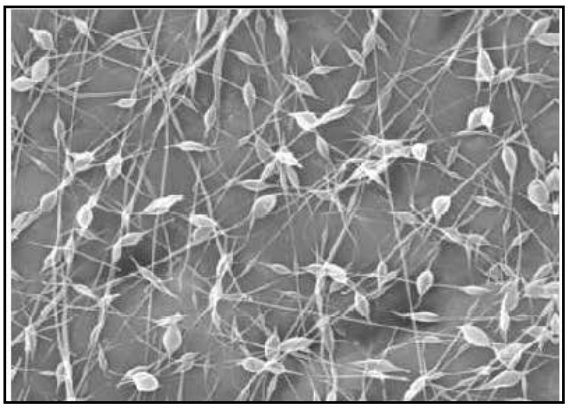

Figure 2.11 The quality of bead on polyethylene oxide from solution that has concentration 3.0% by weight and viscosity 74 cP by using electric potential difference 0.7 kV/cm [26].

2.4.1.2 Viscosity

The solution viscosity is important parameter influencing on the morphology and fiber formation. The difference of solution viscosity can be eletrospun is different such as morphology (bead on the fiber and fiber without bead) and fiber size

(small to large). The bead formation on the fiber decreased with increasing solution viscosity. The fibers size increased with increasing solution viscosity.

2.4.1.3 Solvent system

Solvent system is one of parameters affecting the quality of products from Electrostatic spinning. It includes electrical conductivity, surface tension, conductivity property and evaporation of solvent. If the solvent has thick electrode, there will be electrical force supporting the elongation of charged jet and the fiber size will be small. Therefore, in case to miniaturize the fiber, adding electrode-containing solvent is done to make the solution have more electrode density [26]. The evaporation of solvent is one of parameters that identify the quality, fiber figure. If the evaporation of solvent is too fast, the occlusion at needle's tip of syringe occurs [27]. On the other hand, if the evaporation of solvent is too slow, the fiber will become flat, net-type connecting. Therefore, the hard-evaporating solvent should be avoided to prevent net-type quality [28] shown in picture 2.4. Furthermore, using different solvents causes different fiber's surfaces [27].

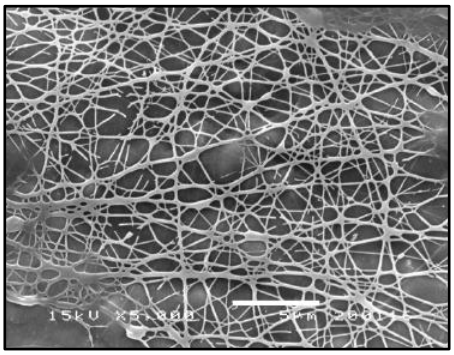

Figure 2.12 Quality of net-type fiber of Fibroin Mai Tai fiber and gelatin with 20% w/v concentration at ratio of mixture by weight of Fibroin Mai Tai and gelatin that is 80/20 by using 20 kV electric potential difference

2.4.1.4 Surface tention

Surface tension is opposite force of charge repulsion force or coulomb repulsion force. The polymer jet will occur, when the charge repulsion force overcome surface tension.

2.4.2 Environment parameters [21]

Environment parameters are external from the production process that considerable results for electrostatic spinning including temperature, humidity, and relative humidity of experimented system. For example, high humidity leads to slow evaporation of solvent. Therefore, to extend the gap distance between the open hole of syringe and collector is required to increase the time of evaporation of solvent out of fiber.

2.4.3 Processing parameters [29]

Processing parameters in molding that are significant and influencing the products from electrostatic spinning includes applied voltage, polymer flow rate, gap distance and spinneret size. For instance, if increasing the electric potential difference, the fiber will be small due to the fact that there is the electrical force elongating the charged jet but increasing spinneret size or polymer rate flow can enlarge the fibers that have beads because the increasing rate flow can elongate the fibers sparsely; so, the beads occur and gap distance parameter slightly affects fiber size.

2.4.3.1 Applied voltage

The applied voltage (V), (kV) induces the charge on the surface polymer jet, The polymer solution will eject from the tip to the collector when charge repulsion overcomes the surface tension. The applied voltage is importance parameter on morphology and fiber formation. The applied voltage increased tends to increase the charge repulsion.

2.4.3.2 Solution flow rate

The polymer solution flow rate is pumped into the spinneret to continuous of Taylor's cone. The feed rate is importance parameter on morphology and fiber formation. Ideally, the feed rate must balance between input and output from the spinneret, there can produce uniform fiber. At lower and higher feed rate influence Taylor's cone and polymer jet that effect on fiber formation.

2.4.3.3 Gab distance

The gap distance (L) is the distance between the tip of spinneret and the surface of the collector. It defines the time for evaporation of the solvent on the polymer jet and influence on the strength of electric field.

2.5 Materials for scaffold fabrication [30, 64]

The major reason is long-term biocompatible issues helping the body to regenerate

and repair damaged tissues. Biomaterials will correlate with biological system to evaluate, treat or replace tissues, organs or body's function. In addition, tissue response to implants relies on particular factors from physical and chemical qualities of materials. Some of biodegradable biomaterials' vital properties can be summed up as follows

1. Materials should not cause lasting inflammatory or toxic response upon implants in the body.

2. Materials should have agreeable shelf life .

3. Materials's degradation time should conform to healing or regeneration process.

4. Mechanical properties of materials should be appropriate to application and variation and degradation should be compatible with healing and regeneration process.

5. Non-toxic degradation products that is not harmful to body.

6. Materials should have appropriate permeability and process ability for particular use.

There are several natural, man-made polymers and ceramics that have high performance and they are biocompatible and biodegradable materials for building scaffolds. Natural ones such as proteins and polysaccharides are included for tissue engineering use. The current research helps verifying the correlation of bioactive materials. Various synthetic biodegradable polymers can be used to fabricate tissue engineering matrices. Mainly, they are structural elements of building scaffolds such as Poly (glycolic acid) (PGA) and poly (lactic acid) (PLA). These three materials are the most commonly used synthetic polymers in tissue engineering. Besides, hydrogels that either composes of synthetic polymer or polysaccharides have been used to immobilize transplanted cells.

Moreover, studies of materials' structure are designed to maximize performance of usage. Materials applied to build nanofibers by using electrospinning process in tissue engineering are very vital. Most-used materials includes substances like polymer synthesis such as poly lactic acid (PLA), poly ethyleneglycol (PEG), polyvinyl an alcohol (PVA), poly urethane (PU), poly lactic glycolic acid (PLGA) and polycarprolactrone (PCL) etc.

2.5.1 Natural materials

Natural polymers like proteins and polysaccharides are included as materials for tissue engineering use.

2.5.1.1 Collagen

Collagen is fibrous protein and main natural extracellular matrix component. It is used for diverse tissue regeneration uses. But, difficulties are available as using collagen require high expense and it is hard to store with poor-mechanical qualities as well as high-rate degradation

2.5.1.2 Polysaccharides

Polysaccharides like Alginate, Chitosan and Hyaluronate are different class of natural polymers used as porous solid-state tissue engineering scaffolds.

2.5.2 Synthetic Materials

2.5.2.1 Hydrolytically degradable polymers

Synthetic polymers are considered by researchers as biomaterials due to the fact that they can induce particular interaction with host cells. Besides, they are degradable for replacement by host tissues. They are cheaper than natural materials. Most extensively used ones for building scaffolds are PLA, PGA or combination of 2 polymers (PLGA). PLA, PGA or PLGA are aliphatic ester with good compatibility and usable as tissue engineering.

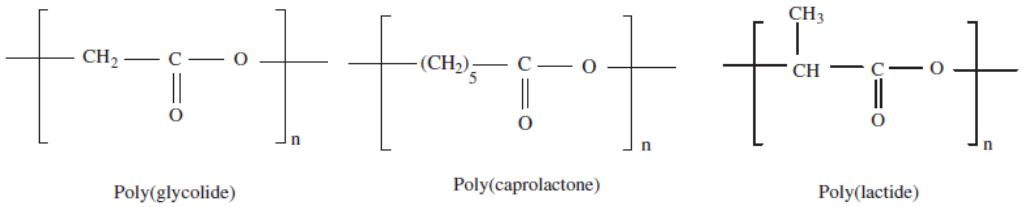

Figure 2.13 Chemical structure of poly(glycolide), poly(lactide) ,and poly(caprolactone) [31].

2.5.2.2 Other polyester

Polyester qualities are assorted by changing polymer backbones' structures. Polycarpolactone (PCL) is studied as substrate for biodegradation and as matrix for drug-releasing system. Its degradation in vivo is much slower than PGA. So, It is appropriate for release devices that is controlled with long in vivo lifetime.

Polyorthoformate, polycarbonate, poly (oxyethylene glycolate), poly (1,4 –

butylenes diglycolate) and polyurethane are biodegradable polymers that may be used in tissue engineering. To sum up, several polyesters are biodegradable and their mechanical properties is controllable by chemical structure of component blocks and they can be varied from tough to elastic forms. The biocompatibility of them is caused by non-toxic degradation products. Many attempts are made to follow bioactive elements to such materials so as to model extracellular matrix molecules.

2.5.2.3 Hydrogels

Hydrogel polymers are being studied for tissues engineering uses. It is called hydrogel due to the fact that materials can absorb 90% of initial dry weight in water. They are much interested as they can be controlled and reproduce [31]. And large amount of water absorption can help superior biocompatibility because of low protein uptake. Moreover, mechanical qualities and hydrophilicity are similar to old tissues' properties. Number of hydrogel monomers consists of half vinyl and that is why methods of free fundamental initial polymerization like fabrication propeller are likely. Photoinitiation, one of such method, let polymers to be structured by using specific light's wavelength. Applying this method, researchers are successful to form complex 3D structure with assorted mechanical qualities. Polyacrylamides is beneficial to hydrogels that have induced regeneration of soft tissues in facial derfects [32] and 2-hydroxyethyl metacrylate is used as fibrillar support for nervous generation [33].

Hydrogel material that is most studied is crosslink PFG approved by FDA for applications in tissue engineering. For instance, researchers parameter that can decelerate growth on to surfaces of biomaterials [34-36]. They accomplishedly use this

technique toward the structure of new biomimetic building. Yet, hydrogels are limitedly used due to highly crosslink hinders degradation that means tissue induction.

2.5.2.4 Other inorganic ceramic materials

Consideration of synthetic and natural inorganic ceramic materials (e.g. hydroxyapatite and tricalcium phosphase) to be materials for scaffold building aimed mostly at bone tissue engineering [37-39]. It is as ceramics are similar to inorganic natural component of bones and have osteoconductive properties. On the other hand, they are fragile and unmatched to mechanical qualities of bones or it should be said that bone is a composite consisting of polymer matrices strengthened by ceramic particles [40-42]. Polymer combines of protein collagen and Hydroxyapatite (HA). Besides, ceramic scaffolds cannot be expected as appropriate for soft tissue's growth 9e.g. cardiac muscle tissue) because these tissues receive different cellular receptors and mechanical properties need. Synthetic and natural polymer is appealing choices for uses to grow largest amount of cells.

CHAPTER III

MATERIALS AND METHODOLOGY

3.1 MATERIALS

3.1.1 Polycaprolactone (PCL)

In this research, poly(caprolactone) (PCL), (Mw 80,000) purchased from Sigma-Aldrich (St. Louis, MO, USA), was selected as our main materials. The Poly(caprolactone) (PCL) chemical structure was show as figure 3.1.

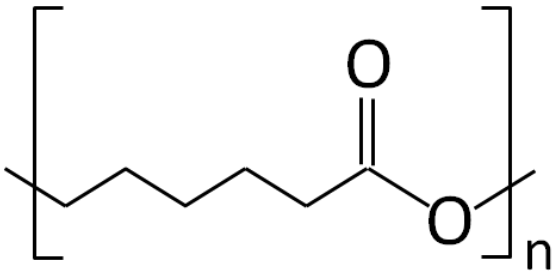

Figure 3.1 Chemical structute of polycaprolactone

3.1.2 Solvent

3.1.2.1 Dichloromethane (DCM) was used as a solvent for solution mixing. It was purchased from Carlo Erba (England).

3.1.2.2 Dimethylformamide (DMF) was used as a solvent for solution mixing with DCM, was supplied from Carlo Erba (England).

3.1.3 Ingredients used for Cell culture and MTT assays

3.1.3.1 Dulbecco's modified eagle medium (DMEM)

DMEM supplemented with 10% Fetal bovine serum (FBS), 1% L-glutamine, 1% antibiotic (penicillin-streptomycin)without Ca^{2+} and Mg^{2+} (PBS(-) powder was supplied by Nissui Pharmaceutical Co. Ltd).

Table 3.1 Dulbecco's modified eagle's liquid medium (DMEM) formulation

Ingredients
10% Fetal bovine serum
1% L-glutamine
1% Antibiotic (penicillin-streptomycin)

3.1.3.2 3-(4,5-Dimethylthiazolyl-2)-2,5-diphenyl tetrazolium bromide

3-(4,5-Dimethylthiazolyl-2)-2,5-diphenyl tetrazolium bromide was obtained from MTT, USB Corporation.

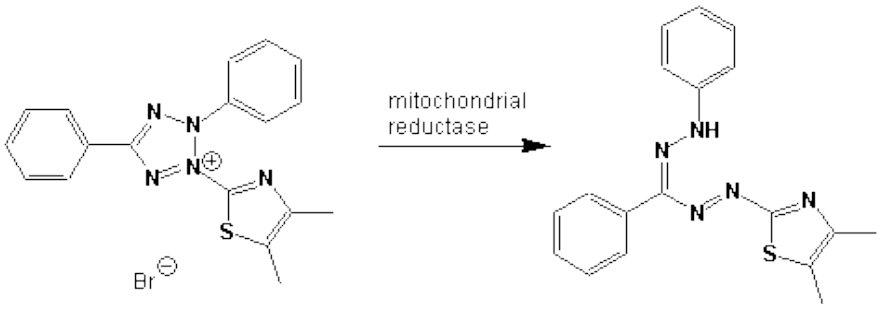

3-(4,5-Dimethylthiazol-2-yl)-2,5-diphenyltetrazolium bromide

Purple formazan in living cells

Figure 3.2 3-(4,5-Dimethylthiazolyl-2)-2,5-diphenyl tetrazolium bromide

3.1.3.3 Dimethyl sulfoxide

Dimethyl sulfoxide using for cell freezing was purchased from DMSO, Sigma, Thailand.

3.1.3.4 Glutaraldehyde

Glutaraldehyde solution (50% GTA) used for crosslinking between proteins in tissue using aldehyde fixatives

3.1.3.5 Hexamethyldisilazane (HMDS)

Hexamethyldisilazane (HMDS) were supplied by Fluka, Thailand.

3.1.3.6 Ethanol (C_2H_5OH)

The absolute ethanol (Analytical grade) was purchased from Normapur, Thailand.

3.2 EQUIPMENT

3.2.1 Negative high-voltage power supply, Model : ES30-5W, USA

3.2.2 Positive high-voltage power supply, Model : ES30-5W, USA

3.2.3 Brookfield viscometer (Model DV-II+),USA

3.2.4 Conductivity meter (Eutech Con510), USA

3.2.5 Syringe 5, 10, and 20 ml.

3.2.6 Needle 23G

3.2.7 Collecter

3.2.8 Scanning Electron Microscopy (Philip, XL 30 CP, USA)

3.2.9 Desicator cabinet (Binder,VD23, Japan)

3.2.10 Digital balance (Mettler TOLEDO, AL204, USA)

3.2.11 Digital balance

3.2.12 Autopipettes 10-100 µl, 100-1000 µl and 1000-5000 µl with tips (Eppendorf, Germany)

3.2.13 Fluorescence microplate reader (Perkin elmer, 1420 multilabel counter, USA)

3.2.14 Fine coat(JEOL Ltd.,JFC-1100E, Japan)

3.2.15 6 cm polystyrene tissue culture discs (Corning)

3.2.16 10 cm polystyrene tissue culture discs (Corning)

3.2.17 24- well polystyrene tissue culture plates (Corning)

3.2.18 96- well polystyrene tissue culture plates(Corning)

3.2.19 Sterilized pipette 2, 10, and 25 ml. (Costar)

3.2.20 Sterilized centrifugal tubes 15, and 50 ml (Corning)

3.2.21 1.5 ml sterilized vials (RCM, 3307-130380)

3.2.22 Hemacytometer (Counting chamber, Boeco, Germany)

3.2.23 Sterilized filter system (0.22 µm)

3.2.24 Paraffin film

3.3 METHODOLOGY

In this research studied both preparation of PCL electrospining; mat (2D) and sponge-liked structure (3D). Optimization of processing parameter conditions were investigated, characterization of cell viability was studied, the different method of sponge-liked structure preparation was prepared, Comparison the properties of different electrospinging structure were also studied.

3.3.1 Preparation of PCL electrospinging fiber (mat; two-dimentional (2D))

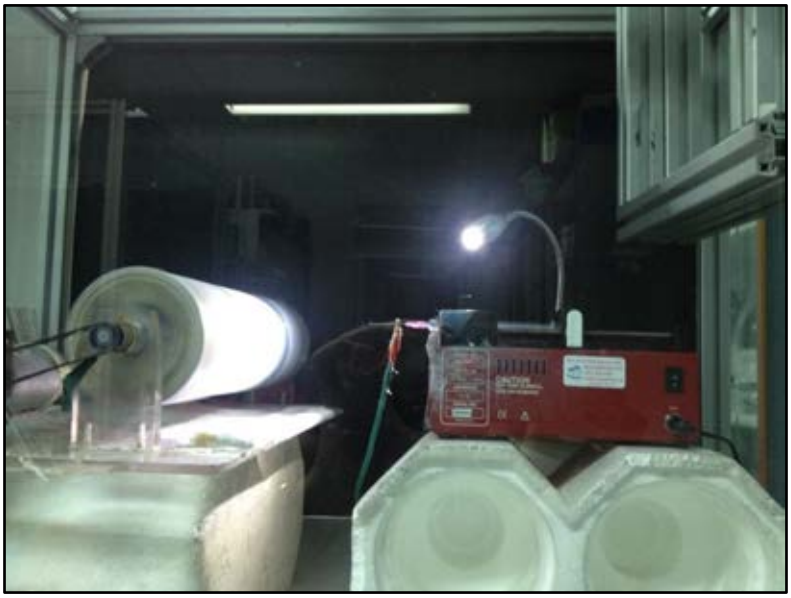

Figure 3.3 Simple electrospinning set up

In this part, the effect of different processing parameters on morphologies, fiber diameter, pore size and porosity of PCL electrospun were studied. The different of concentration of PCL solution, applied voltages, gap distance between spinneret and collector, flow rate were prepared.

PCL solutions at various concentrations (5, 10, 15, 20, 25 and 30 wt%) were prepared by dissolving appropriate amount of PCL in a mixed-solvent of dichloromethane(DCM): dimethylformamide(DMF) (1:1). PCL solutions were electrospun into fibers under applied voltage 10, 15, 20 and 25 kV, a solution flow rate was varied at 0.1, 0.5, 1.0 and 2.0 ml/h, the effect of distance between the syringe tip and rotating fiber collector was also studied at 10 and 20 cm. The obtained fiber mats (2D) were kept in a desiccator for at least 24 h at room temperature to dissipate remaining solvent before undergone morphological evaluation with SEM. All samples list with different concentration, applied voltage, flow rate and collecting distance between the syringe tip and rotating fiber are shown in table 3.2.

Table 3.2 PCL electrospun samples with different processing parameters at various PCL solution concentration

Applied voltages (kV)	Flow rate (ml/h)	Collecting distance (cm.)
5,10, 15, 20, 25, and 30 % PCL solution		
10	0.1	10
		20
	0.5	10
		20
	1.0	10
		20
	2.0	10
		20
15	0.1	10
		20
	0.5	10
		20
	1.0	10
		20
	2.0	10
		20
20	0.1	10
		20
	0.5	10
		20
	1.0	10
		20
	2.0	10
		20
25	0.1	10
		20
	0.5	10
		20
	1.0	10
		20
	2.0	10
		20

3.3.2 Preparation of 3D structure fabrication by Dual-Polarity Co-Electrospinning Process

We have invented and developed a new process that involves positive and negative charge in electrospinning system with collected the sponge-liked polycaprolactone (PCL) electrospun (3D) on vertical collector. The variation of process parameters; the applied opposite charge, flow rate, fiber size, and distance between collector were applied. The morphologies and porosity (distribution of pore and pores size) of a 3D PCL were observed using scanning electron microscope (SEM) and porosimeter.

In experiments, the PCL solution of 15%, 20% and 30% were selected to prepared in sponge-liked the structure. Due to the effect of fiber size, and application method on morphology, pore size, porosity and mechanical property of the obtained fiber mat.

3.3.2.1 Dual-polarity co-electrospinning process set up

The opposite charge electrospinning had been invented in this experiment, there are composed of negative high voltage, positive high voltage, vertical collector to collect the sponge-liked electrospun and spinneret. The both of PCL solutions were connected to a negative and positive applies voltage. The distance between both of spinneret was fixed at 40 cm and vertical collector was at a center. A voltage of 10 to 25 kV on the both of high voltage power supply were applied to the spinneret, and the flow rate of the solution was varied 1.0, and 2.0 ml/h. The polymer solution was ejected onto vertical collector, the distance between the fiber and the vertical collector was taken vary to study the structure of the 3D morphology. The 3D polycaprolactone (PCL) electrospun were dried

in a desicator for 24 h at room temperature to remove the remaining solvent. The setup is the following the figure 3.11.

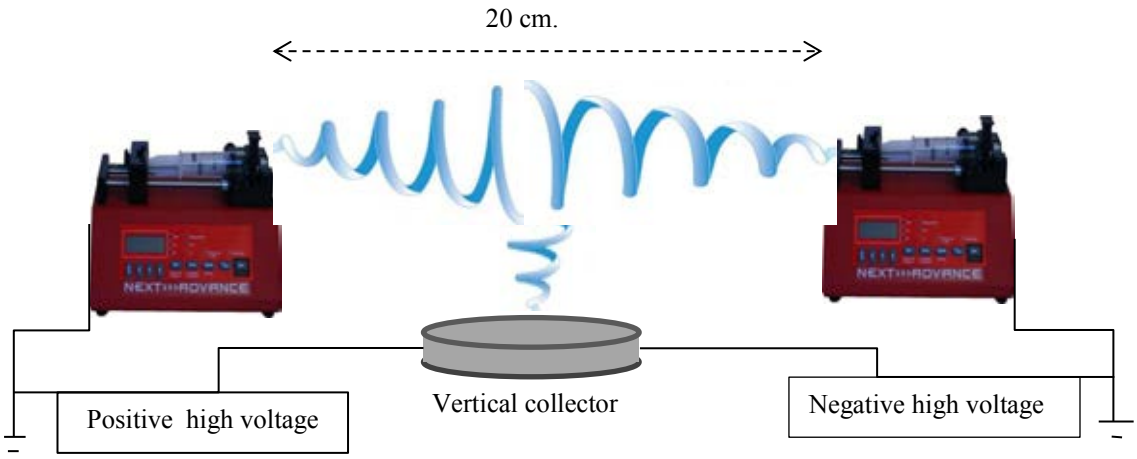

Figure 3.4 Dual-polarity co-electrospinning process set up

The futher works, L929 mouse fibroblast cells were used to study the cell activity (cell penetration, cell infiltration and cell proliferation rate) on a 3D scaffold via SEM micrographs and MTT assays.

Table 3.3-1PCL electrospun samples with different processing parameters at 15%, 20%,30% and mixed 15%, and 30% PCL solution

Concentration (wt%)	Positive		Negative	
	V (kV)	F(ml/h)	V (kV)	F(ml/h)
15,20 and 30	10	0.1	10	0.1
			10	0.5
			10	1
			10	2
			15	0.1
			15	0.5
			15	1
			15	2
			20	0.1
			20	0.5
			20	1
			20	2
			25	0.1
			25	0.5
			25	1
			25	2
		0.5	10	0.1
			10	0.5
			10	1
			10	2
			15	0.1
			15	0.5
			15	1
			15	2
			20	0.1
			20	0.5
			20	1
			20	2
			25	0.1
			25	0.5
			25	1
			25	2

Table 3.3-2 PCL electrospun samples with different processing parameters at 15%, 20%,30% and mixed 15%, and 30% PCL solution

Concentration	Positive		Negative	
(wt%)	V (kV)	F(ml/h)	V (kV)	F(ml/h)
15,20 and 30	10	1		0.1
			10	
			10	0.5
			10	1
			10	2
			15	0.1
			15	0.5
			15	1
			15	2
			20	0.5
			20	1
			20	2
			25	0.1
			25	0.5
			25	1
			25	2
		2	10	0.1
			10	0.5
			10	1
			10	2
			15	0.1
			15	0.5
			15	1
			15	2
			20	0.1
			20	0.5
			20	1
			20	2
			25	0.1
			25	0.5
			25	1
			25	2

Table 3.3-3 PCL electrospun samples with different processing parameters at 15%, 20%,30% and mixed 15%, and 30% PCL solution

Concentration	Positive		Negative	
(wt%)	V (kV)	F(ml/h)	V (kV)	F(ml/h)
15,20 and 30	15	0.1	10	0.1
			10	0.5
			10	1
			10	2
			15	0.1
			15	0.5
			15	1
			15	2
			20	0.5
			20	1
			20	2
			25	0.1
			25	0.5
			25	1
			25	2
		0.5	10	0.1
			10	0.5
			10	1
			10	2
			15	0.1
			15	0.5
			15	1
			15	2
			20	0.1
			20	0.5
			20	1
			20	2
			25	0.1
			25	0.5
			25	1
			25	2

Table 3.3-4 PCL electrospun samples with different processing parameters at 15%, 20%,30% and mixed 15%, and 30% PCL solution

Concentration (wt%)	Positive		Negative	
	V (kV)	F(ml/h)	V (kV)	F(ml/h)
15,20 and 30	15	1.0	10	0.1
			10	0.5
			10	1
			10	2
			15	0.1
			15	0.5
			15	1
			15	2
			20	0.1
			20	0.5
			20	1
			20	2
			25	0.1
			25	0.5
			25	1
			25	2
		2.0	10	0.1
			10	0.5
			10	1
			10	2
			15	0.1
			15	0.5
			15	1
			15	2
			20	0.1
			20	0.5
			20	1
			20	2
			25	0.1
			25	0.5
			25	1
			25	2

Table 3.3-5 PCL electrospun samples with different processing parameters at 15%, 20%,30% and mixed 15%, and 30% PCL solution

Concentration	Positive		Negative	
(wt%)	V (kV)	F(ml/h)	V (kV)	F(ml/h)
15,20 and 30	20	0.1	10	0.1
			10	0.5
			10	1
			10	2
			15	0.1
			15	0.5
			15	1
			15	2
			20	0.5
			20	1
			20	2
			25	0.1
			25	0.5
			25	1
			25	2
		0.5	10	0.1
			10	0.5
			10	1
			10	2
			15	0.1
			15	0.5
			15	1
			15	2
			20	0.1
			20	0.5
			20	1
			20	2
			25	0.1
			25	0.5
			25	1
			25	2

Table 3.3-6 PCL electrospun samples with different processing parameters at 15%, 20%,30% and mixed 15%, and 30% PCL solution

Concentration (wt%)	Positive		Negative	
	V (kV)	F(ml/h)	V (kV)	F(ml/h)
15,20 and 30	20	1.0	10	0.1
			10	0.5
			10	1
			10	2
			15	0.1
			15	0.5
			15	1
			15	2
			20	0.1
			20	0.5
			20	1
			20	2
			25	0.1
			25	0.5
			25	1
			25	2
		2.0	10	0.1
			10	0.5
			10	1
			10	2
			15	0.1
			15	0.5
			15	1
			15	2
			20	0.1
			20	0.5
			20	1
			20	2
			25	0.1
			25	0.5
			25	1
			25	2

Table 3.3-7 PCL electrospun samples with different processing parameters at 15%, 20%,30% and mixed 15%, and 30% PCL solution

Concentration	Positive		Negative	
(wt%)	V (kV)	F(ml/h)	V (kV)	F(ml/h)
15,20 and 30	25	0.1		0.1
			10	
			10	0.5
			10	1
			10	2
			15	0.1
			15	0.5
			15	1
			15	2
			20	0.5
			20	1
			20	2
			25	0.1
			25	0.5
			25	1
			25	2
		0.5	10	0.1
			10	0.5
			10	1
			10	2
			15	0.1
			15	0.5
			15	1
			15	2
			20	0.1
			20	0.5
			20	1
			20	2
			25	0.1
			25	0.5
			25	1
			25	2

Table 3.3-8 PCL electrospun samples with different processing parameters at 15%, 20%,30% and mixed 15%, and 30% PCL solution

Concentration (wt%)	Positive		Negative	
	V (kV)	F(ml/h)	V (kV)	F(ml/h)
15,20 and 30	25	1.0	10	0.1
			10	0.5
			10	1
			10	2
			15	0.1
			15	0.5
			15	1
			15	2
			20	0.1
			20	0.5
			20	1
			20	2
			25	0.1
			25	0.5
			25	1
			25	2
		2.0	10	0.1
			10	0.5
			10	1
			10	2
			15	0.1
			15	0.5
			15	1
			15	2
			20	0.1
			20	0.5
			20	1
			20	2
			25	0.1
			25	0.5
			25	1
			25	2

Based on the experiment, we selected the morphology of 3D structure from various parameters for studied on the next experiment.

In this part, our studies the effect of the position of the fiber collection on sponge-liked structure that shows in figure 3.5. The position C is the first gathering point of fiber from the both sides around 5 cm. From the center of pararel line (orange line). For position D is the point from C to collector about 5 cm.

\

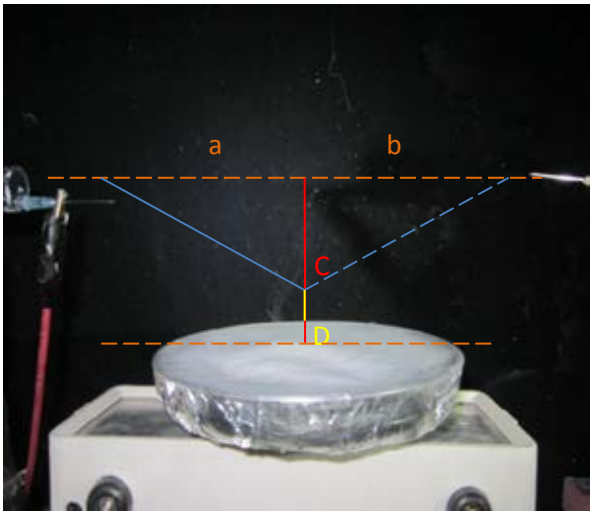

Figure 3.5 The position of fiber collection

3.4 Characterization of properties of electrospun nanofiber

3.4.1 Characterization of solution

3.4.1.1 Viscosity

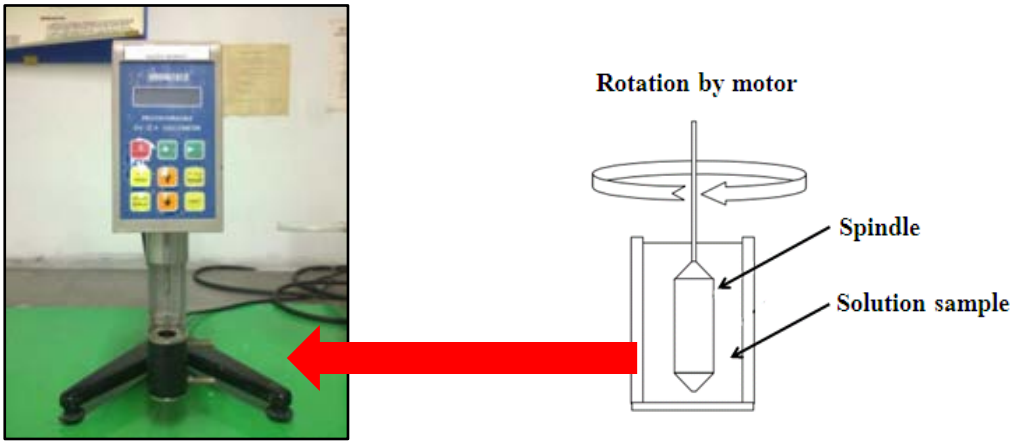

Figure 3.6 Rotational viscometer

3.4.1.2 Conductivity

Figure 3.7 Conductivity meters instrument.

The viscosity and conductivity of as prepared PCL solutions were determine and measured using rotational viscometer and conductivity meters (Eutech Con510) instrument that show in figure 3.6 and 3.7, respectively.

3.4.2 Porosimetry

Porosimetry is an analytical technique used to determine the various quantifiable aspects of a materials porous nature, such as pore diameter, total pore volume, surface area, and bulk and absolute densities. Porosity measurement was used to investigate the total porosity of the electrospun nanofiber. In this work, the porosimetry was referring to S.Soliman et al (2009). A liquid intrusion procedure, scaffolds were weighed prior to immersion in ethanol (intruding liquid of density qEtOH = 0.789 g ml_1), left overnight on a shaker table to allow diffusion of ethanol into the void volume, blotted with a Kimwipe and reweighed. The porosity was calculated as

$$\varepsilon = V_{EtOH}/(V_{EtOH} + V_{PCL}) \qquad (3.1)$$

By dividing the volume V_{EtOH} of the intruded ethanol (i.e. the ratio of the observed mass change after intrusion and ρEtOH) by the total volume after intrusion (equaling the sum of V_{EtOH} and the volume of the PCL fibers V_{PCL} computed as the ratio between the initial scaffold mass before intrusion and ρPCL)

3.4.3 Morphology of PCL electrospun nanofiber

3.4.3.1 SEM, Optical and Confocal microscope

Firstly, the sheets of electrospun fibers were cut approximately 8x8 mm^2. Then the thin gold layer was sputtered plated using Pularon SC500 sputter coater for 2 min.

The samples were prepared to study the morphology using scanning electron microscopy (SemAfore 5.21, SEM) with magnification of 2000x and 5000x. SEM images the sample by scanning with a high-energy beam of electrons. The electrons interact with the atoms that make up the sample producing signals that contain information about the sample's surface topography, after measuring the diameter of the fibers were selected randomly from 50 points of SEM images at magnification 2000x. The morphology and pore size of cell, electrospun nanofiber and cell activity were investigated.

Figure 3.8 Scanning Electron Microscopy (SEM)

3.4.4 Characterisation of Cell culture

3.4.4.1 Mesurement by Methylthiazol Tetrazolium Assay (MTT)

The MTT assay is colorimetric assays for measuring the activity of enzymes that reduce MTT to formazan dyes, giving a purple color. A main application allows assessment the viability (cell counting) and the proliferation of cells (cell culture assays). It

can also be used to determine cytotoxicity of potential medicinal agents and toxic materials, since those agents would stimulate or inhibit cell viability and growth.

For cell culture and cell viability test, selected electrospun fiber mats of approximately equal thickness were cut into a circular shape scaffold with diameter about 14.3 mm and sterilized with 70% ethanol. These scaffolds were placed in a 24 well treated tissue culture plate (TCP), before soaked with 0.5 ml of DMEM overnight prior to L929 seeding. Then L929 cells were seeded in each well with a density of 2 x10^4 cells/scaffold. The plates were incubated for specific time at 37 ºC and 5% CO_2 atmosphere, with culture media being replaced every 48 hr to ensure optimum cell growth. Cellular adhesion and proliferation were determined from number of cell at 6, 24, 72 and 168 hr using MTT assays. At first the 0.5 mg/ml of MTT in PBS was prepared in dark area. The existing DMEM in scaffold was removed by washing using PBS. After that, 1 ml of MTT solution was added in each well and incubated at temperature of 37 $^{\circ}$C, 5% CO_2 for 2 hr. The MTT solution in each well was removed leaving the purple ice crystals of MTT on the fiber which reveals the existence of cell. One ml of DMSO was added into the well to dissolve the crystals. Cell number was then determined from the absorbance of the solution using microplate reader (Perkin elmer, 1420 multilabel counter, USA) at 570 nm. Cell morphology was assessed by SEM micrograph. For this tissue culture experiment, two set of triplicate samples were carried out.

3.5 Workplace research

1. Electrospinning Labrolatory, 10th floor,

2. Tissue culture Labrolatory, 9th and 10th floor Faculty of Medical, Chulalongkorn University, Bangkok, Thailand
3. Biotechnology Labrolatory

3.5 Overall research flow chart

3.5.1 Overall PCL solution preparation flow chart is presented in figure 3.9

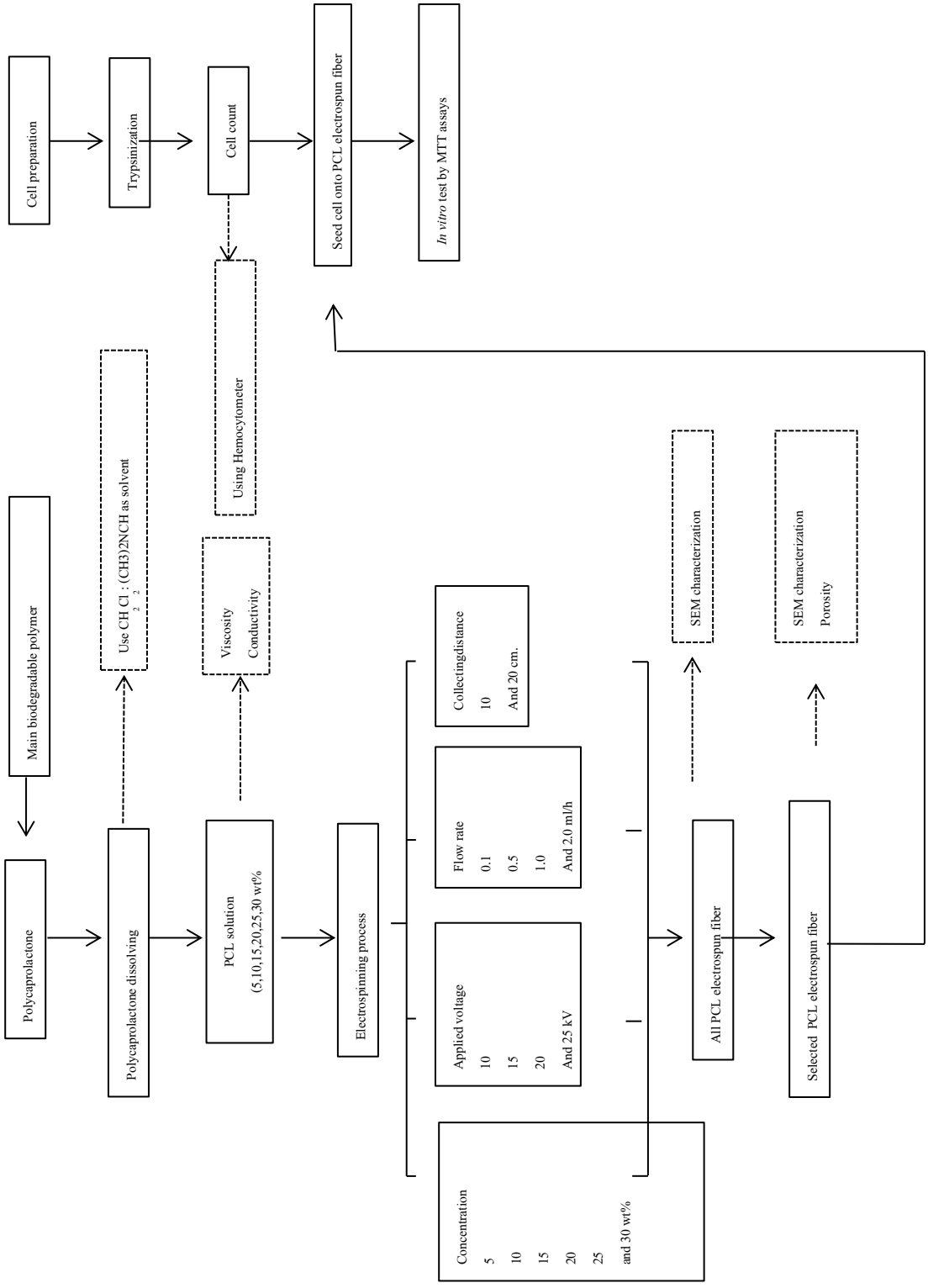

Figure 3.9 Overall PCL electrospun fiber preparation flow chart

3.5.2 Overall PCL 3D structure preparation flow chart is presented in figure 3.10

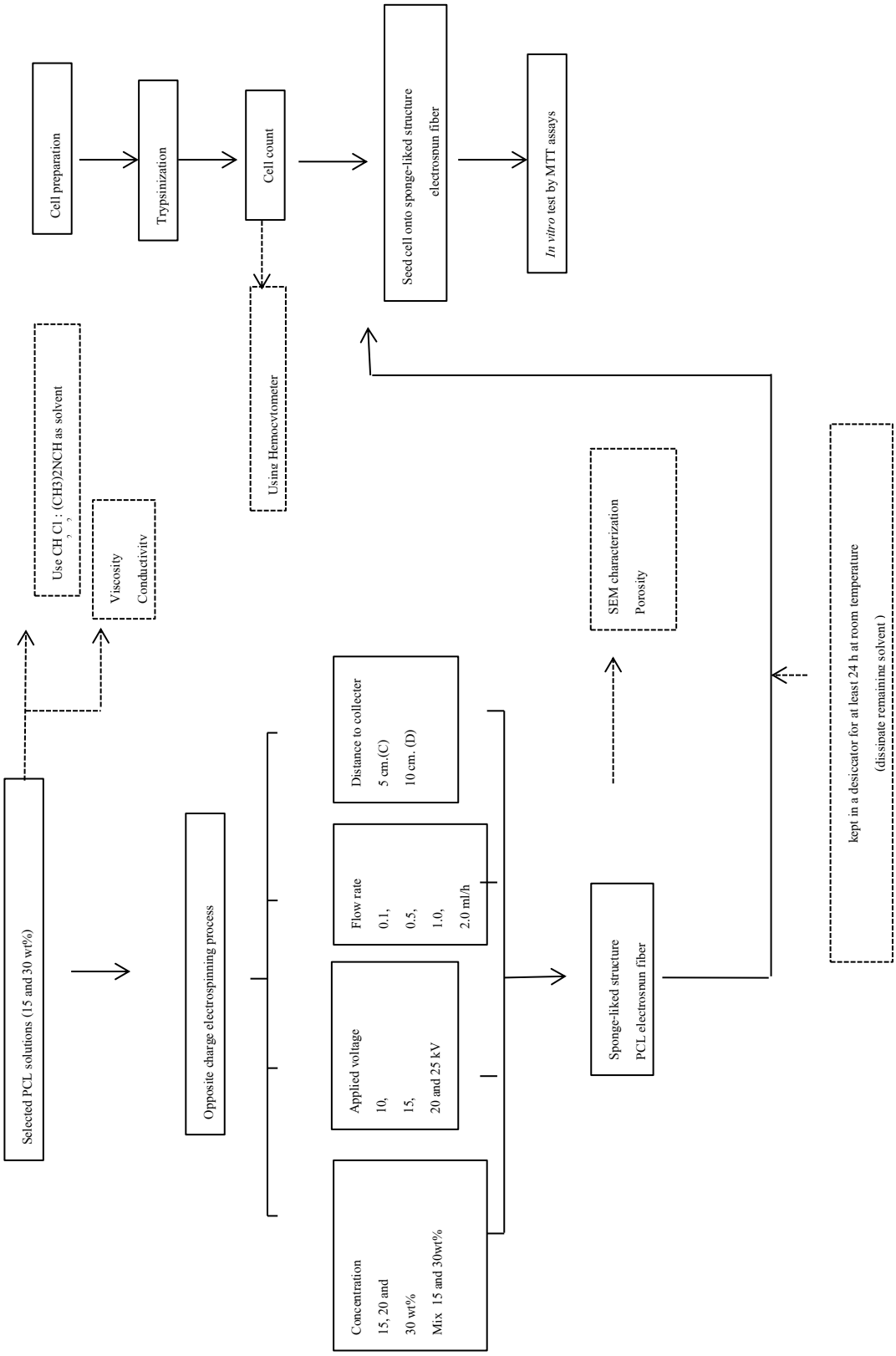

Figure 3.10 Overall PCL 3D structure preparation flow chart

CHAPTER IV

RESULT AND DISCUSSION

The results of this research were separated into 3 main parts. The first part related to the study of the effect of processing parameters on fiber size and fiber formation for electrospinning of PCL. Second part of the content was related to the development of 3D-structure of PCL electrospun fiber using a novel dual-polarity co-electrospinning process, which had been developed here. In the last section, we assessed effect of PCL electrospun fiber size on cell adhesion and proliferation. We also demonstrated the potential use of a newly developed 3D-structure as an artificial tissue engineering scaffold.

4.1 Effect of processing parameter on PCL electrospinning process

In this section, we investigated the effect of PCL polymer solution concentration, applied voltage, solution flow rate and collecting distance on size, morphology and formation of PCL fibers. Polymer concentration was varied from 5, 10, 15, 20, 25, to 30 wt%, the applied voltages used for electrospinning process were varied from 10,15,20, to 25 kV., the polymer solution flow rate was varied from 0.1, 0.5, 1.0 to 2.0 ml/h, and the gap distance between spinneret and collector was varied between 10 and 20 cm.

In the following discussion section, only selected data were presented to give an overview on how the processing parameter affects obtained PCL fiber. Full data of the experiment was included in the Appendix A.

4.1.1 Propeties of polymer solution

Properties of polymer solutions

From table 4.1 and figure 4.1 (a), the viscosity of polymer solution was increased with the increasing of the concentration of the PCL solution from 5 to 30 wt%. As PCL was a polymer containing long molecular chains which involves high entanglement in solution [21]. Processing parameters considered have included solution concentration and viscosity effects. Solution viscosity has been found to influence fiber diameter [5,16], Increasing solution viscosity has been associated with the production of larger diameter fibers [5].

Table 4.1. Characteristic of PCL solution viscosity and conductivity at various concentrations.

Polymer concentration	Viscosity (cP) at 30°c	Conductivity (µs)
PCL 5 wt%	15.1	10.32
PCL 10 wt%	117.1	6.26
PCL 15 wt%	153.2	6.05
PCL 20 wt%	544.4	5.23
PCL 25 wt%	1443.2	3.42
PCL 30 wt%	3704.0	1.19

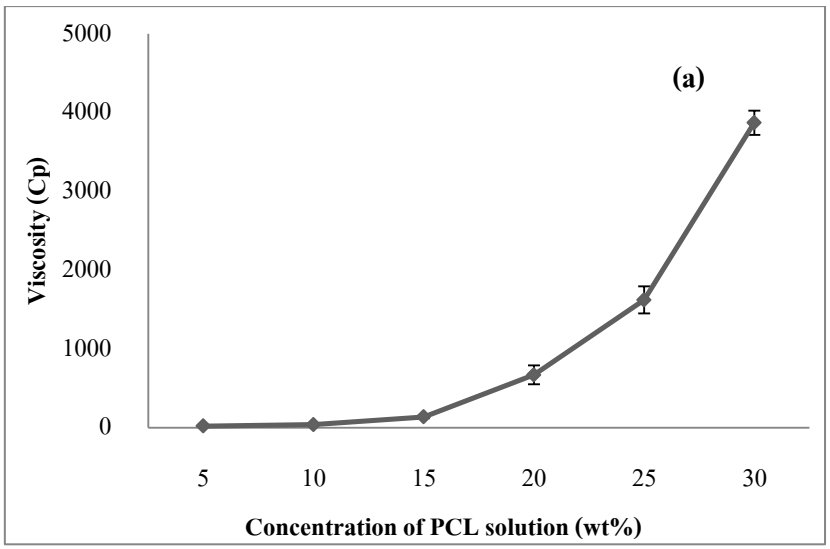

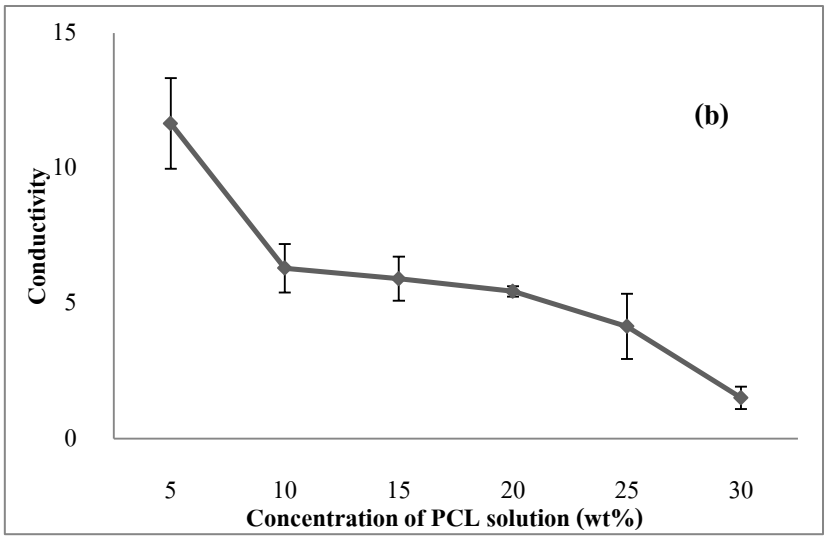

Figure 4.1 Properties of polymer solutions (a) Viscosity of PCL, and (b) Conductivity solution, respectively.

From table 4.1 and figure 4.1 (a), the viscosity of PCL solution increased gradually with the increasing of the concentration of the PCL solution from 5 to 15 wt%, and increased drastically when the concentration rosed 30 wt%. This findings was constistant with numberous report [a, b,c] and is infact a universal fact for polymer solution. Since the

viscosity of the polymer is a result of molecular entanglement, increasing concentration increased number of polymer molecule, which increase intermolecular entanglement and hence solution viscosity.Hence, the higher concentration of PCL solution gave higher viscosity. Similar to the Yu and colleagues's reported, they was found that the concentration of polyacrylonitrile (PAN) solution enhanced the the viscosity proportionally which is an important factor for producing the spinning fibers [22].

On the contrary study of the effect of concentration on the conductivity reveals that the concentration of the solution resulted in increased conductivity. The conductivity is an indication of number of mobile charges or ions in the solution and the mobility of the charges within the solution. Thus it is an indication of charge diffusion ability to the surface of the the ability to lead the charge to the surface of the solution process while the solution is higher conductivity result in higher a charge to the surface, which are factors that contribute to forming fibers by the electrospinning process. The results showed that the conductivity decreased with increasing amount of PCL concentration (Figure 4.1 (b)). The initial concentration, the conductivity increased but at the critical of concentration the conductivity will decrease.

As for the electrical conductivity of the solution, we observed a sharp drop of the conductivity when the concentration rose from 5 to 10 wt%, after that the conductitvity declined steadily. In general, the conductivity depends on number of mobile charges or ions in the solution, and the mobility of the ions. Increasing solution concentration raised the solution viscosity, as the result from the previous section shown, which in turn, hinder the mobility of the ions in the solution, and led to conductivity reduction.

4.1.2 Effect of solution concentration on fiber formation and morphology

PCL polymer solutions with concentration of 5, 10, 15, 20, 25, and 30 wt% were prepared and electrospun into fibers using applied voltage, solution flow rate and collecting distance of 15 kV, 0.1 ml/h, and 10 cm, respectively.

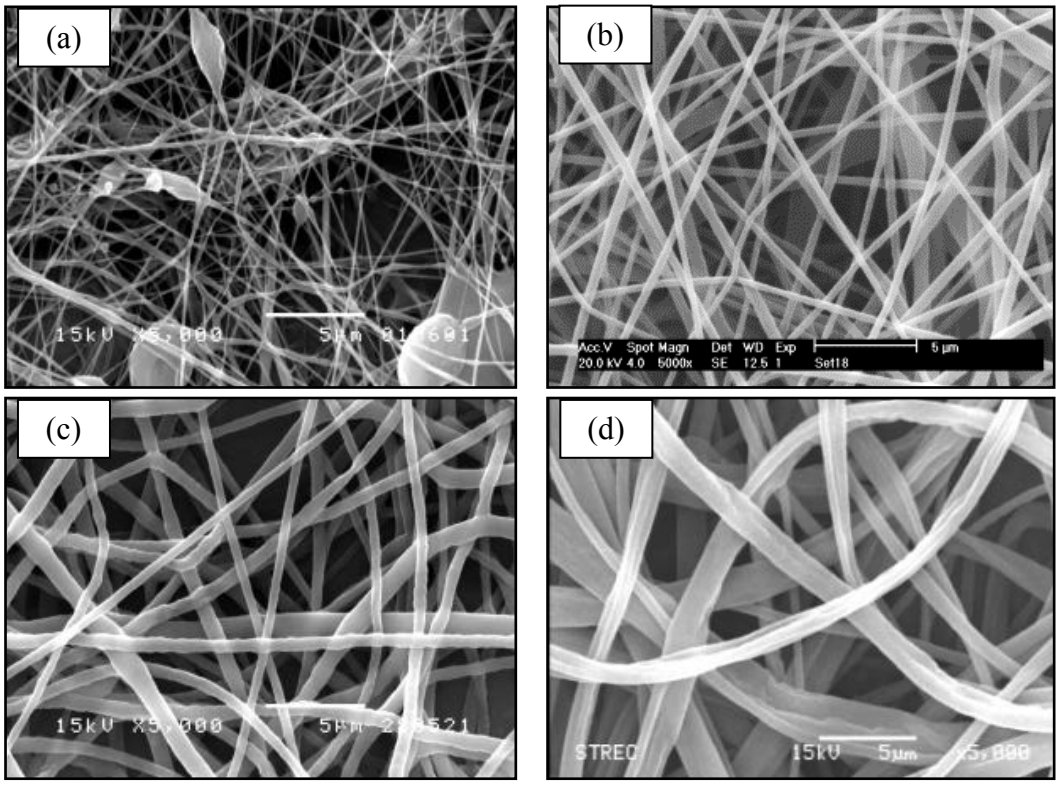

Figure 4.2 SEM micrographs of PCL electrospun fiber mats at varied concentration 5, 10, 15 and 20 wt%. At fixed voltage 15 kV, collecting distance 10 cm. and flow rate 0.1 ml/h.

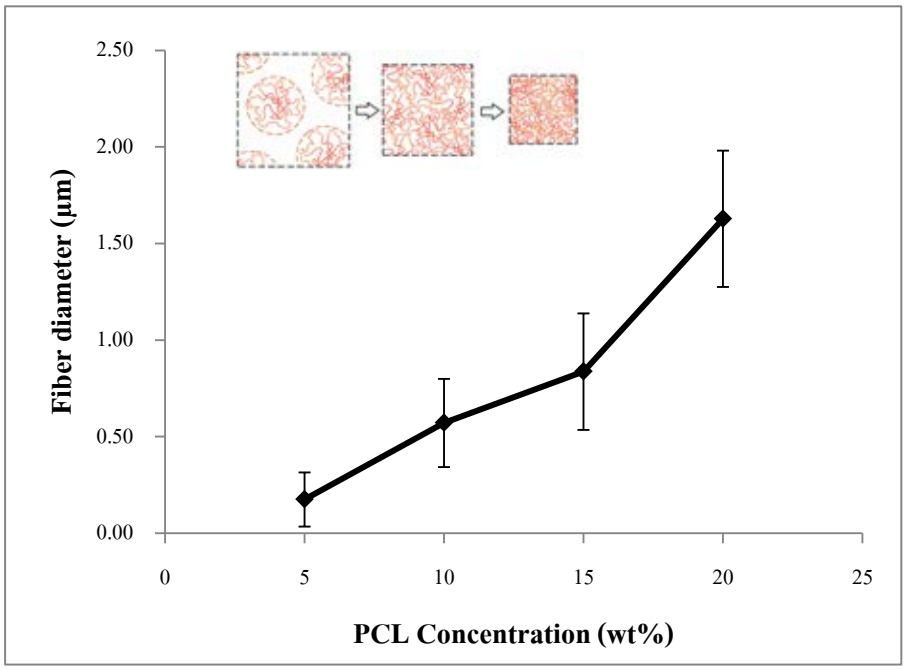

Figure 4.3 Influence of PCL concentration on fiber diameter of PCL electrospun fiber mats. At fixed voltage 15 kV, collecting distance 10 cm and flow rate 0.1 ml/h.

Figure 4.2 showed SEM micrograph of PCL electrospun fiber mats at varied concentration 5, 10, 15 and 20 wt%. At fixed voltage 15 kV, collecting distance 10 cm and flow rate 0.1 ml/h. and figure 4.3 clearly showed that the result of PCL electrospun fiber size increased as the concentration increased. Also, significant morphological changes of the fibers were noticed when the concentration of the polymer solution was altered. At low concentration, 5 wt%, the fiber appeared to have many beads on the straight segment of the fiber, or so called, bead on strings morphology, which indicated an insufficient polymer chain entanglement to suppress a capillary instability. Smooth and uniform fibers started to be formed as the concentration increased to 10 to 30 wt%. The results confirmed that the concentration of polymer solution is one of the most dominant processing parameters that can be used to control both fiber size and morphology.

4.1.3 Effect of applied voltage on fiber formation and morphology

From figure 4.4 showed the SEM micrograph of PCL electrospun fiber mats with varied applied voltage 5, 10, 15 and 20 kV. At fixed voltage 15 wt%, collecting distance 10 cm and flow rate 0.1 ml/h. In figure 4.5, the fiber diameter gradually increased with increased the applied voltage.

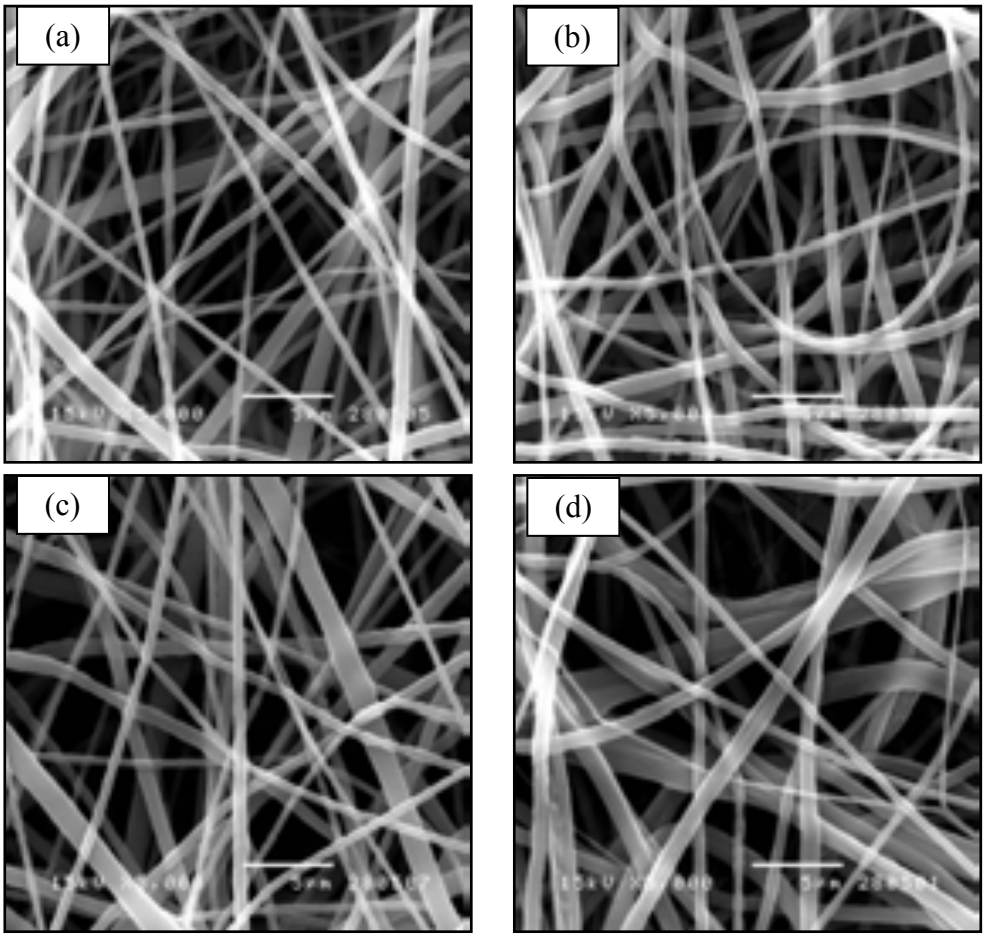

Figure 4.4 SEM micrograph of PCL electrospun fiber mats with varied applied voltage 5, 10, 15 and 20 kV. At fixed voltage 15 wt%, collecting distance 10 cm. and flow rate 0.1 ml/h.

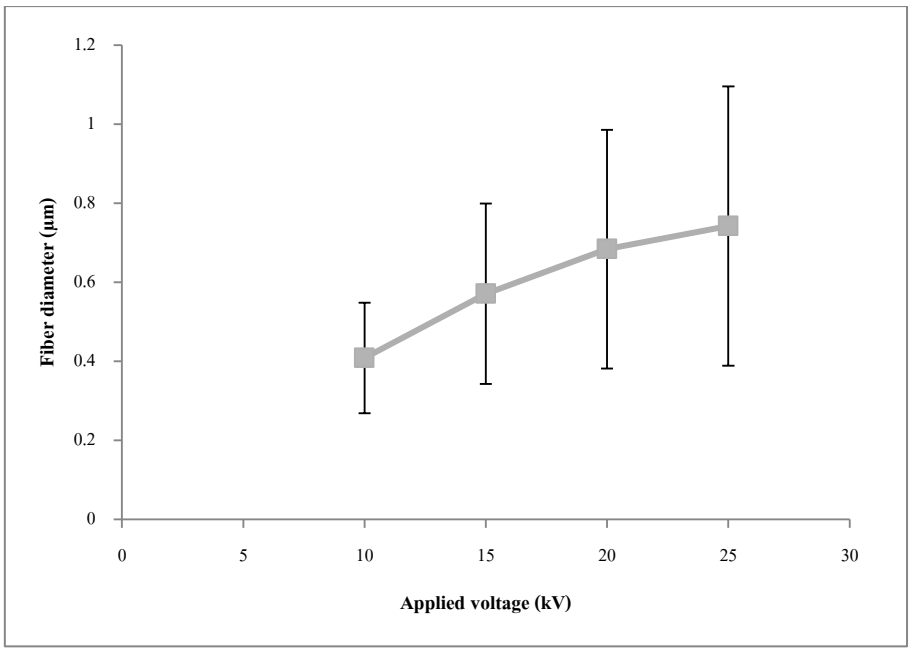

Figure 4.5 Influence of applied voltage on fiber diameter of PCL electrospun fiber mats. At fixed voltage 15 wt%, collecting distance 10 cm and flow rate 0.1 ml/h.

The electrical potential different between the spinneret and the collector played play important role in the process, since it is the only diving force that induce free charges or ions from within the solution body to migrate to the surface of the solution at the opening in the spinneret. The Columbia repulsion force between these surface charges then destabilizes the surface and cause the charged jet, which later solidify into solid fiber, to emit from the spinneret. Increasing applied voltage has both positive and negative effects on fiber formation from fiber size standpoint. Higher potential difference, or higher applied voltage, can induce more charges to the surface, resulting in a higher magnitude of the repulsive force. In the ideal case, the higher repulsive force led to a larger elongation of the charged jet when it is still a liquid state, which solidifies into smaller fibers as compare to the case of using lower repulsive force. However, the higher repulsive force from higher applied voltage also draw more charged jet to emit from the spinneret making the diameter

of the initial charged jet to be bigger than that when using lower applied voltage. The large volume of the initial charged jet affects the fiber size in 2 ways. First, There is more solution volume to solidify, and second, there is more visco-elastic resistant associated with having larger volume. These effects compensate and play each other out, and depend on the polymer system and processing parameters range under investigation, can lead to either fiber reduction or enlargement as the applied voltage being increased. For our system here, increasing applied voltage led to the fiber size enlargement.

4.1.4 Effect of polymer flow rate on fiber formation and morphology

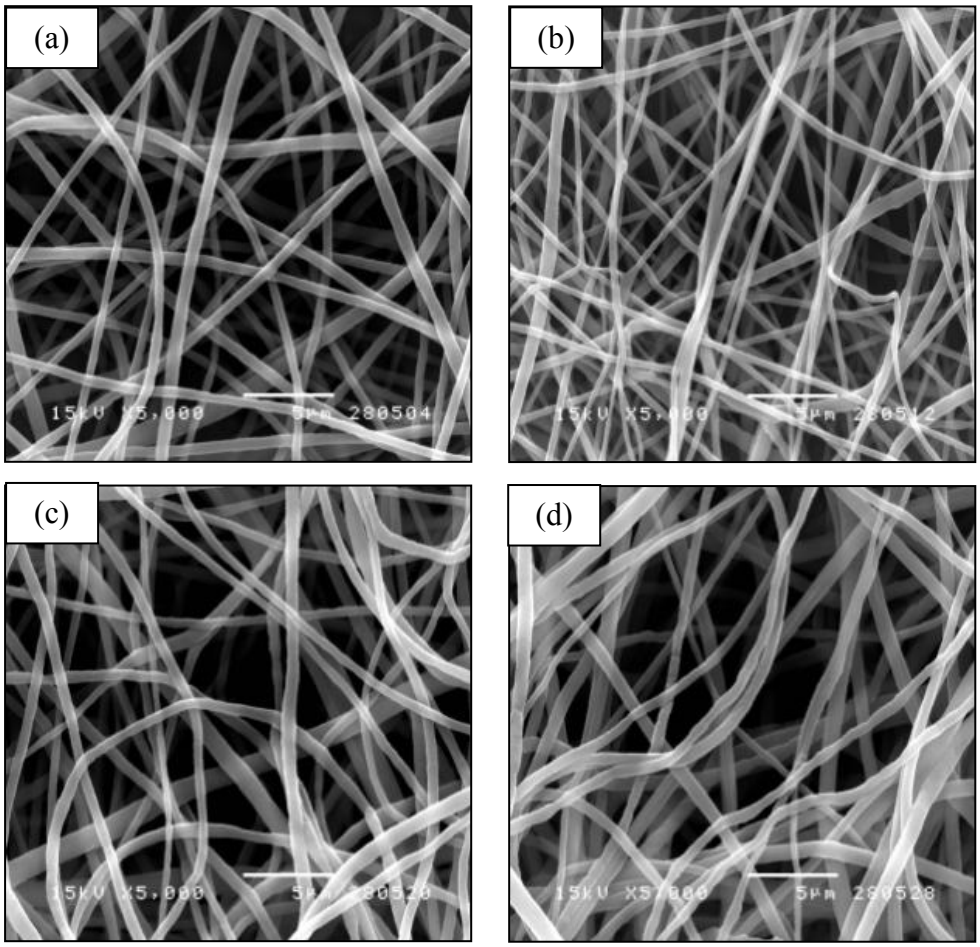

Figure 4.6 SEM micrograph of PCL electrospun fiber mats with varied flow rate 0.1, 0.5, 1 and 2 ml/h. At fixed voltage 15 wt%, applied voltage 15 kV and collecting distance 10 cm.

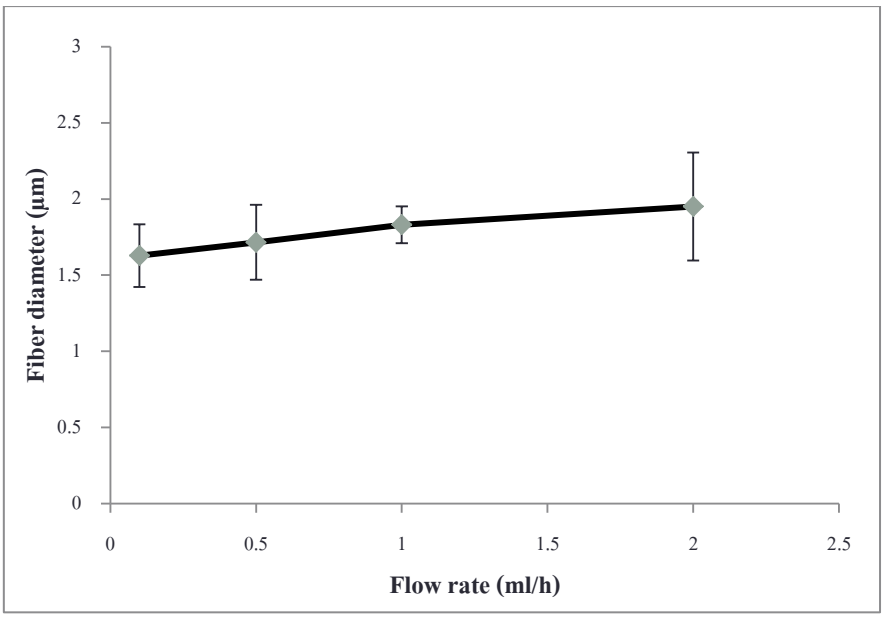

Figure 4.7 Influence of flow rate on fiber diameter of PCL electrospun fiber mats. At fixed voltage 15 wt%, applied voltage 15 kV and collecting distance 10 cm.

From figure 4.6 showed SEM micrograph of PCL electrospun fiber mats with variable flow rate 0.1, 0.5, 1 and 2 ml/h. At fixed voltage 15 wt%, applied voltage 15 kV and collecting distance 10 cm. The flow rate was also effected on fiber diameter. Interestingly, the feed rate was sufficient for fibers forming. Higher feed rate could be provided more polymer solution than needed, since it was observed that the amount of the excess polymer solution formed at the needle tip increased with increasing feed rate. The rate must be tuned so that a stable Taylor cone is formed. High flow rates could potentially cause a buildup of solution at the needle tip. As the flow rate increases, the surface charge density decreases therefore the rate of charge withdrawal into the solution is dependent upon the residence time of ions in contact with the needle. The polymer solution used for less time to contact with the tip. It can be concluded that the surface charge density is the driving force behind electrospinning, which is directly affected by flow rate. It was observed that the amount of excess polymer solution formed at the needle tip increased with

increasing feed rate (figure 4.7). That was described as a higher amount of polymer solution was repulsed. It showed the smaller size when flow rate increased at similar voltage at high concentration of polymer solution.

4.1.5 Effect of collecting distance on fiber formation and morphology

The last parameter effect for investigated is collecting distance . Figure 4.8 showed the effect of collecting distance on the fiber size. It observed the difference in distance is affected on fiber sizes as shown in figure 4.8.

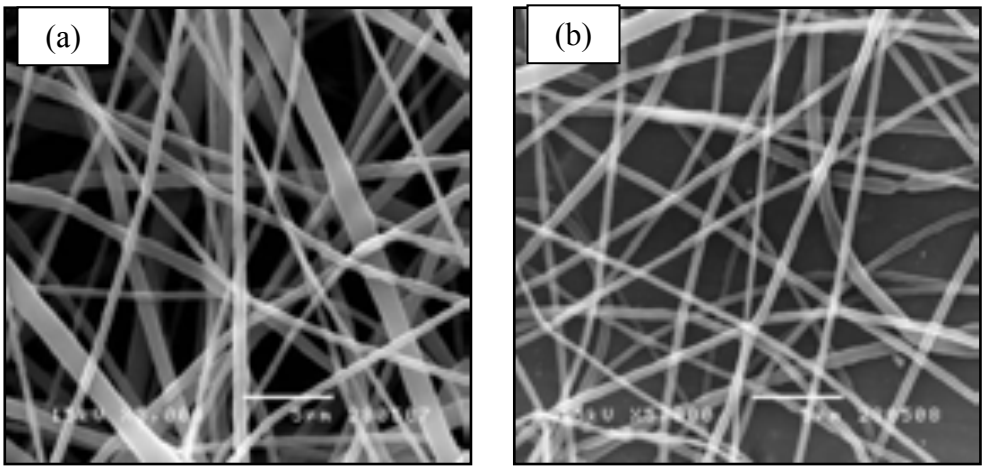

Figure 4.8 Morphology of PCL electrospun fiber mats with varied collecting distance from 10 to 20 cm. At fixed voltage 15 wt%, collecting distance 10 cm and flow rate 0.1 ml/h.

The last parameter effect for investigated is collecting distance. Figure 4.8 showed the effect of collecting distance on the fiber size. It observed the difference in distance is affected on fiber sizes. The enlargement of distance in a constant of flow rate and electric field. It was observed that, the fact that the volume charge density decreases as the distance increases. That results in a decrease the electric field strength and increased in solvent evaporation rate. It was found the fiber diameters decreased as the gap between the needle and collector was increasing. The distance between the needle and collector results was

longer pass time for the charged fluid jet ejected from the needle. Therefore the distance increases induced the fibers tend to become more elongated and slightly smaller in diameter from 0.57±0.22 μm to 0.58±0.18 μm (figure 4.8).

From the experiment, we found that the solution concentration was the most dominant parameter on PCL electrospun fiber size. It can be seen obviously that the fiber size increase when the concentration increased. In the next part of the experiment, we studied the effect of fiber size on the cellular behavior by the preparation of fibers with different sizes at different concentrations.

4.2 3D-structure fabrication by dual-polarity co-electrospinning process

In this part, an achievement was made to fabricate a 3D-structure of polycaprolactone (PCL) electrospun through the electrospinning process which is usually produced the fiber mat (2D) using this simple electrospining process and also study the ingrowth of cell that growing through the gap between the 3D nano-fibers structure or mats.

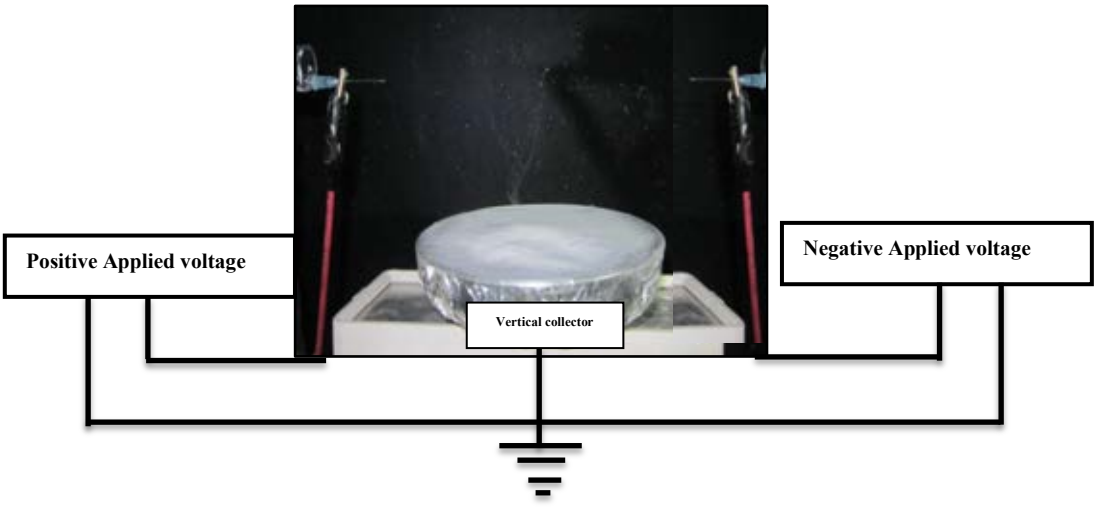

Figure 4.9 Dual-polarity co-electrospinning process set up.

The goal of this part was to fabricate the 3D nano-fibers scaffold in dual-polarity co-electrospinning process. The eletrospining process was applied and set up using the negative high voltage, positive high voltage, vertical collector to collect the sponge-liked electrospun and spinneret addition to installing in traditional electrospinning process. The effected of processing parameters on morphology and porosity of the obtained fiber mat were investigated.

In the experiment, PCL 3D-structure was produced from dissolved in DCM:DMF (1:1) mixed solvent at concentration 15, 20, and 30 wt%. Table 4.2 listed all experimental conditions carried out in this part of the research. Since for most conditions, the as spun fiber mats were in the form of regular non woven fiber mat typically obtained from a normal electrospinning process, the discussion part here would emphasis only on the experimental condition that produced 3D structure.

It was found that the forming a three-dimensional structure of PCL electrospun fiber at concentration 15, 20 and 30 wt%. It was done at the specific conditions of the positive voltage at10 kV with the flow rate of 1.0 ml/h and negative voltage at 10 kV with the flow rate 1.0 or 2.0 ml/h.

Table 4.2 Data of initial trial experimental of preparation of 3D structure via dual-polarity co-electrospinning process

Positive		**Negative**		**Concentration (wt%)**		
V (kV)	**F(ml/h)**	**V (kV)**	**F(ml/h)**	**15**	**20**	**30**
10	0.1	10	0.1	2D Structure	2D Structure	No fiber formation
			0.5	2D Structure	2D Structure	No fiber formation
			1.0	2D Structure	2D Structure	No fiber formation
			2.0	2D Structure	2D Structure	No fiber formation
	0.5		0.1	2D Structure	2D Structure	No fiber formation
			0.5	2D Structure	2D Structure	No fiber formation
			1.0	2D Structure	2D Structure	No fiber formation
			2.0	2D Structure	2D Structure	No fiber formation
	1.0		0.5	2D Structure	2D Structure	No fiber formation
			1.0	2D Structure	2D Structure	No fiber formation
			2.0	*3D Structure*	*3D Structure*	*3D Structure*
			2.0	*3D Structure*	*3D Structure*	*3D Structure*
	2.0		0.1	2D Structure	2D Structure	No fiber formation
			0.5	2D Structure	2D Structure	No fiber formation
			1.0	2D Structure	2D Structure	2D Structure
			2.0	2D Structure	2D Structure	2D Structure
15	0.1	15	0.1	2D Structure	2D Structure	No fiber formation
			0.5	2D Structure	2D Structure	No fiber formation
			1.0	2D Structure	2D Structure	No fiber formation
			2.0	2D Structure	2D Structure	No fiber formation
	0.5		0.1	2D Structure	2D Structure	No fiber formation
			0.5	2D Structure	2D Structure	No fiber formation
			1.0	2D Structure	2D Structure	No fiber formation
			2.0	2D Structure	2D Structure	No fiber formation
	1.0		0.5	2D Structure	2D Structure	No fiber formation
			1.0	2D Structure	2D Structure	No fiber formation
			2.0	2D Structure	2D Structure	No fiber formation
			2.0	2D Structure	2D Structure	No fiber formation
	2.0		0.1	2D Structure	2D Structure	No fiber formation
			0.5	2D Structure	2D Structure	No fiber formation
			1.0	2D Structure	2D Structure	2D Structure
			2.0	2D Structure	2D Structure	2D Structure

Table 4.2 (cons) Data of initial trial experimental of preparation of 3D structure via dual-polarity co-electrospinning process

Positive		Negative		Concentration (wt%)		
V (kV)	**F(ml/h)**	**V (kV)**	**F(ml/h)**	**15**	**20**	**30**
20	0.1	20	0.1	2D Structure	2D Structure	No fiber formation
			0.5	2D Structure	2D Structure	No fiber formation
			1.0	2D Structure	2D Structure	No fiber formation
			2.0	2D Structure	2D Structure	No fiber formation
	0.5		0.1	2D Structure	2D Structure	No fiber formation
			0.5	2D Structure	2D Structure	No fiber formation
			1.0	2D Structure	2D Structure	No fiber formation
			2.0	2D Structure	2D Structure	No fiber formation
	1.0		0.5	2D Structure	2D Structure	No fiber formation
			1.0	2D Structure	2D Structure	No fiber formation
			2.0	2D Structure	2D Structure	2D Structure
			2.0	2D Structure	2D Structure	2D Structure
	2.0		0.1	2D Structure	2D Structure	No fiber formation
			0.5	2D Structure	2D Structure	No fiber formation
			1.0	2D Structure	2D Structure	2D Structure
			2.0	2D Structure	2D Structure	2D Structure
25	0.1	25	0.1	2D Structure	2D Structure	No fiber formation
			0.5	2D Structure	2D Structure	No fiber formation
			1.0	2D Structure	2D Structure	No fiber formation
			2.0	2D Structure	2D Structure	No fiber formation
	0.5		0.1	2D Structure	2D Structure	No fiber formation
			0.5	2D Structure	2D Structure	No fiber formation
			1.0	2D Structure	2D Structure	No fiber formation
			2.0	2D Structure	2D Structure	No fiber formation
	1.0		0.5	2D Structure	2D Structure	No fiber formation
			1.0	2D Structure	2D Structure	No fiber formation
			2.0	2D Structure	2D Structure	No fiber formation
			2.0	2D Structure	2D Structure	No fiber formation
	2.0		0.1	2D Structure	2D Structure	No fiber formation
			0.5	2D Structure	2D Structure	No fiber formation
			1.0	2D Structure	2D Structure	2D Structure
			2.0	2D Structure	2D Structure	2D Structure

4.2.1 Observations

In this experiment, the fiber formation in this process was followed using digital video camera recording at 30 frames per second. Due to experiment set up limitation, the recording has been done with off angle (camera setup) at low speed recording, which would affected our analysis in the part. Nonetheless, the obsearvation and estimation of fiber collecting speed made hear would still be relavent and useful for future work.

From this system, we obsearved the bending instability on a polymer jet of 20 % PCL in DCM:DMF (32 frame/second) via dual-polarity co-electrospinning process, figure 4.10 showed 30 successive images of a region that includes most of the straight segment, the onset of the bending instability and the region small closed loops were observed. The onset of the bending instability is shown in the first 10 frames. The exposure time for each frame was 0.3125 s. Various parts of the jet moved downward at slightly different velocities near 0.230 m/s. calculated by linear velocity (v) formulation as follow ;

$$\mathrm{v} = \frac{\Delta s}{\Delta t} \qquad (4.1)$$

The straight segment, by frame 1, the path reached the dimensions and the level of complexity that was typical of this region. The several fiber loops in the middle of the both sides meet in the center caused the fibers gradually settled down as the fiber overlap. The centers of many of the loops were displaced radially from the center point onto the vertical collector. As the collector spun around radially, the aggromolation loops falled downward and collected mostly in the center region of the collector. If segments of these agglomerate

loop were not fully elongate, then the loops would remained interact and acted as scaffold which pretuded from the floor upward and raised up next fiber layer. After numerous fiber collecting cycle, the fiber formed into 3D-structure.

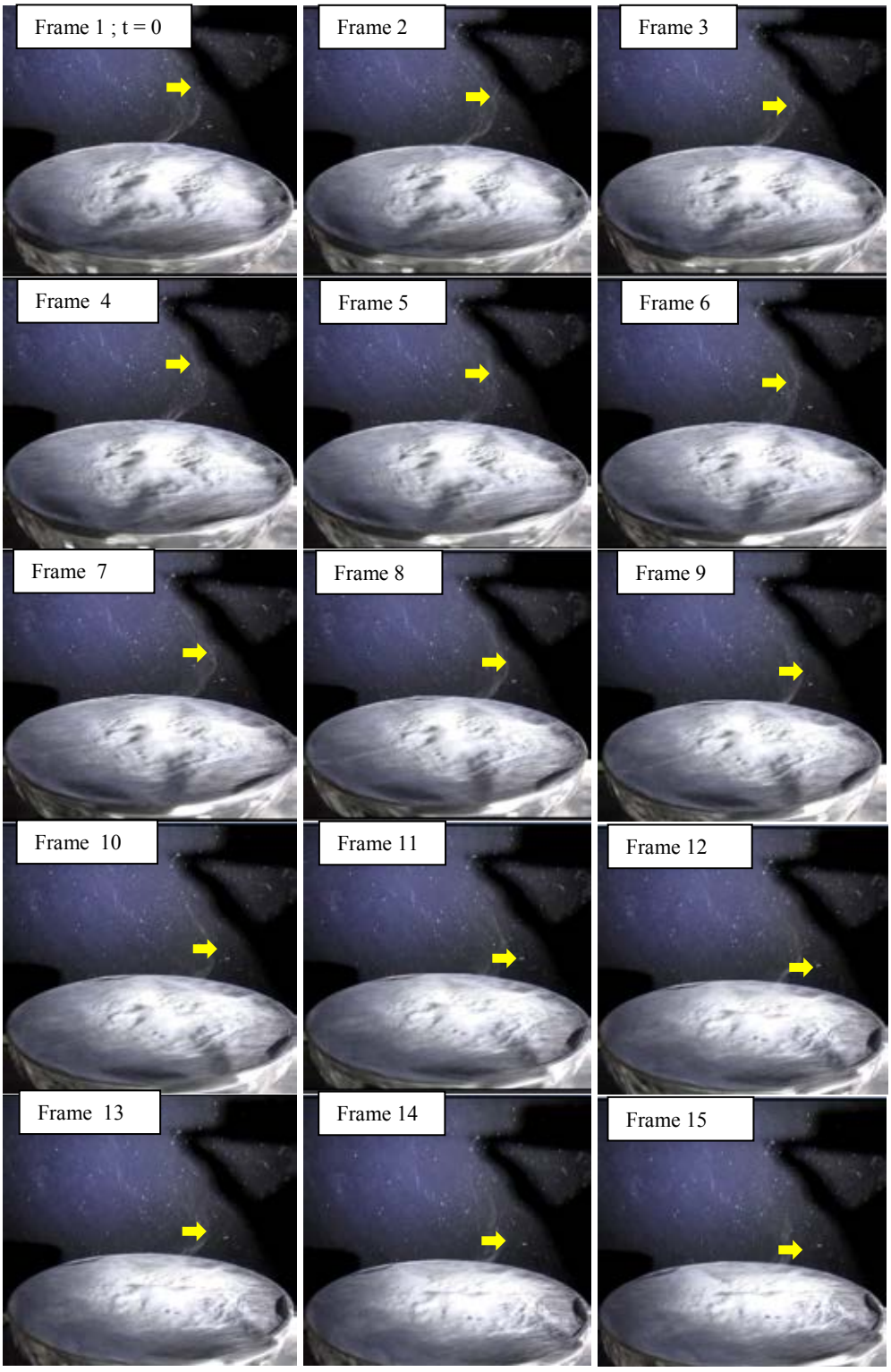

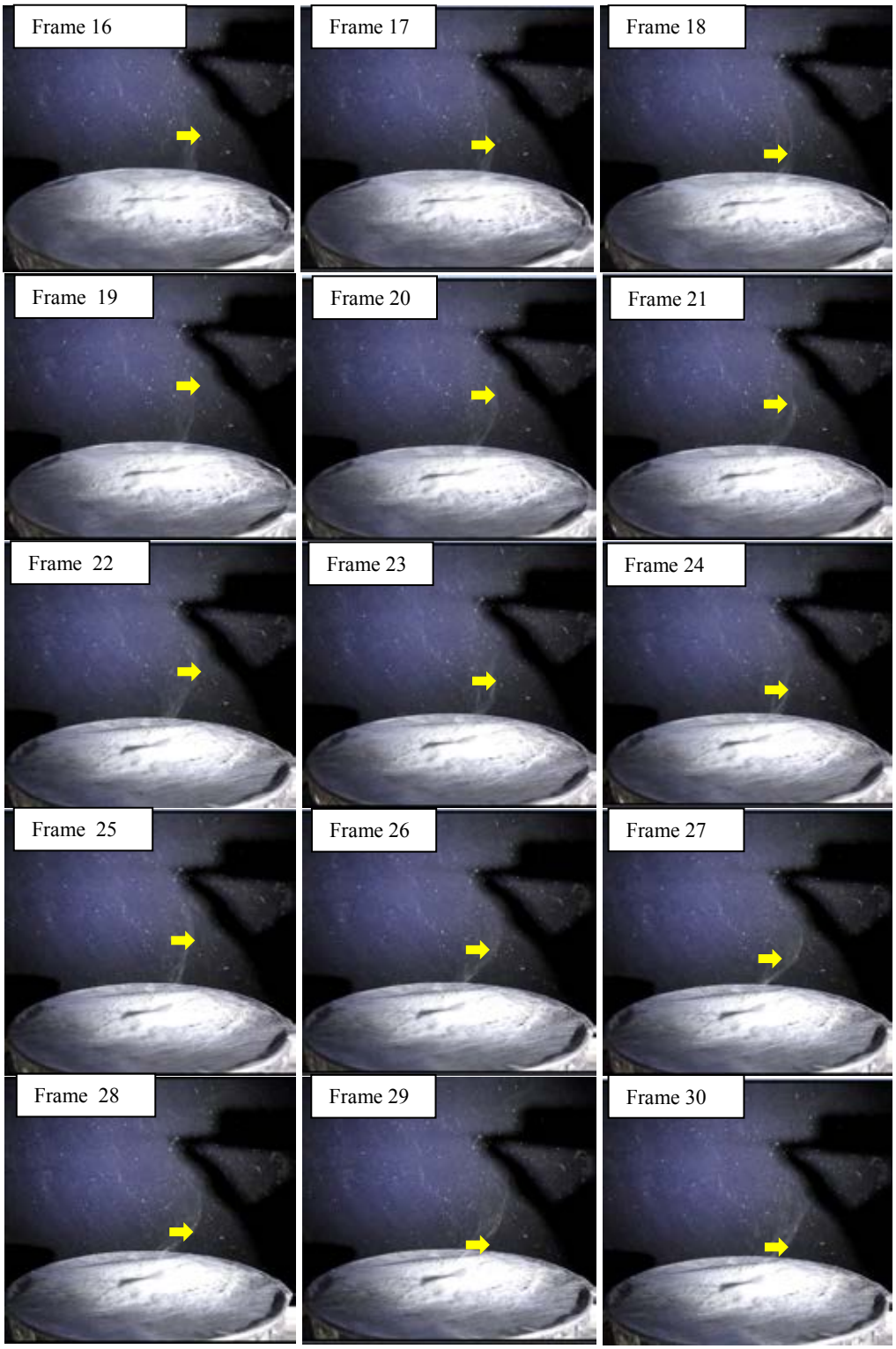

Figure 4.10. Frame to frame images that show the bending instability on a jet of 20 % PCL in DCM:DMF (32 frame/second) via dual-polarity co-electrospinning process.

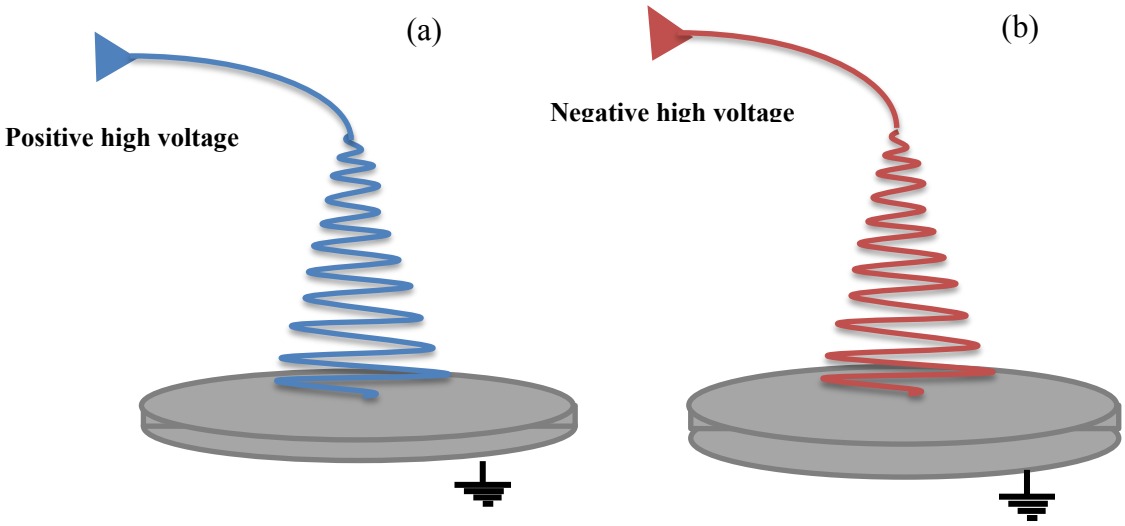

Figure 4.11 (a), (b) Conventional positive and negative electrospinning process

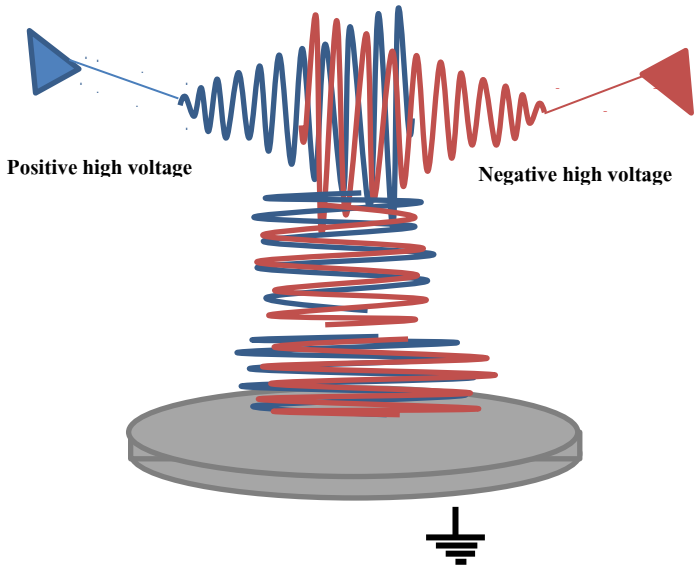

Figure 4.12 3D-structure via dual-polarity co-electrospinning process

4.2.2 Formation of merged contacts

The merged contacts were established when the segment of the fiber agglomolation contact to contact with another segment.By comparison, in conventional electrospinning process (from figure 4.11 (a)), when applied the positive high voltage the positive polymer nanofibers are formed by the creation and elongation of a positive electrified fluid jet. The path of the jet is from a fluid surface that is often, but not necessarily constrained by an orifice, through a straight segment of a tapering cone, then through a series of successively smaller electrically driven bending coils, with each bending coil having turns of increasing radius, and finally solidifying into a continuous positive thin fiber. Likewise, in the case of applied the negative high voltage, it would be a continuous negative fiber. In the present study, this technique allowed the formation of nanofibers into the 3D-structure via combinding of positive electrospun fiber and negative electrospun fiber and floated in the air before the fibers were collected on the vertical collector. Using the charge neutralization strategy, and hence, employing positive applied voltage and negative applied voltage simultaneously. As can be seen in figure 4.10 , showed snap shot of 3D formation between processing. Each electric field line between the positive charged and the negative charged is continuous (figure 4.12).

This contacting and merging together of the fiber agglomolation segments created a three-dimensional structure. In 2006, D.K Reneker et. al reported the formation of 3D garland fibers. However, they did not report that these garland fibers could form a 3D structure in a macro scale as we observed here.

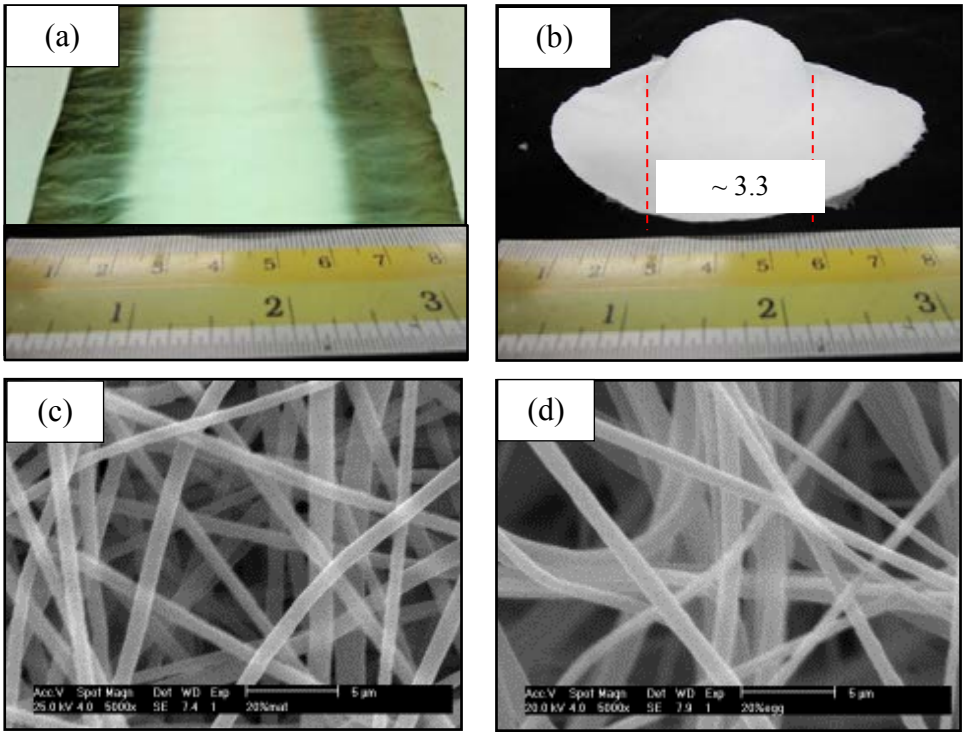

Figure 4.13 Digital photographs of (a) electrospun mats from electrospinning at 20 wt% 2D-structure , (b) 20 wt% 3D-structure from novel technique, and SEM micrographs (c) 20 wt% 2D-structure, and (d) 20wt% 3D-structure .

Table 4.3. Characteristics of electrospun mats from electrospinning (2D) at 20wt% PCL concentration, 20% 3D-structure .

Samples	Fiber diameter (nm)	%Porosity
20wt% (2D)	961 ± 263	77.1 ± 1.2
20 wt% (3D)	1637 ± 77	93.4 ± 0.8

The digital photographs from the visual obsearvation the thickness of as spun 2D and 3D mats were shown in figure 4.13 (a, b). 2D mats was less than 100 μm, while that of

3D-structure were much higher in the range of centimeters that were shown in figure 4.14 (a) and (b), respectively. Qualitatively, it was clearly observed that nanofibers which were fabricated by electrospinning showed a much more dense structure with lesser porosity compared to those fabricated by dual-polarity co-electrospinning process. Hence, from table 4.2, it could be explained that the 3D scaffold could be prepared using this new technique with giving low density light scaffold and a higher porosity about 93.4 ± 0.8% when compare with conventional structure giving a porosity about 77.1 ± 1.2%.

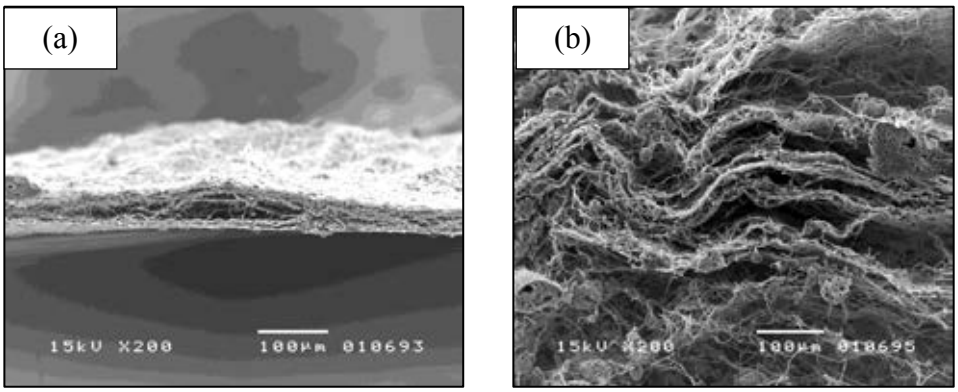

Figure 4.14. SEM micrographs (cross section) of (a) 20 wt% 2D-structure, and (b) 20wt% 3D-structure using difference technique condition.

From figure 4.14 (a,b) showed SEM micrographs (cross section) of (a) 20 wt% 2D-structure, and (b) 20wt% 3D-structure using difference technique condition. However, fiber in the image appeared to be deformed and compressed from sample preparation.

4.2.3 Effect of concentration on morphology

The structure of scaffolds and fibers prepared from PCL solution with concentration of 10, 20 and 30 wt% were most stable using these two conditions; -10 (negative 10 kV), 2.0 ml/h and +10 (positive 10 kV), 2.0 ml/h. The samples of 3D-structure

were shown in figure 4.13 (a) with figure 4.13 (b), (c) and (d) showed the 3D scaffold of solution concentrate 15, 20 and 30wt%, respectively, with flow rate of 2.0 ml/h both negative and positive charge of 10 kV by novel dual-polarity co-electrospinning process.

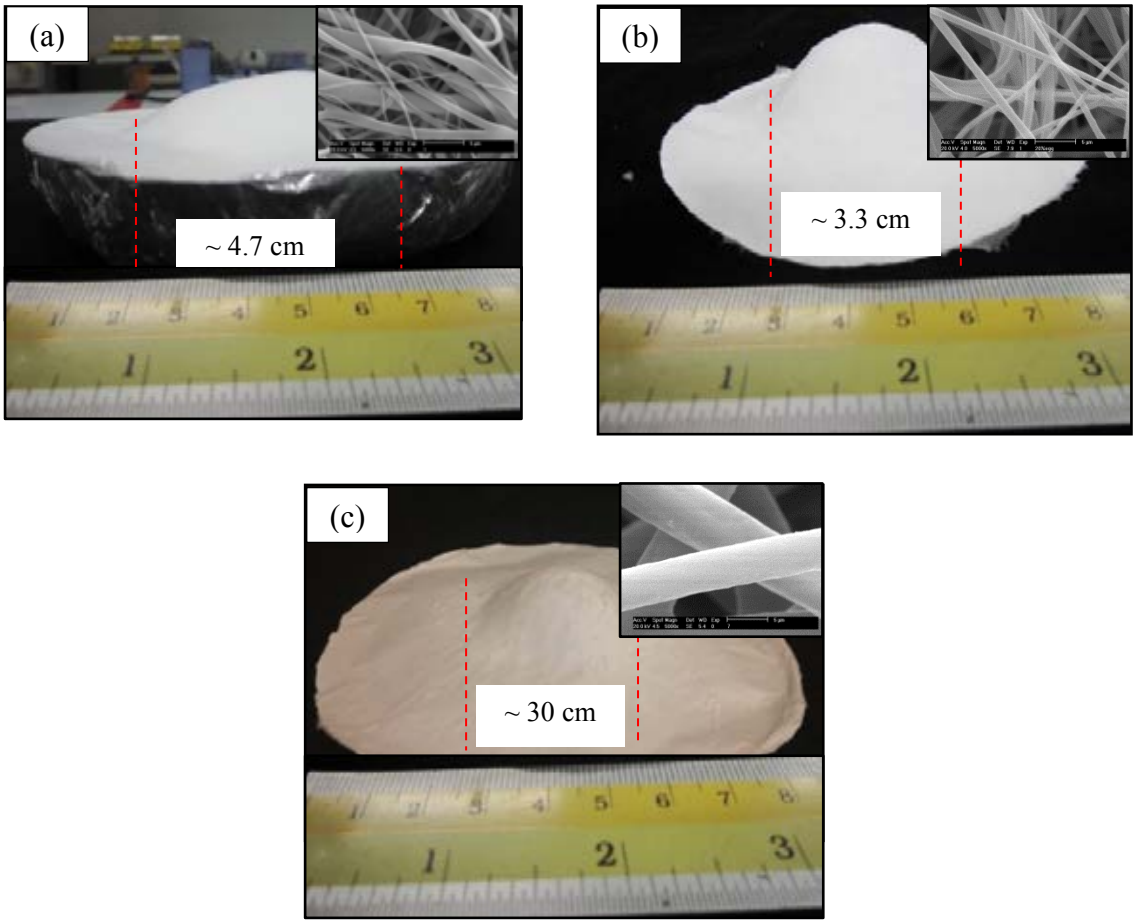

Figure 4.15 Digital photographs and SEM micrographs of (a)15% 3D-structure, (b) 20% 3D-structure, and (c) 30% 3D-structure using difference technique condition

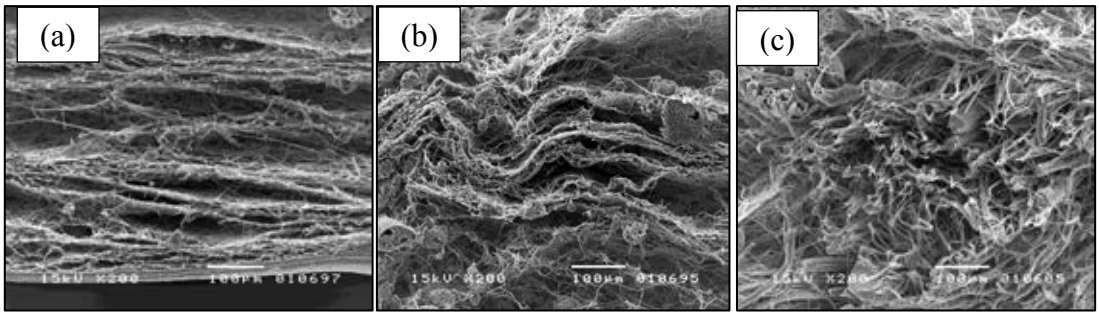

Figure 4.16 SEM micrographs (cross section) of (a)15% 3D-structure, (b) 20% 3D-structure, and (c) 30% 3D-structure using difference technique condition

Table 4.3 Characteristics of electrospun mats from electrospinning (2D) at 20wt% PCL concentration, 15%, 20%, and 30% 3D-structure .

Samples	Fiber diameter (nm)	%Porosity
20wt% Mats(2D)	961 ± 263	77.1 ± 1.2
15% (3D)	758 ± 187	96.8 ± 0.3
20% (3D)	1637 ± 77	93.4 ± 0.8
30% (3D)	6225 ± 136	95.5 ± 0.2

From figure 4.15, 4.16 and table 4.3, it was found that as solution concentration increased, the size of 3D-structure segment in fiber mats decreased, while the fiber size in the structure increased dramatically. This was because the higher concentration of PCL solution had higher viscosity.

4.2.4 Effect of flow rate on morphology

In this section, The structure of scaffolds and fibers at concentration 20 wt% not be seen the 3D structure when these various conditions (flow rate); -10kv (negative), and +10 kv (positive), 0.1, 0.5, 1.0 ml/h. The samples were shown in Figure 4.17.

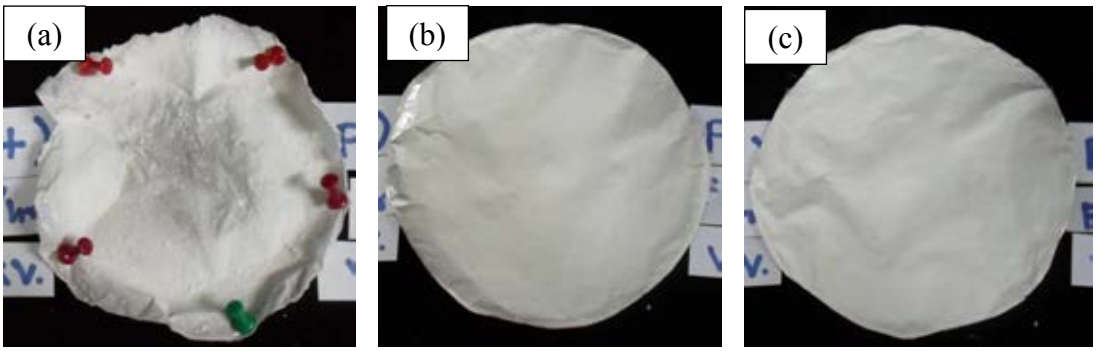

Figure 4.17 Digital photographs of 20wt% PCL concentration at ± 10 kV and flow rate (a) 0.1, (b) 0.5, and (c) 1.0 ml/h using dual-polarity co-electrospinning process.

As a figure 4.17, the mats could not be produced using this study due to when the flow rate increased then the polymer trend to form at high flow rate. Thus it was found low flow rate gave 2D mats scaffold form.

4.2.5 Effect of applied voltage on morphology

In this section, the structure of scaffolds and fibers at concentration 20 wt% could not be seen the 3D structure when these various applied voltage: 15, 20 and 25 kV (negative kV), and (positive kV), respectively. The samples were shown in Figure 4.18 (a)-(c).

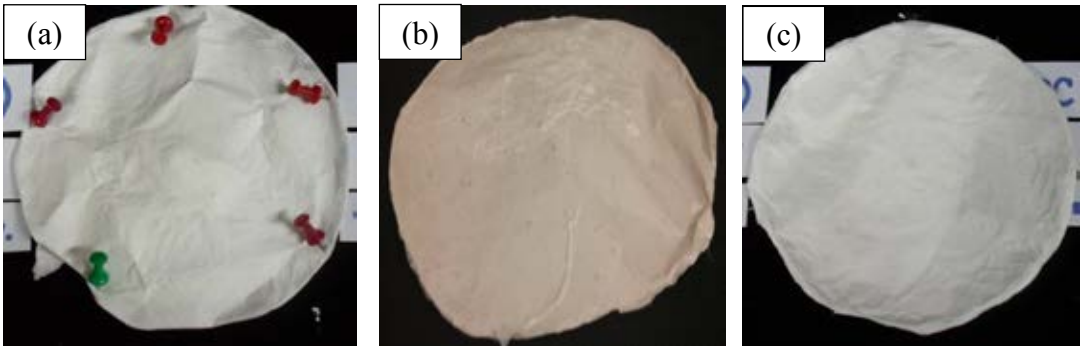

Figure 4.18 Digital photographs of 20wt% PCL concentration at flow rate 2.0 ml/h and applied voltage (a) ±15 kV, (b) ±20 kV, and (c) ±25 kV using dual-polarity co-electrospinning process.

From figure 4.18 showed digital photographs of 20wt% PCL concentration at flow rate 2.0 ml/h and applied voltage (a) ±15 kV, (b) ±20 kV, and (c) ±25 kV using dual-polarity co-electrospinning process. It could not be seen the 3D-structure of these systems. No 3D-structure was formed from these system.

4.2.6 Effect of the sample collecting position on 3D-structure morphology

For our studied, those three conditions as shown in figure 4.13 from previous part were produced a 3D-structure by were also studied the morphology which was collected from a different position as shown in figure 4.19 showed the position C is the first gathering point of fiber from both side (usually collect). Position D was about 5 cm. below position C. The photographs of both positions were shown in figure 4.19.

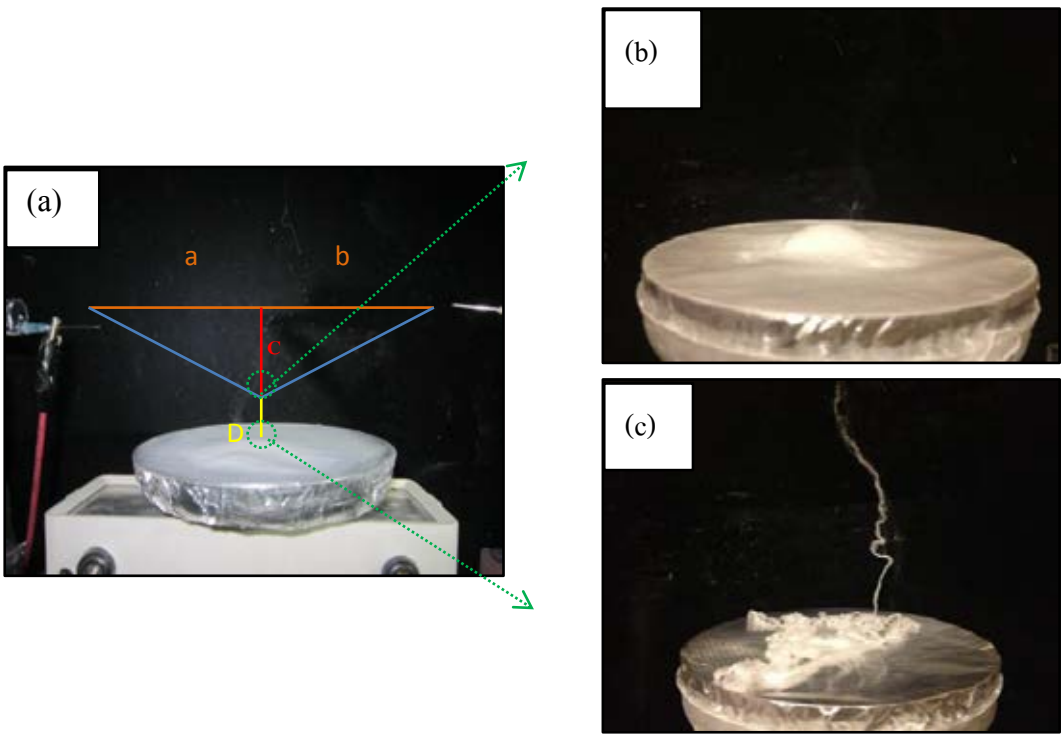

Figure 4.19 Illustration of the collection position (a) position C. and (b) position D. of electrospunfiber

As figure 4.20 showed the digital photographs of 3D-structure at two different morphology i.e. 3D-structure (i), and fluffy yarn structure (ii)). The basic assumsion of the 3D structure from previous experiment, we studied the effect of collecting position on 3D-structure morphology. In addition to producing a 3D structure, when we increase the distance that can produce fibers with different structures.

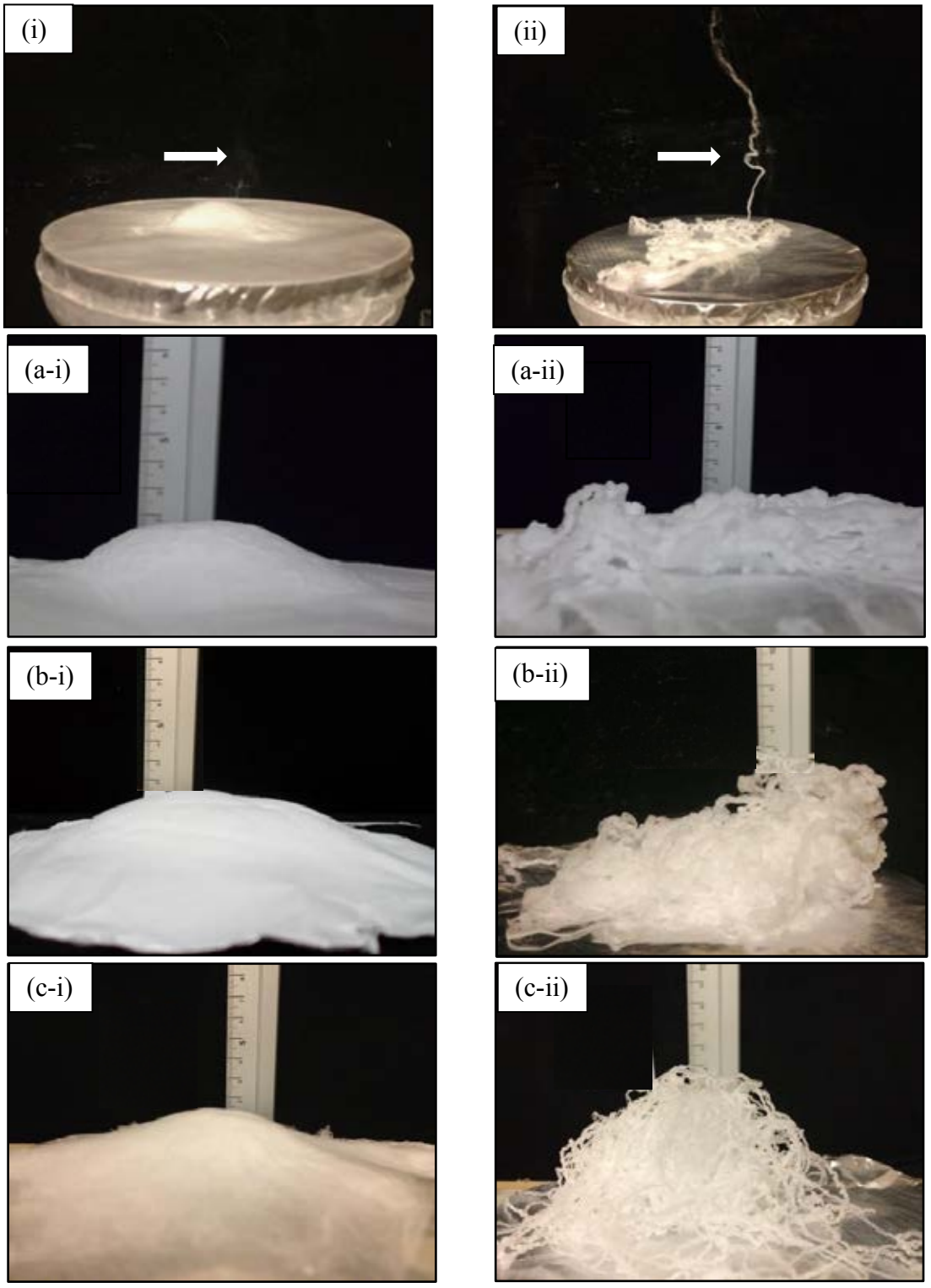

Figure 4.20 Photograph of PCL 3D structure at difference distance (i) distance C, (ii) D, (a-i,ii) 15%-3D, and fluffy, (b-i,ii)) 20%- 3D, and fluffy, and (c-i,ii)) 30%-3D, and fluffy.

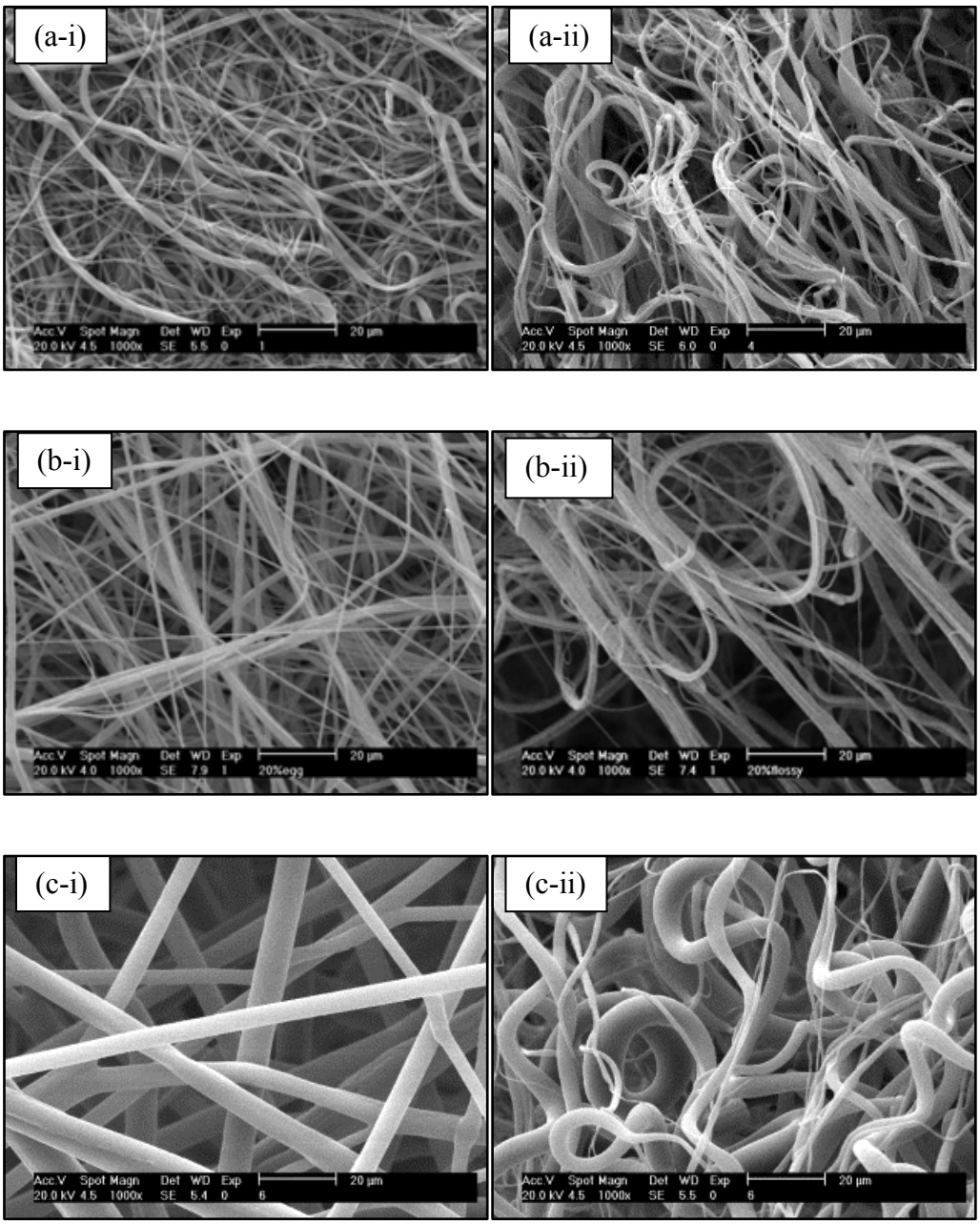

Figure 4.21 SEM micrograph of (a-i,ii) 15%-3D-structure, and fluffy structure, (b-i,ii)) 20%-3D-structure, and fluffy structure, and (c-i,ii)) 30%-3D-structure, and fluffy structure.

Table 4.4 Characteristics of 3D-structure.

Samples	Fiber diameter (nm)	%Porosity
15%-3D-structure	758 ± 187	96.8±0.3
15%-fluffy structure	964 ± 205	98.1±0.4
20%-3D-structure	1637 ± 77	93.4±0.8
20%-fluffy structure	1434 ± 72	97.7±0.7
30%-3D-structure	6225 ± 136	95.5±0.2
30%-fluffy structure	5128 ± 93	97.5±0.4

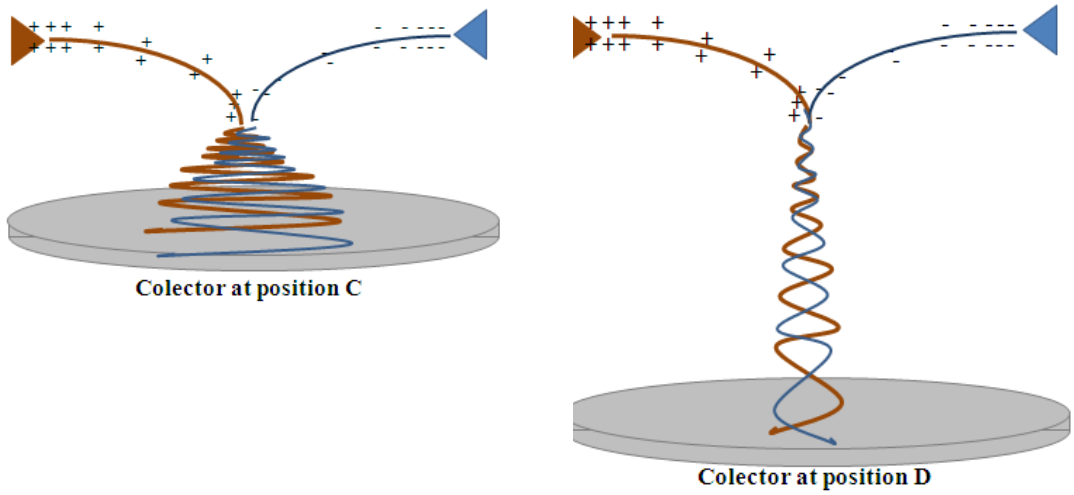

(a) (b)

Figure 4.22 Model of 3D structure from dual-polarity co-electrospinning process

Figure 4.22 showed the model of 3D structure from dual-polarity co-electrospinning process. The SEM image as shown in figure 4.21. It could be seen that the morphology was

obviously difference hence the scaffold may selected depends on the application which need in 3D-structure and fluffy structure. Currently, exact mechanism of how these structure were formed was still unknown. However, our best explanation on how they were formed as followed. From figure 4.20 (a-i), (b-i) and (c-i) , at position C when this loop segment collected on the vertical collector. It formed the proturbed growth up in the space above the flat layer of previously collected fibers. The protuberance would stack up, leave on opening void beneath itself, and hence, act as the building scaffold for the next step as can be seen model from figure 4.22 (a). In the case of fiber collecting at the D position (figure 4.20 (a-ii, b-ii, and c-ii), the mechanism of fiber formation would be similar to fiber collected at C position, except that increasing distance of fiber collection gave more space and time for the fiber remained in the bending instability state to stretch and fully pulled into the spinal loop before collecting on the vertical collector, as depicted in figure 4.2 (b). After several cycles of these occurance. At the end, fiber gain more volume and form into fluffy yarn.

The results also showed that while 3D-structure and fluffy yarn were different in global structure, their porosity were in the same range about 96.8% and 98.1% at 15%wt PCL, 93.4% and 97.7% at 20%wt, and 95.5% and 97.5% at 30%wt, respectively.

4.3 The morphology of polycaprolactone electrospun fiber size on L929 cellular behavior

In this section composed of two part, the first, we studied the effect of diferent PCL electrospun fiber size on L929 cell behavior. And the second, we studied the effect of morphology on L929 cell behavior also.

From the experiment above, PCL solutions at various concentrations 15, 20, and 30wt% were prepared by dissolving appropriate amount of PCL in a mixed-solvent of dichloromethane: dimethylformamide (1:1). PCL solutions were electrospun into fibers under applied voltage 15 kV, a constant solution flow rate of 1.0 ml/h and a 20 cm distance between the syringe tip and rotating fiber collector.

4.3.1 Morphology and appearance of electrospun fiber mat

The porosities of PCL-A, PCL-B, and PCL-C electrospun nanofibrous mats were determined by density measurement. Porosity of 73.2%, 77.1%, and 65.5% for PCL-A, PCL-B, and PCL-C electrospun nanofibrous mats were summarized in table 4.3. It showed that the scaffolds were highly porous structure due to the formation of very fine fibers imparting large surface area.

From figure 4.23 (i-iii) showed SEM micrographs of electrospun fibers morphology of the fibers diameter in range of 146±42 nm to 4.6±0.5 μm were prepared by PCL 15wt%, 20wt% and 30wt% concentration. We called them PCL-A, PCL-B and PCL-C, respectively**.** Using image analysis software for measuring 50 randomly selected fibers, average value of fiber diameter as well as fiber diameters distributions was determined and presented in table 4.3 and figure 4.24, showing a normal distribution with average and values of 440 ± 78.65 nm, 961 ± 263.27nm, and 4.6 ± 0.5 μm, respectively.

Interior morphology, as seen in 4.22 (i-iii) contains a network of interconnected pores with a pattern. The porosity developed into the structure during electrospinning could

be the best described about degradation period of mats [66]. Figure 4.24 (i-iii) showed the thickness of electrospun mats 1.27, 1.85, and 1.42 mm., respectively.

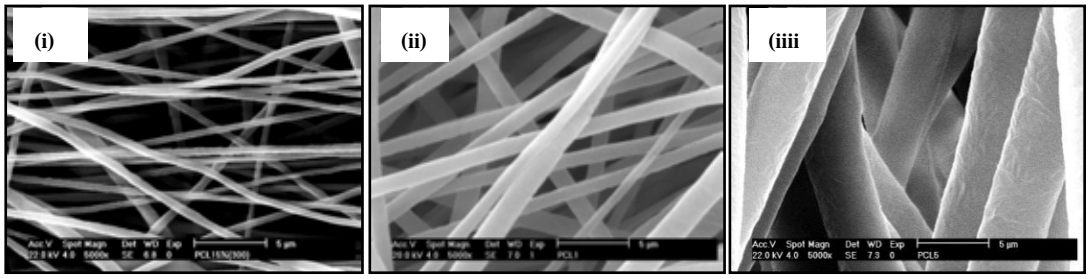

Figure 4.23 SEM micrographs of electrospun fibers morphology using different PCL fiber sizes (i) 440±78.65 nm (PCL-A), (ii)961±263.27 nm (PCL-B) (iii) and 4.6±0.5 µm (PCL-C), respectively at V=15 kV and flow rate =1.0.

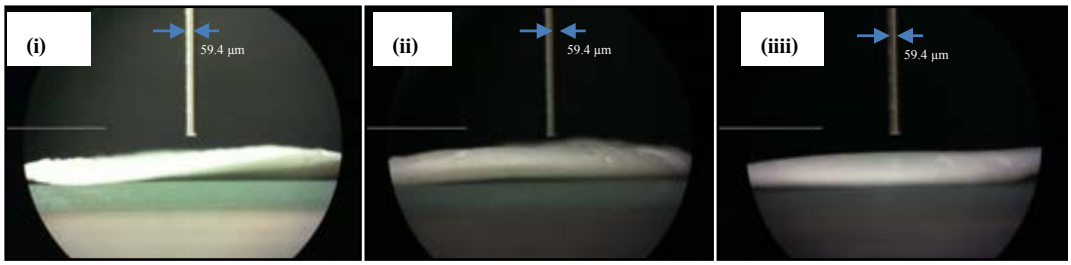

Figure 4.24 Photographs of (i) PCL-A, (ii) PCL-B, and (iii) PCL-C thickness, respectively.

Table 4.5 Characteristics of PCL-A, PCL-B, and PCL-C electrospun nanofibrous mats.

Samples	Fiber diameter (nm)	Thickness (mm)	%Porosity
PCL-A	440 ± 78.65	1.27 ± 0.18	73.2 ± 3.4
PCL-B	961 ± 263.27	1.85 ± 0.24	77.1 ± 1.2
PCL-C	4.6 ± 0.5 µm	1.42 ± 0.13	65.5 ± 5.3

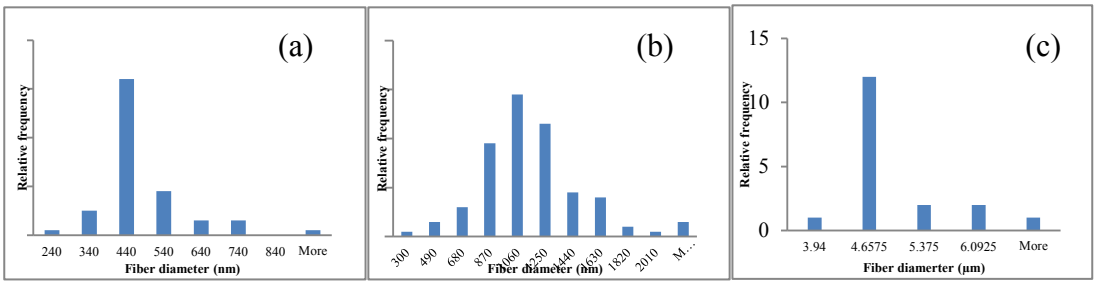

Figure 4.25 (a)-(c) Diameter distribution of fibers electrospun from 15 wt%, 20 wt.%, and 30 wt% in DCM/DMF solvent

4.3.3 Cell viability by MTT assays on polycaprolactoneelectrospun fiber size

As above experiments, we studied the effect of varying fiber size for investigated the effect of fiber size on cell attachment and proliferation, fibers with three different size of PCL-A (440 ± 78.65 nm), PCL-B (961 ± 263.27nm) and PCL-C(4.6 ± 0.5 µm) were used as culture scaffold for L929 mouse fibroblast cell. The treated tissue culture plate was used as a control in the experiment. Cell adhesion and proliferation were assessed by MTT assays.

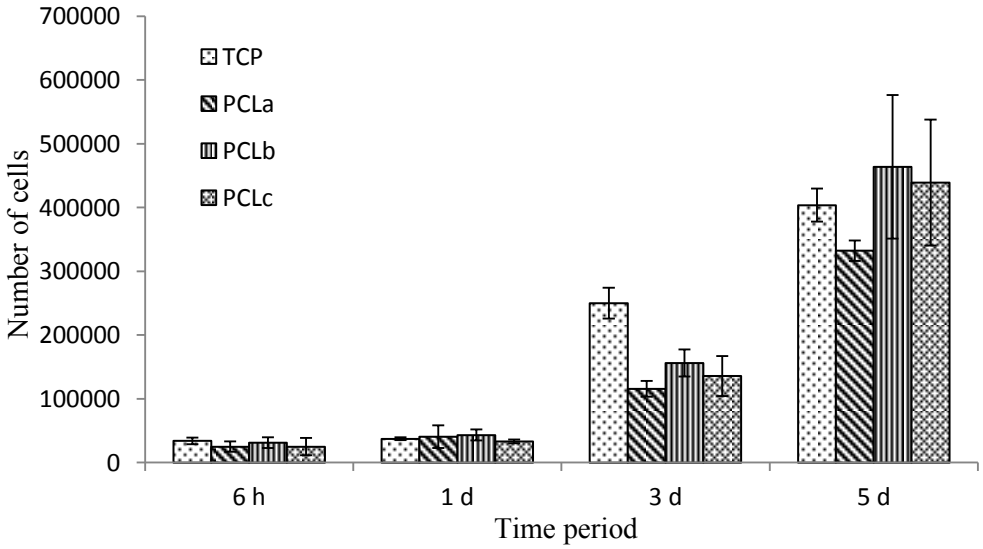

*Significant difference relative to TCP (tissue culture plate) control at $p < 0.05$

Figure 4.26 In vitro attachment and proliferation of L929 on various PCL fiber mats

Figure 4.26 shows the number of cells after 6 hr, 1, 3, and 5 days culture period. The cell number after 6 hr incubation time indicated that PCL fiber size appeared to have no effect on initial cell adhesion. The cell number after 24 hr incubation also supported that result as the cell number for each sample, including the control, showed no significant difference. However, after 5 days, the results indicated that cell proliferation in PCL-B and PCL-C fibers, were higher that of PCL-A considerably. For all incubation period, no significant difference in term of cell number was observed between PCL-B and PCL-C, despite the fact that fiber size of PCL-C was much bigger than that of PCL-B. In spite of that similarity between PCL-B and PCL-C, SEM micrographs of PCL fibers after each incubation period revealed drastic different of cell matrix-interaction for PCL-B and PCL-C, as shown in figure 4.27.

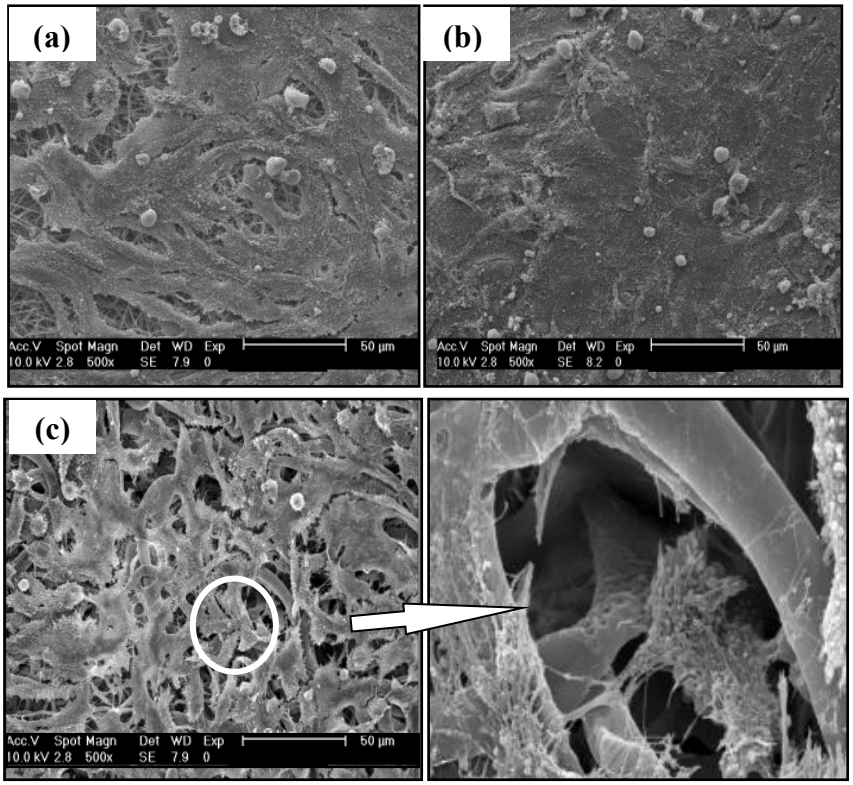

Figure. 4.27. SEM micrographs of attachment and proliferation of L929 mouse fibroblasts on PCL fiber mats at 5 days ; (a) PCL-A, (b) PCL-B, and (c) PCL-C

For PCL-A and, to a lesser extent, PCL-B, the cells appeared to spread out over the entire surface of the fiber mat after 5 days, with no evidence of cell spreading or migrating inside fibrous structure for PCL-A. This could be because the pore size of PCL-A mats was smaller than the cell size, thus, preventing them from penetration or migration into the under layer of the scaffolds. PCL-B, with larger fiber size and widerfiber size distribution than PCL-A, could have limited number of pore with size large enough to allow cell penetration into under layer, as evidence by high cell number from figure 4.27. For PCL-C fiber mat, on the other hand, in addition to spreading over the top fiber layers, many cells appeared to wrap themselves around individual fibers and spreading along fiber axis. We observed some cells located deep inside fibrous structure, which could be due to the fact that pore size of these PCL-C mats was much larger than the size of the cell, and therefore could allowed the cell to penetrate or slip into under layer by mean of gravitational force during cell seeding or by other mechanism such as cellular migration during cell culture period. Similar observations were also reported by Soliman and Shalumon [11, 12]. Our result suggested that while a very fine electrospun fiber mat could offer a great cellular adhesion effect, it could restrict or entirely prohibit cellular migration into the scaffold. Bigger electrospun fiber mat, however, while possesses lower surface area, its bigger pore size could allow a better cellular migration or cellular distribution inside the scaffold compare to the very fine fibers. Therefore, the scaffold composed of electrospun fibers of various size could be a good candidate for tissue engineering scaffold application that requires a three dimensional structure.

4.3.3 Cell viability by MTT assays on 2D and 3D PCL electrospun

From previous experiments, macroscopic photographs from fabricated PCL 3D-structure compare with PCL electrospun mats structure (2D). The thickness of the mats

from novel electrospinning was about one millimeter. Qualitatively, figure 4.28 (b, c, and d) were clearly obvious that nanofibers fabricated by dual-polarity co-electrospinning showed a much less dense structure compared to conventional fabricated.

Hence, this study reported and discussed a results of cellular behavior on the 20%wt PCL mats structure, 20 wt% PCL 3D-structure and fluffy formation, and 30 wt% PCL 3D-structure and fluffy formation.

Samples	**Fiber diameter (nm)**	**%Porosity**
PCL20%Mats	1460 ± 78.65	92.1 ± 1.1
PCL20%-3D	1311 ± 345	97.9 ± 0.3
PCL20%-Fluffy	1596 ± 1223	98.0 ± 1.2
PCL30%-3D	1456 ± 720	98.4 ± 0.4

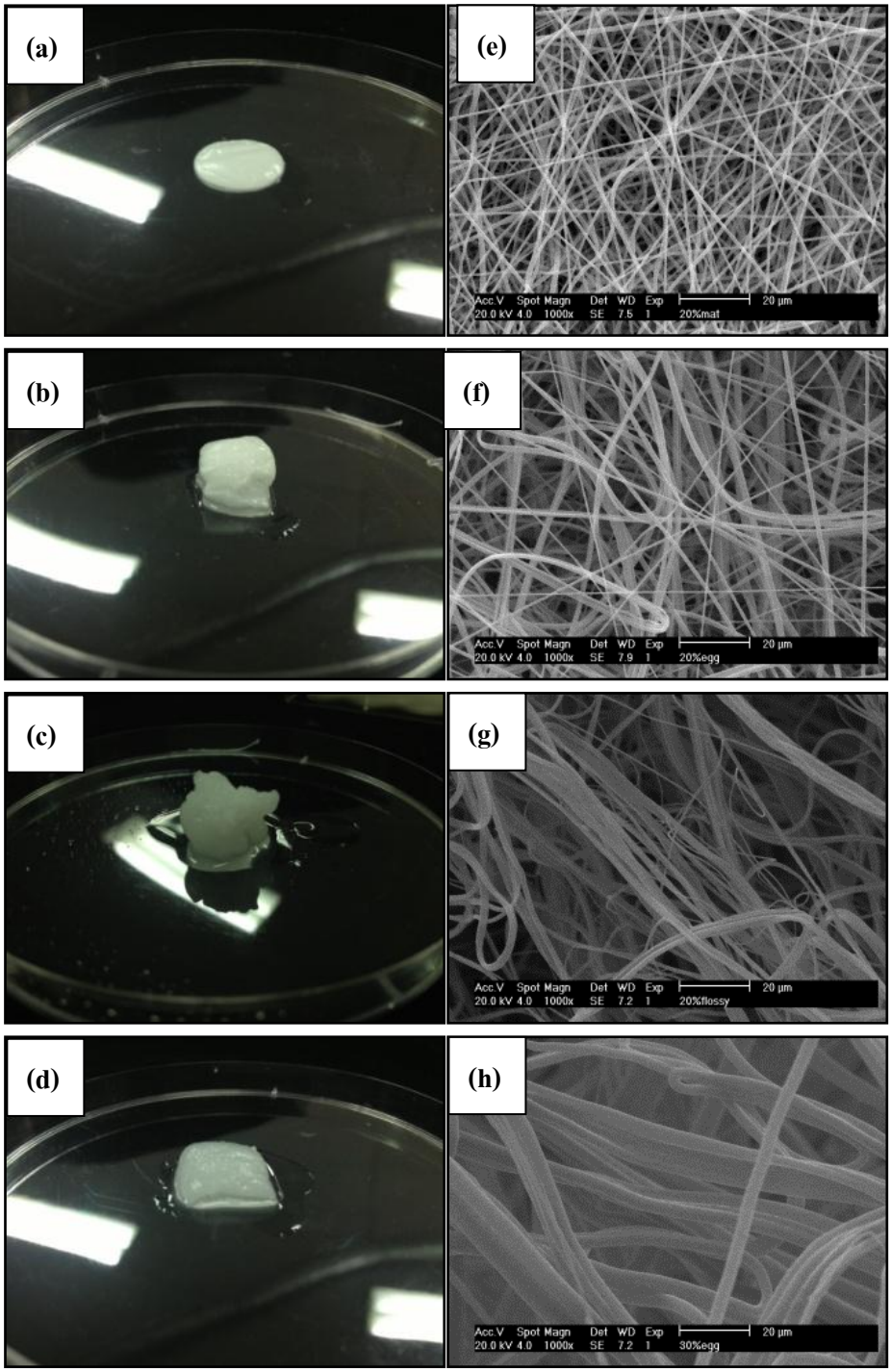

Figure 4.28 (a)-(d) morphology of sample, and (e)-(h) SEM of electrospun mats and 3D-structure, respectively.

PCL20%Mats PCL20%-3D PCL20%-Fluffy PCL30%-3D

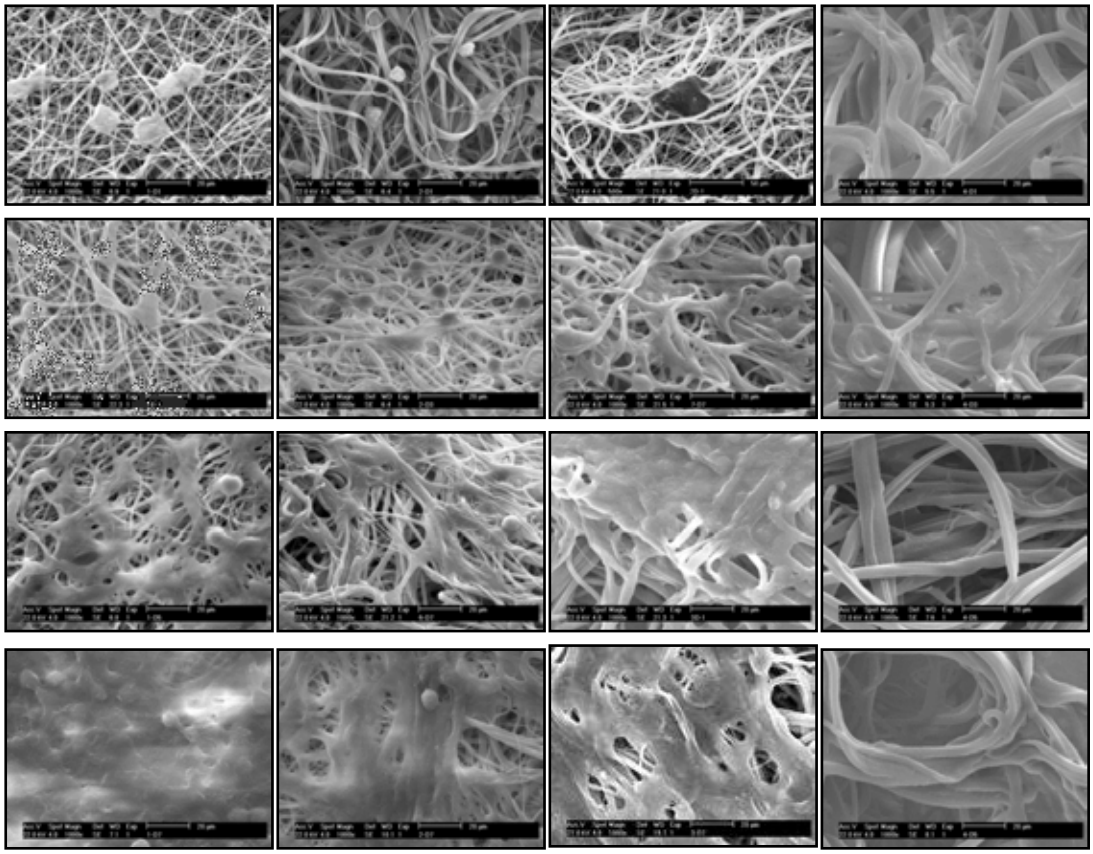

Figure 4.29 SEM photographs of cell behavior on sample (a) 20% mats - (d) 30% 3D-structure at culture period 1 day, 3 days, 5 days and 7 days .(1000x)

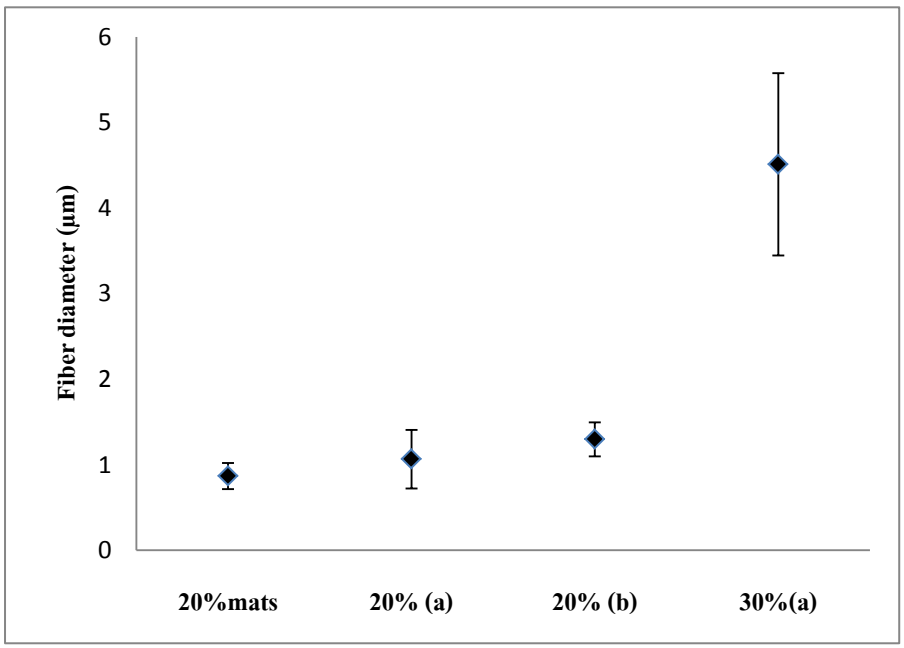

Figure 4.30 Fiber diameter of PCL electrospun fiber mat and 3D-structure

In this studied, we would evaluated and compared cell seeding capacity and cellular behavior (i.e. adhesion, proliferation and migration) of selected 3D-structures against a conventional electrospun fiber mat.

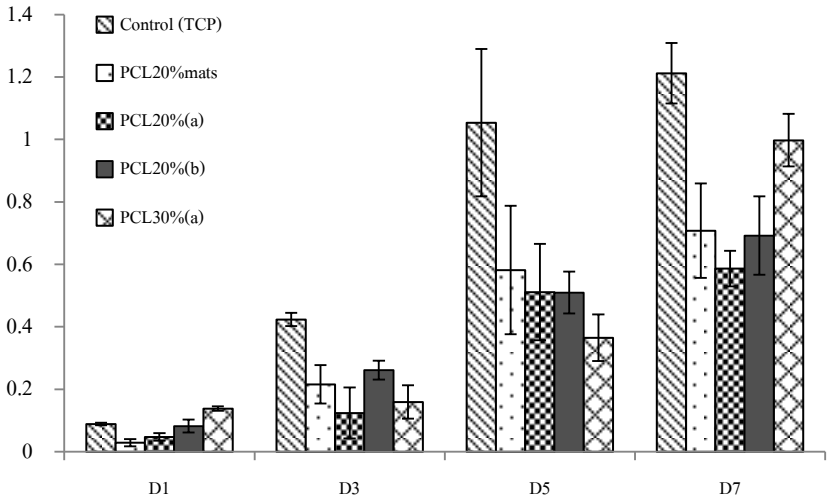

Figure 4.31 In vitro attachment and proliferation of L929 on sample (a) 20% mats - (d) 30% 3D-structure at culture period 1 day, 3 days, 5 days and 7 days .

MTT assay was performed to evaluate the viability of L929 mouse fibroblast cells in the 2D and 3D structure of PCL[[PCL (20 wt.% and 30 wt% in DCM:DMF] for in-vitro studies. Figure 4.30 showed the amount of cell in different scaffolds platform at incubation ranging from 1 day to 7 days. 2D and 3D structure of 20wt% PCL showed that the amount of cell increases when the culture period increased that could be seen the increasing due to those cells were growing up comfortably. However, when those cells cover all the limited areas, it has no significant increasing even though the period was continuously increased that can be seen from Day1 to Day5 due to those cells grow up tightly in limited areas whereas Day7 the 3D structure of 30 wt% PCL nanofibrous scaffold showed dramatically induced cell viability under similar experimental conditions. These results indicate that 3D-30wt% PCL had a fiber size more than smaller size. As seen SEM micrographs of PCL 20% mat, PCL 20% (a) and PCL 20% (b) at D7 showed those PCL were fully covered by cells except PCL 30% (a). It is due to the fiber size of PCL30% are bigger than others, then the pore size also bigger. It leads amount of cells could infiltrate into PCL 30% scaffold more than other scaffolds that can be seen in table 4.6. Cells in PCL20%, PCL20%(a) and PCL20%(b) trend slowly increase whereas PCL30%(a) obviously from D5 to D7.

CHAPTER V

CONCLUSION

Based on this research work devoted to develop the PCL 3D-structure structure from electrospun mats. The processing characteristic, and morphological properties were investigated.

From the study, it can be concluded that new processing has a potential to produce the 3D scaffold PCL. The conclusion can be divided as following:

In this study, we found that the concentration of polymer solution is the main parameter that affects to the fiber size, anyway other parameters also affect but not much. The fiber size affected to the cellular morphology on the top layer of the scaffold. The finer fiber size expressed the smaller pore size. It results the spreading of cell (L929 mouse fibroblast cells) are over the entire surface of these mate rather than penetrate into under layer whereas the bigger fiber size allowed those cells penetrated deep under layer.

In addition, an achievement of fabrication a 3D-structure polycaprolactone (PCL) electrospun (3D) through the electrospinning process was done. The novel technique was developed that involves positive and negative charge in electrospining system with collected the 3D-structure polycaprolactone (PCL) electrospun (3D) on vortical collector. The 3D-structure PCL scaffolds show structure with better regular pore size and well-distribute porosity compare to the previous technique. The excellence improvement of cell activity using L929 mouse fibroblast cells on 3D scaffold by new technique was observed

compare to previous one and mat scaffold . It could be concluded that this new technique is a new potential design for fabrication of the unique 3D-structure fiber with the better cell activity results.

Future work

This work has succeeded to fabricate the unique 3D-structure and fluffy yarn fiber by the new difference-charge technique. However, more characterization and work are needed for further understanding and to be used in the potential real application.

REFERENCES

[1] http://www.nano.org.uk/what-is-nanotechnology

[2] Anthony A., David J. M., Josept P. V., and Robert L. Synthetic biodegradable polymer scaffolds.

[3] Chan B. P. and Leong K. W. , Scaffolding in tissue engineering: general approaches and tissue-specific considerations. Eur. Spine J. 2008 December; 17 (Suppl 4) : 467–479.

[4] Martins A., Reis R. L., and Neves N. M.. Electrospinning: processing technique for tissue engineering scaffolding.

[5] Ranjna C. D. and Aroop K. D. Cell-interactive 3D-Scaffold; Advances and Applications.

[6] Langer R, Vacanti JP. Tissue engineering. Science 26 (1993) : 920–6.

[7] Joydip K.,Falguni P.,Young H. J.,Dong-Woo C. Biomaterials for Biofabrication of 3D Tissue engineering.

[8] Smith L.A., Maa P.X.. Nano-fibrous scaffolds for tissue engineering. Colloids and Surfaces B: Biointerfaces 39 (2004) : 125–131

[9] Sang B. L., Yong H.K., Moo S. C., Seung H. H., Young M. L. Study of gelatin-containing artificial skin V: Fabrication of gelatin scaffolds using a salt-leaching method. Biomaterials 26 (2005) : 1961–1968.

[10] McIntosh L., Cordell J.M., Wagoner J. Impact of bone geometry on effective

properties of bone scaffolds. Biomaterialia 5 (2009) : 680–692.

[11] Hyeon J. K., Ung-Jin K., Gordana Vunjak-N., Byoung-H. M., David L. K.Influence of

macroporous protein scaffolds on bone tissue engineering from bone marrow stem

cells. Biomaterials 26 (2005) : 4442–4452.

[12] Boissard C.I.R., Bourban P.-E., Tami A.E., Alini M., Eglin D.Nanohydroxyapatite /poly(ester urethane) scaffold for bone tissue engineering. Acta Biomaterialia 5

(2009) : 3316–3327.

[13] Niki J. C., Rachel H. B., Gary A. L., Liam M. G. Particle seeding enhances interconnectivity in polymeric scaffolds foamed using supercritical CO_2. Acta Biomaterialia 6 (2010) : 1055–1060.

[14] Claire M. T., Matthew G. H., Jakob L., Fergal M., Brian H., Fergal J. O. Brien. The effects of collagen concentration and crosslink density on the biological, structural and mechanical properties of collagen-GAG scaffolds for bone tissue engineering. Mechanical behavior biomedical materials 2 (2009) : 202-209.

[15] Amir A. Al-Munajjed, Fergal J. O. Brien. Influence of a novel calcium-phosphate coating on the mechanical properties of highly porous collagen scaffolds for bone repair. Mechanical behavior biomedical materials 2 (2009) : 138-146.

[16] Xiaohua L. , Laura A. S., Jiang H., Peter X. M. Biomimetic nanofibrous gelatin/apatite

composite scaffolds for bone tissue engineering. In press. Biomaterials (2009) :

1–7.

[17] Travis J. S., Horst A. V. R. Electrospinning: Applications in drug delivery and tissue engineering. Biomaterials 29 (2008) : 1989-2006.

[18] Doshi and D.H. Reneker. Electrospinning process and applications of electrospun fibers. Electrostatics **35** (1995) : 151–160.

[19] Sangamesh G. Kumbar, Syam P. Nukavarapu, Roshan James, Lakshmi S. Nair, Cato T. Laurencin. Electrospun poly(lactic acid-co-glycolic acid) scaffolds for skin tissue engineering. Biomaterials 29 (2008) : 4100–4107.

[20] Andrady, A. Science and Technology of Polymer Nanofibers. Australia: Wiley-Interscience (2008).

[21] Bhardwaj, N., and Kundu, S.C. Electrospinning: A fascinating fiber fabrication technique. Biotechnology Advances 28 (June 2010) : 325-347

[22] Sukigara, S., Gandhi, M., Ayutsede, J., Micklus, M., and Ko, F. Regeneration of Bombyxmori silk by electrospinning-part 1: processing parameters and geometric properties. Polymer 44 (September 2003) : 5721-5727.

[23] Weiwei, B. et al, 2008

[24] Cui, W., Li, X., Zhou, S., and Weng, J. Investigation on process parameters of electrospinning system through orthogonal experimental design. Polymer 103 (September 2006) : 3105-3112.

[25] Fong, H., Chun, I., and Reneker, D.H. Beaded nanofibers formed during electrospinning. Polymer 40 (July 1999) : 4585-4592.

[26] Megelski, S., Stephens, J.S., Chase, D.B., and Rabolt, J.F. Micro- and

nanostructured surface morphology on electrospun polymer fibers. Macromolecules 35 (September 2002) : 8456-8466.

[27] Jarusuwannapoom, T., and others. Effect of solvents on electro-spinnability of Polystyrene solutions and morphological appearance of resulting electrospun polystyrene fibers. European Polymer Journal 41 (March 2005) : 409-421.

[28] Amiraliyan, N., Nouri, M., and Kish, M.H. Electrospinning of silk nanofibers. I. An investigation of nanofiber morphology and process optimization using response surface methodology. Fibers and Polymer 10 (April 2009) : 167-176.

[29] Materials for scaffold

[30] Peppas N.A. and Ward. J.H. Biomimatic materials and micropatterned structures using iniferter. Advance Drug Delivery 56 (2004) : 2587-2597.

[31] Von Buelow, S., Von Heimburg, D. Effecacy and safty to polyacrylamide hydrogel for facial soft tissue augmentation. Plast.Reconstruct Surgery 116(2005) : 1137-1146.

[32] Flynn, L., Dalton., P.D. Fiber templating of poly(2-hydroxyethyl methacrylate) for neural tissue engineering. Biomaterials 24 (2003) : 4265-4272.

[33] Mann B.K., Schmedlen R.H. Tethered-TGF-beta increase extracellular matrix production of vascular smooth muscle cells. Biomaterials 22 (2001) : 439-444.

[34] Gonzalez. A.L., Gobin, A.S. Integrin interactions with immobilized peptides in

polyethylene glycol diacrylate hydrogels. Tissue engineering 10 (2004) : 1775-1786.

[35] Delong, S.A., Moon, J.J. Covalently immobilized gradients of bFGF on hydrogel scaffolds for directed cell migration. Biomaterials 26 (2005) : 3227-3234.

[36] Simone S., Anna T., Giancarlo C., Elena L. Development of hydroxyapatite/calcium silicate composites addressed to the design of load-bearing bone scaffolds. Mechanical behavior of biomedical materials 2 (2009) : 147-155.

[37] Yang F., Wolke J.G.C., and Jansen J.A. Biomimetic calcium phosphate coating on electrospun poly(e-caprolactone) scaffolds for bone tissue engineering. Chemical Engineering Journal 137 (2008) : 154–161.

[38] Moncy V. Jose, Vinoy T., Kalonda T. Johnson, Derrick R. Dean , Elijah Nyairo. Aligned PLGA/HA nanofibrous nanocomposite scaffolds for bone tissue engineering. Acta Biomaterialia 5 (2009) : 305–315.

[39] Cevat E., Dilhan M. Kalyon, Hongjun Wang. Functionally graded electrospun polycaprolatone and B-tricalcium phosphate nanocomposites for tissue engineering applications. Biomaterials 29 (2008) : 4065–4073.

[40] Xiaohua L. , Laura A. Smith , Jiang H. , Peter X. Ma. Biomimetic nanofibrous gelatin/apatite composite scaffolds for bone tissue engineering. In press. Biomaterials (2009) : 1–7.

[41] Yanzhong Z., Jayarama R. V., Adel El-Turki, Seeram R.,Bo Su, Chwee Teck Lim. Electrospun biomimetic nanocomposite nanofibers of hydroxyapatite/chitosan or bone tissue engineering. Biomaterials 29 (2008) : 4314–4322.

[42] Nitar N., Tetsuya F., Hiroshi T.. The Mechanical and Biological properties of Chitosan

Scaffolds for Tissue Regeneration. Materials 2 (2009) : 374-398.

[43] Wan J. L., Rocky S. T.. Fabrication and Application of Nanofibrous Scaffolds in Tissue Engineering.

[44] Taek G.K., Hyun J. C., Tae G. P.. Macroporous and nanofibrous hyaluronic acid/collagen hybrid scaffold fabricated by concurrent electrospinning and deposition/leaching of salt particles. Acta Biomaterialia 4 (2008) : 1611–1619.

[45] Laleh G.-M., Molamma P. P., Mohammad M., Mohammad-hossein Nasr-Esfahani, Seeram Ramakrishna. Electrospun poly(e-caprolactone)/gelatin nanofibrous scaffolds for nerve tissue engineering. Biomaterials 29 (2008) : 4532-4539.

[46] Deepika G., Venugopal J., Molamma P. Prabhakaran, V.R. Giri Dev, Sharon Low, Aw Tar Choon, S. RamakrishnaDehai Liang, , Benjamin S. Hsiao, Benjamin Chu. Functional electrospun nanofibrous scaffolds for biomedical applications. Advanced Drug Delivery Reviews 59 (2007) : 1392–1412.

[47] Nitar N., Tetsuya F., Hiroshi T.. The Mechanical and Biological properties of Chitosan

Scaffolds for Tissue Regeneration. Materials 2 (2009) : 374-398.

[48] Soliman S., Pagliari S., Rinaldi A., Foate G., Fiaccavento R., Pagiali F., Franzes O. , Minieri M., Nardo P. Di, Licoccia S., and E. Traversa: Acta Biomaterialia. In Press.

[49] Shalumon K.T., Chennazhi K.P., Tamura H., Kawahara K., Nair S.V., and R. Jayakumar: IET Nanobiotechnology 69 (2012) : 16-25.

[50] Deitzel J.M., Beck T. N.C, Kleinmeyer J.D., Rehrmann J., Tevault D.,Reneker D., Sendijarevic I., The effect of processing variables on the morphology of electrospun nanofibers and textiles. Polymer 42 (2001) : 261–272.

[51] Peter K. S. Electrostatic spinning of acrylic microfibers Original Research Article. Journal of Colloid and Interface Science, 36, Issue 1, (May 1971) : 71-79.

[52] Torres-Ginera S., Gimenez E., J.M. Lagaron. Characterization of the morphology and thermal properties of Zein Prolamine nanostructures obtained by electrospinning Food Hydrocolloids 22 (2008) : 601-614.

[53] Thompson C.J. , Chase G.G., Yarin A.L. , D.H. Reneker Effects of parameters on nanofiber diameter determined from electrospinning model Polymer 48 (2007) : 6913-6922.

[54] Shu Z., Woo S. S., Jooyoun K. Design of ultra-fine nonwovens via electrospinning of

Nylon 6: Spinning parameters and filtration efficiency Materials and Design 30 2009) : 3659–3666.

[55] Jason L., Christopher L., Frank K. Melt-electrospinning part I: processing

parameters and geometric properties. Polymer 45 (2004) : 7597–7603.

[56] Pirjo H., Ali H. Parameter study of electrospinning of polyamide-6. European Polymer

Journal 44 (2008) : 3067–3079.

[57] Tana S-H., Inaia R., Kotakib M., S. Ramakrishna Systematic parameter study for

ultra-fine fiber fabrication via electrospinning process. Polymer 46 (2005) : 6128–6134.

[58] Vince B., Xejun W. Effect of electrospinning parameters on the nanofiber diameter and

length. Materials Science and Engineering C 29 (2009) : 663-668.

[59] Tamer U., Flemming B. Electrospinning of uniform polystyrene fibers: The effect of

solvent conductivity. Polymer 49 (2008) : 5336–5343.

[60] Yun P. Neo, Sudip R., Allan J. E., Marija G. N., Siew Y. Q.. Influence of solution and

processing parameters towards the fabrication of electrospun zein fibers with sub-micron diameter. Journal of Food Engineering 109 (2012) : 645–651.

[61] Ioannis S. ChronakisMicro-/Nano-Fibers by electrospinning Technology:

Processing, Properties and Applications

[62] Xiuyan Li a, Huichao Liu a, Jiaona Wang a,b, Congju Li Preparation and characterization of poly(3-caprolactone) nonwoven mats via melt electrospinning. Polymer 53 (2012) : 248-253.

[63] Qiuxiang S., Peina S., Mongna G., Xuechan Y., Yuxin L., Ling L.,Yabin Zhu. Review

Progress on materials and scaffold fabrications applied to esophageal tissue engineering. Materials Science and Engineering C 33 (2013) : 1860–1866.

[64] Joe R. , Michel A. Huneault. Preparation of interconnected poly(3-caprolactone) porous scaffolds by a combination of polymer and salt particulate leaching. Polymer 47 (2006) : 4703–4717.

[65] C.L. Pai, M.C. Boyce, G.C. Rutledge, Morphology of porous and wrinkled fibers of polystyrene electrospun from dimethylformamide. Macromolecules 42 (2009) : 2102–2114.

[66] Balendu S. Jha a, Raymond J. C., James R. B., Scott A. S., Kangmin D. Lee d, John W.

Bigbee a, Gary L. Bowlin e, Woon N. Chow b, Bruce E. Mathern d, David G. Simpson Two pole air gap electrospinning: Fabrication of highly aligned, three-dimensional scaffolds for nerve reconstruction. Acta Biomaterialia 7 (2011) : 203–215.

[67] Jelena R.-K., Steven G. Wise Z. L., Peter K.M. M., Cara J. Young d, Yiwei Wang c, Anthony S. Weiss a,*. Tailoring the porosity and pore size of electrospun synthetic human elastin scaffolds for dermal tissue engineering. Biomaterials 32 (2011) : 6729-6736.

[68] Wei J., Fang Y., Jeroen J.J.P. van den B., Zhuan B., Mingwen F., Zhi C., John A. J. Fibrous scaffolds loaded with protein prepared by blend or coaxial electrospinning. Acta Biomaterialia 6 (2010) : 4199–4207.

[69] Sangwon C., Nilesh P. I., Gerardo A. Montero , S. H. K.,Martin W. King Bioresorbable

elastomeric vascular tissue engineering scaffolds via melt spinning and electrospinning. Acta Biomaterialia 6 (2010) 1958–1967

[70] Jongwan L., Jinah Jang,1, Hana O., Young H. J., Dong-W.C.Fabrication of a three-dimensional nanofibrous scaffold with lattice pores using direct-write electrospinning.

[71] Antoniya Tonchevaa, Dilyana Panevaa, Nevena Manolovaa, Iliya Rashkova,

Luigi Mitab,c, Stefania Crispi d, Damiano Gustavo Mitac. Dual vs. single spinneret electrospinning for the preparation of dual drug containing non-woven fibrous materials, Colloids and Surfaces A: Physicochem. Eng. Aspects (2012).

[72] Sandeep Kumar Tiwari , Subbu S. Venkatraman Importance of viscosity

parameters in electrospinning: Of monolithic and core–shell fibers.

[73] Nandana B., Subhas C. Kundu. Research review paper Electrospinning: A

fascinating fiber fabrication technique. Biotechnology Advances 28 (2010) : 325–347.

[74] Sachiko S., Milind G., Jonathan A., Michael M., Frank Ko. Regeneration of Bombyx mori silk by electrospinning—part 1: processing parameters and geometric properties. Polymer 44 (2003) : 5721–5727.

[75] Awal A. a, Sain M. a, M. Chowdhury. Preparation of cellulose-based nano-composite fibers by electrospinning and understanding the effect of processing parameters. Composites: Part B 42 (2011) : 1220–1225.

[76] Fashandi H., Karimi M. Pore formation in polystyrene fiber by superimposing temperature and relative humidity of electrospinning atmosphere. Polymer 53 (2012) : 5832-5849.

APPENDICES

Appendix A: SEM micrographs of PCL electrospun fiber mats (2D) at various processing parameters

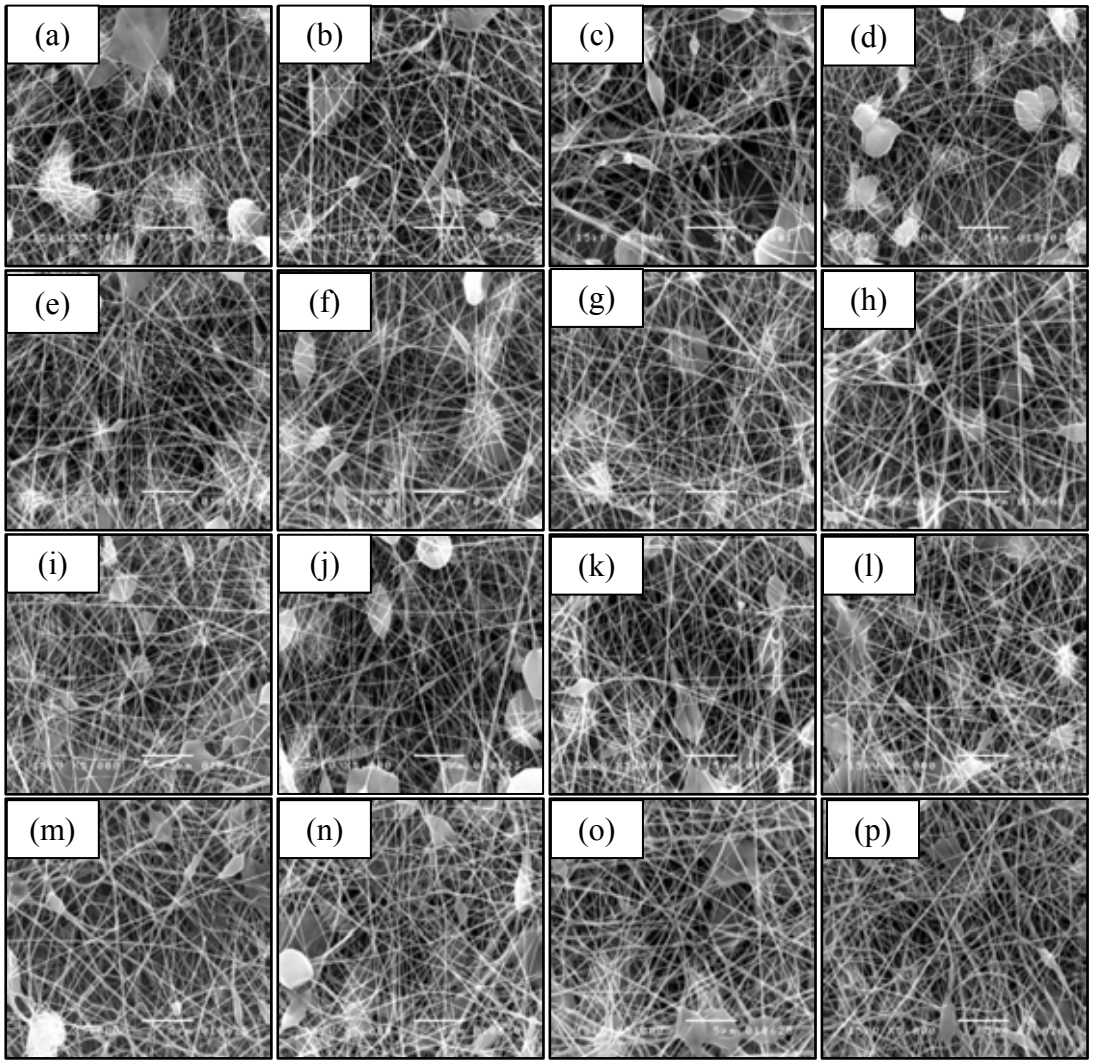

Figure a. SEM micrograph of PCL electrospun fiber mats at various flow rate (1-d), (e-h), (i-l),(m-p) 0.1 at applied voltage 10 kV., 0.5 at applied voltage 15 kV, 1.0 at applied voltage 20 kV and 2.0 ml/h at applied voltage 25, respectively. At fixed concentration 5wt%, and distance 10 cm.

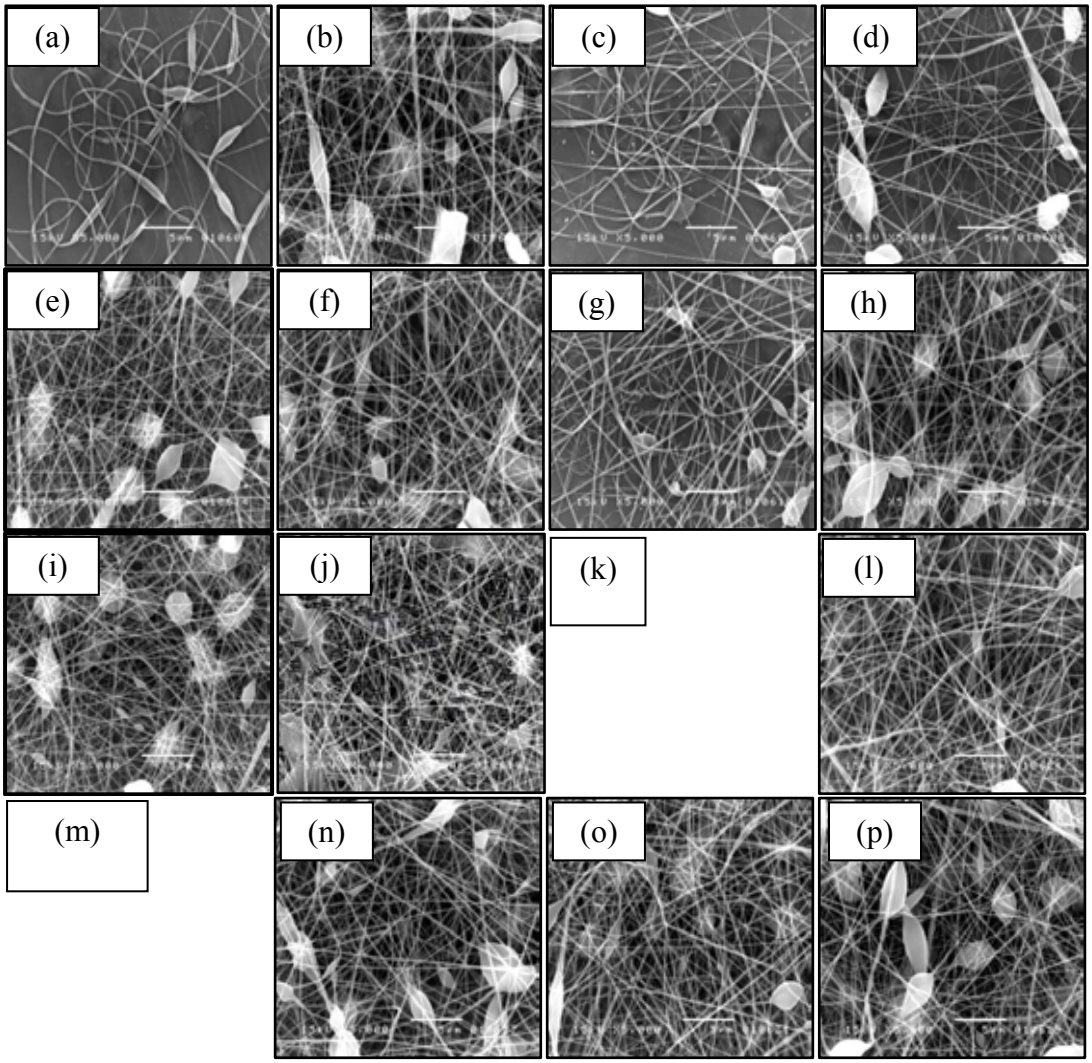

Figure b. SEM micrograph of PCL electrospun fiber mats at various flow rate (1-d), (e-h), (i-l),(m-p) 0.1 at applied voltage 10 kV., 0.5 at applied voltage 15 kV, 1.0 at applied voltage 20 kV and 2.0 ml/h at applied voltage 25, respectively. At fixed concentration 5wt%, and distance 20 cm.

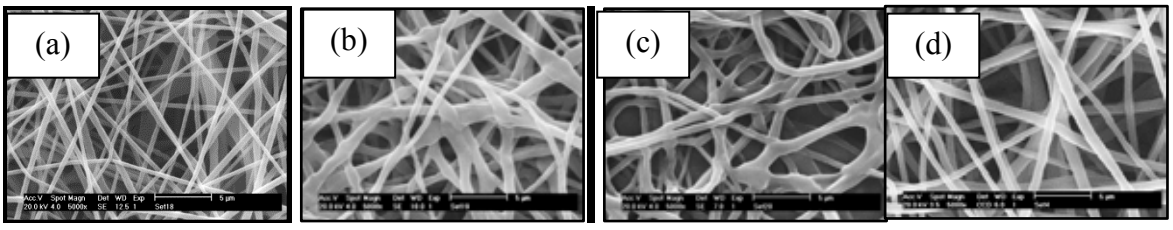

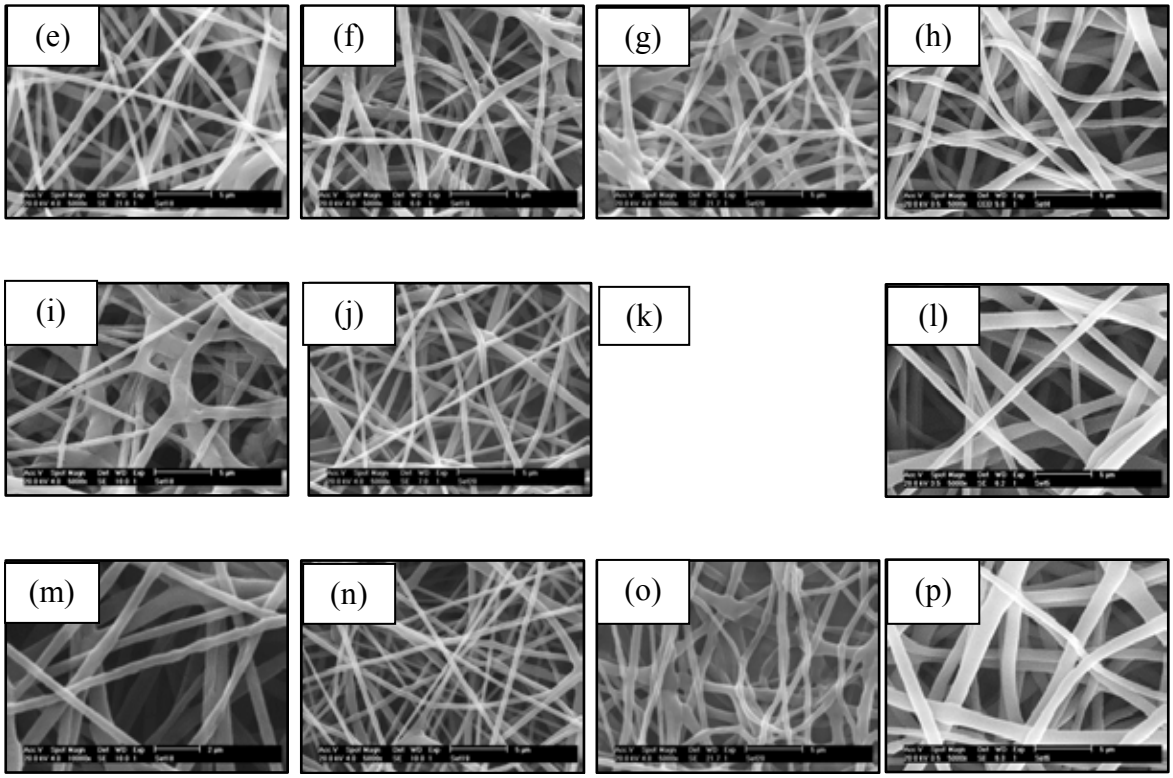

Figure c. SEM micrograph of PCL electrospun fiber mats at various flow rate (1-d), (e-h), (i-l),(m-p) 0.1 at applied voltage 10 kV., 0.5 at applied voltage 15 kV, 1.0 at applied voltage 20 kV and 2.0 ml/h at applied voltage 25, respectively. At fixed concentration 10 wt%, and, distance10 cm.

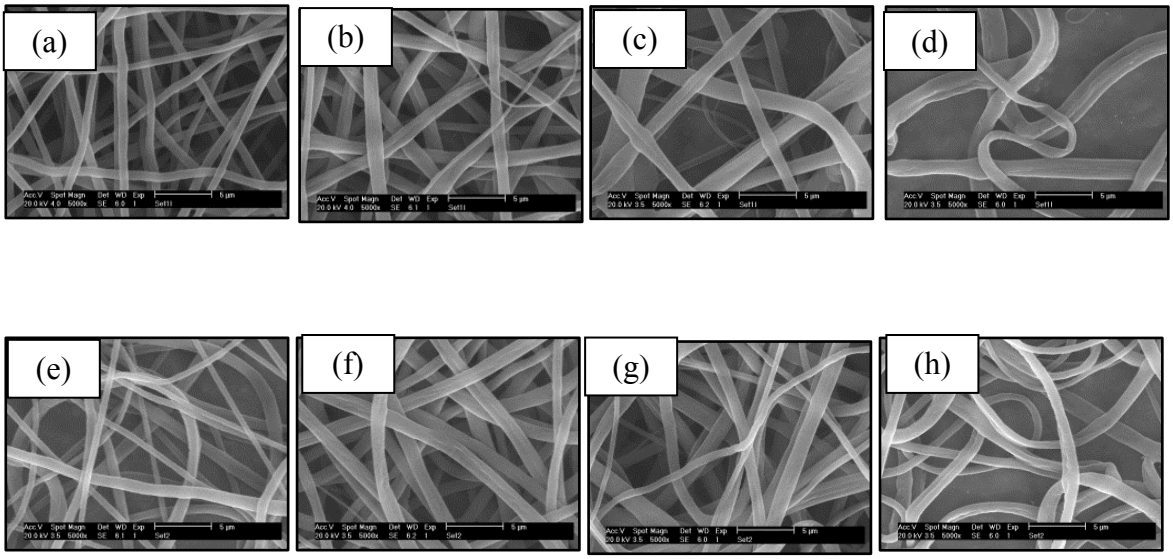

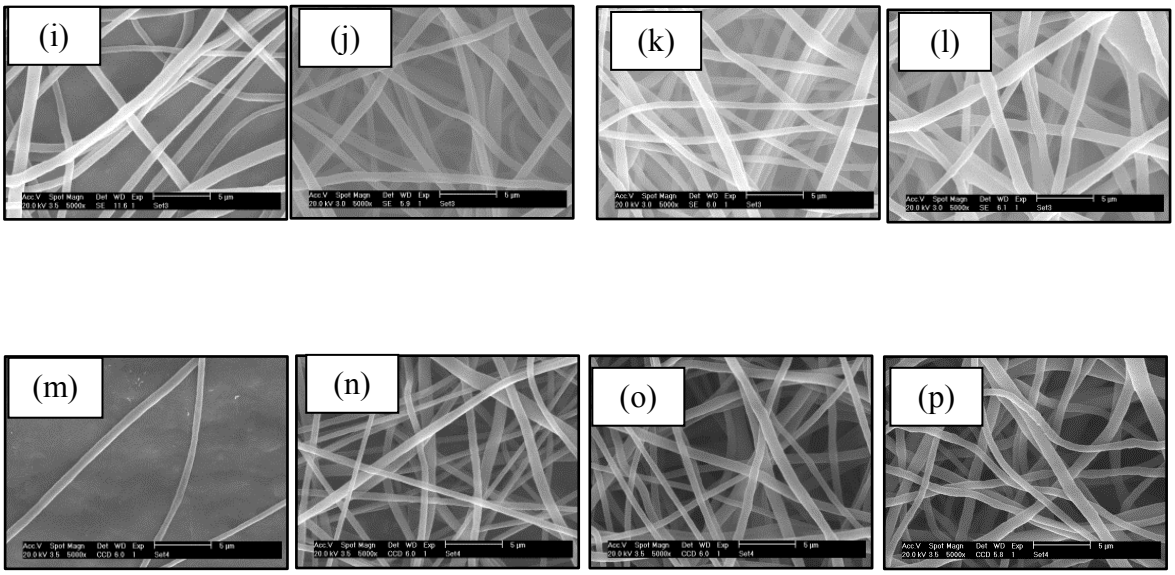

Figure d. SEM micrograph of PCL electrospun fiber mats at at various flow rate (1-d), (e-h), (i-l),(m-p) 0.1 at applied voltage 10 kV., 0.5 at applied voltage 15 kV, 1.0 at applied voltage 20 kV and 2.0 ml/h at applied voltage 25, respectively. At fixed concentration 10 wt%, and distance20 cm.

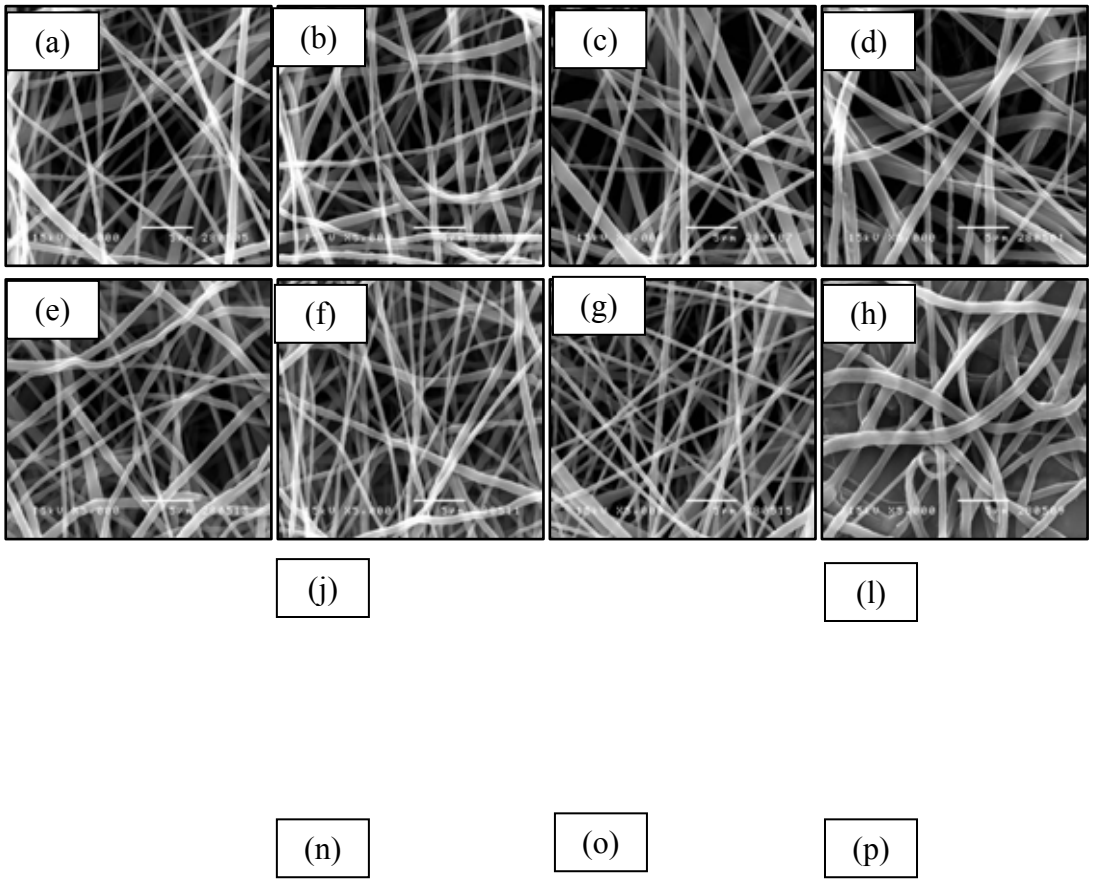

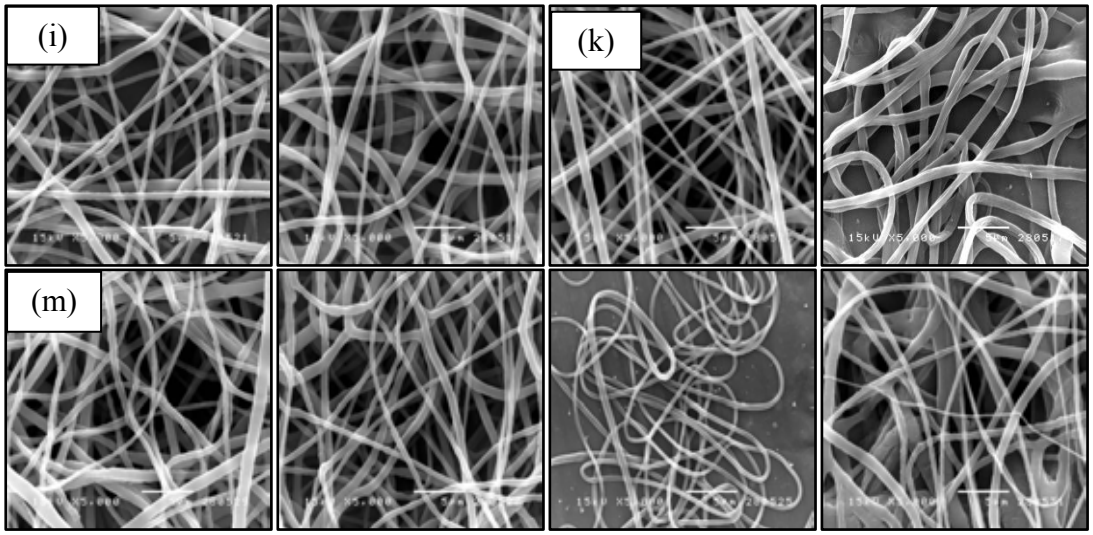

Figure e. SEM micrograph of PCL electrospun fiber mats at at various flow rate (1-d), (e-h), (i-l),(m-p) 0.1 at applied voltage 10 kV., 0.5 at applied voltage 15 kV, 1.0 at applied voltage 20 kV and 2.0 ml/h at applied voltage 25, respectively. At fixed concentration 15 wt%, and distance 10 cm.

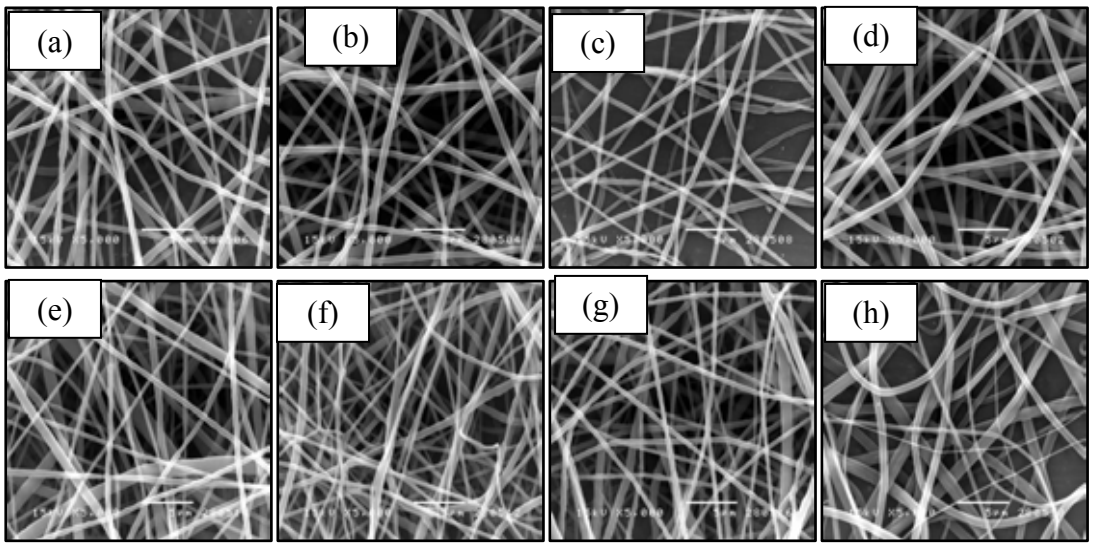

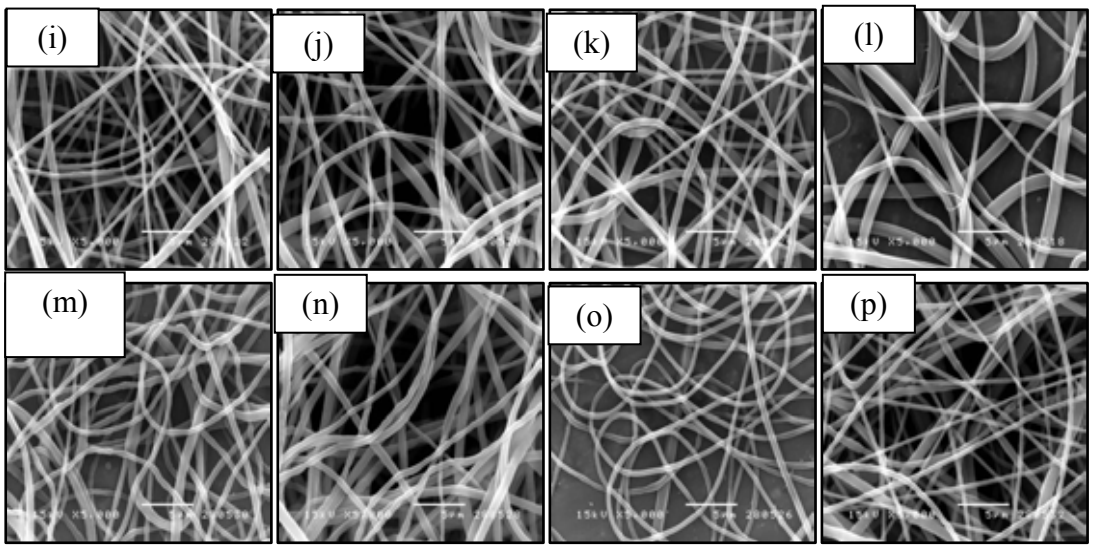

Figure f. SEM micrograph of PCL electrospun fiber mats at various applied voltage concentration 15wt%, distance20 cm.

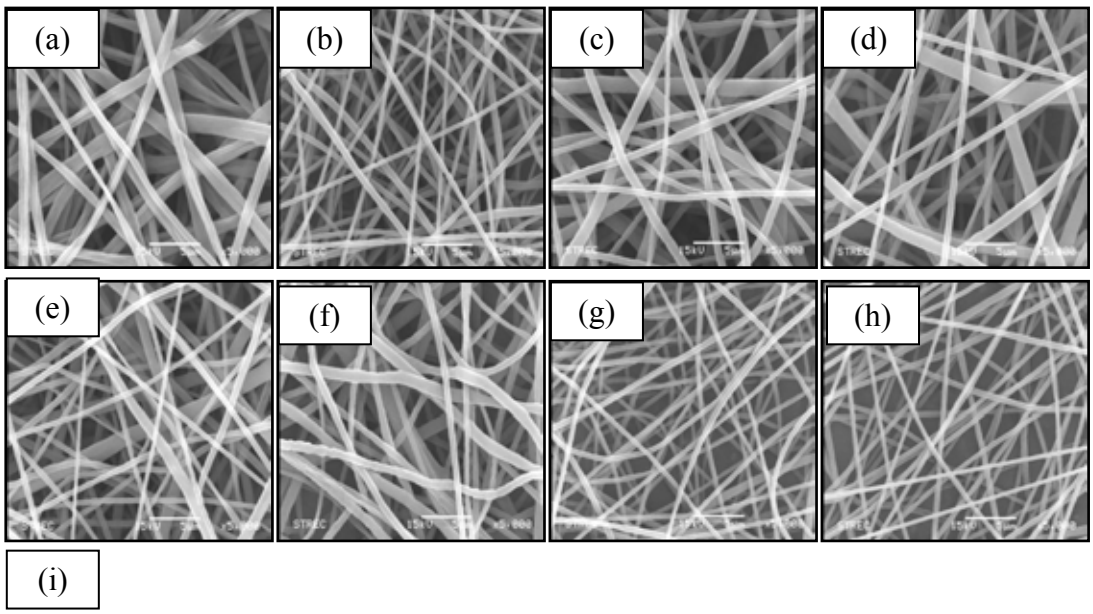

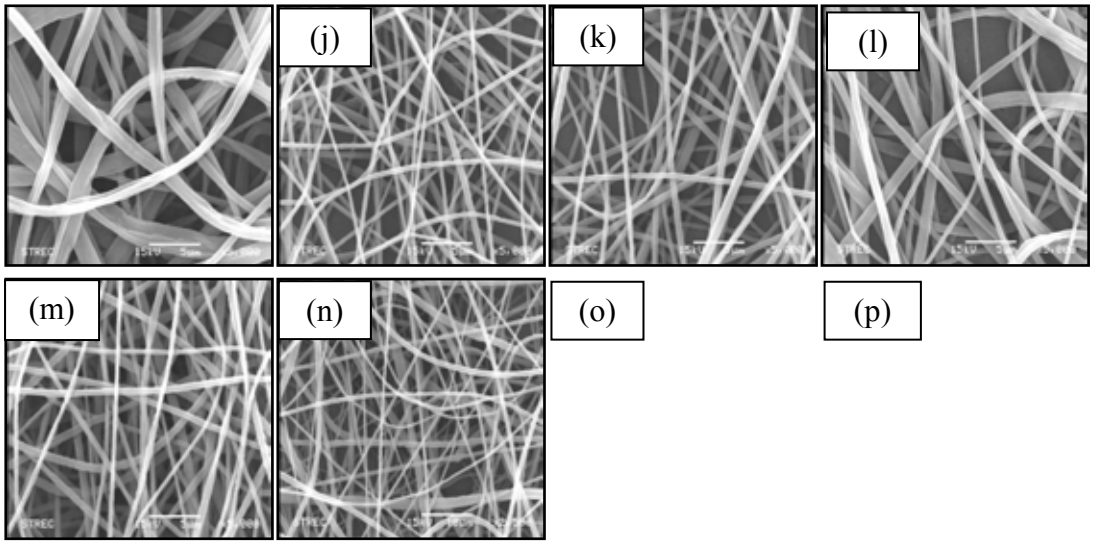

Figure g. SEM micrograph of PCL electrospun fiber mats at various flow rate (1-d), (e-h), (i-l),(m-p) 0.1 at applied voltage 10 kV., 0.5 at applied voltage 15 kV, 1.0 at applied voltage 20 kV and 2.0 ml/h at applied voltage 25, respectively. At fixed concentration 20 wt%, and distance 10 cm.

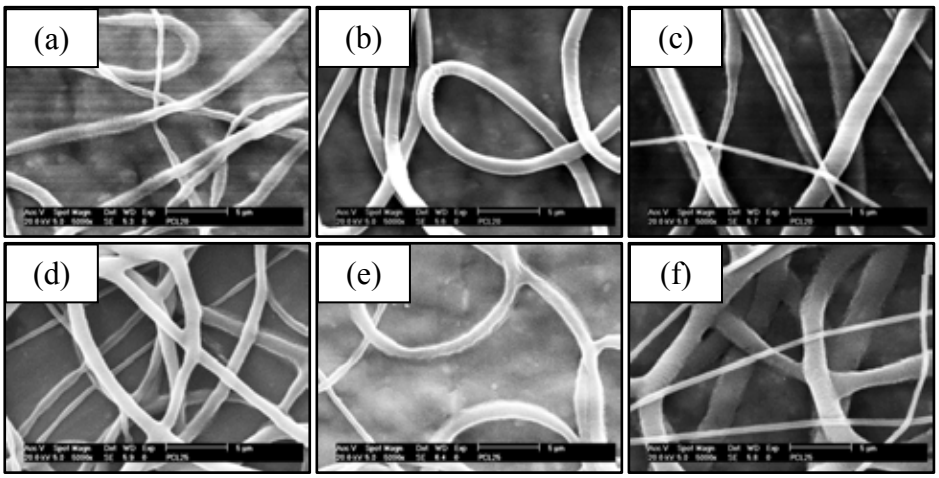

Figure h. SEM micrograph of PCL electrospun fiber mats at various flow rate (a-c), (d-f), 0.5 at applied voltage 10 kV, 1.0 at applied voltage 15 kV, respectively. At fixed concentration 25 wt%, and distance 10 cm.

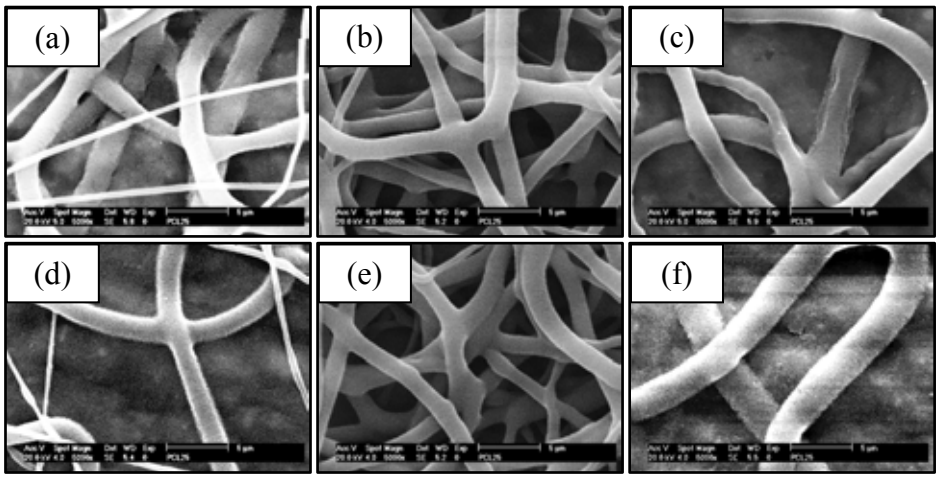

Figure i. SEM micrograph of PCL electrospun fiber mats at various flow rate (a-c), (d-f), 0.5 at applied voltage 10 kV, 1.0 at applied voltage 15 kV, respectively. At fixed concentration 25 wt%, and distance 20 cm.

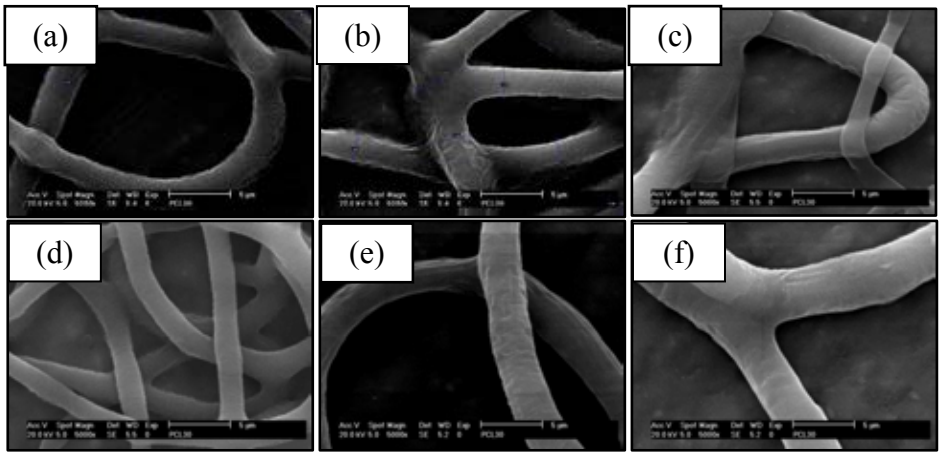

Figure j. SEM micrograph of PCL electrospun fiber mats at various flow rate (a-c), (d-f), 0.5 at applied voltage 10 kV, 1.0 at applied voltage 15 kV, respectively. At fixed concentration 30 wt%, and distance 10 cm.

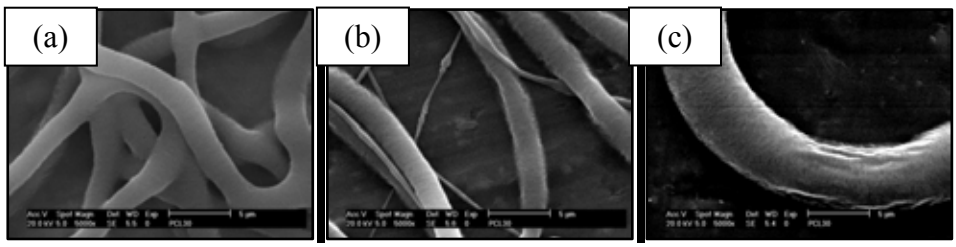

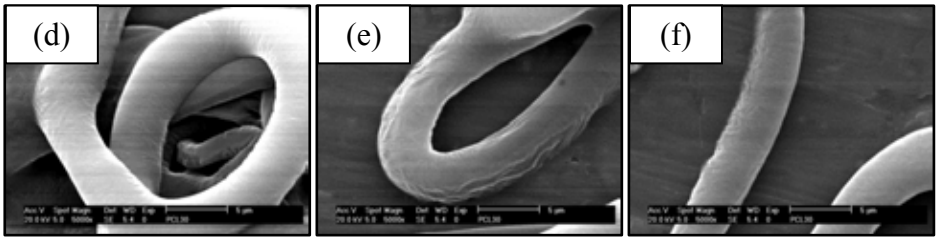

Figure k. SEM micrograph of PCL electrospun fiber mats at various flow rate (a-c), (d-f), 0.5 at applied voltage 10 kV, 1.0 at applied voltage 15 kV, respectively. At fixed concentration 30 wt%, and distance 20 cm.

Appendix B: Fiber diameter size at various processing parameters

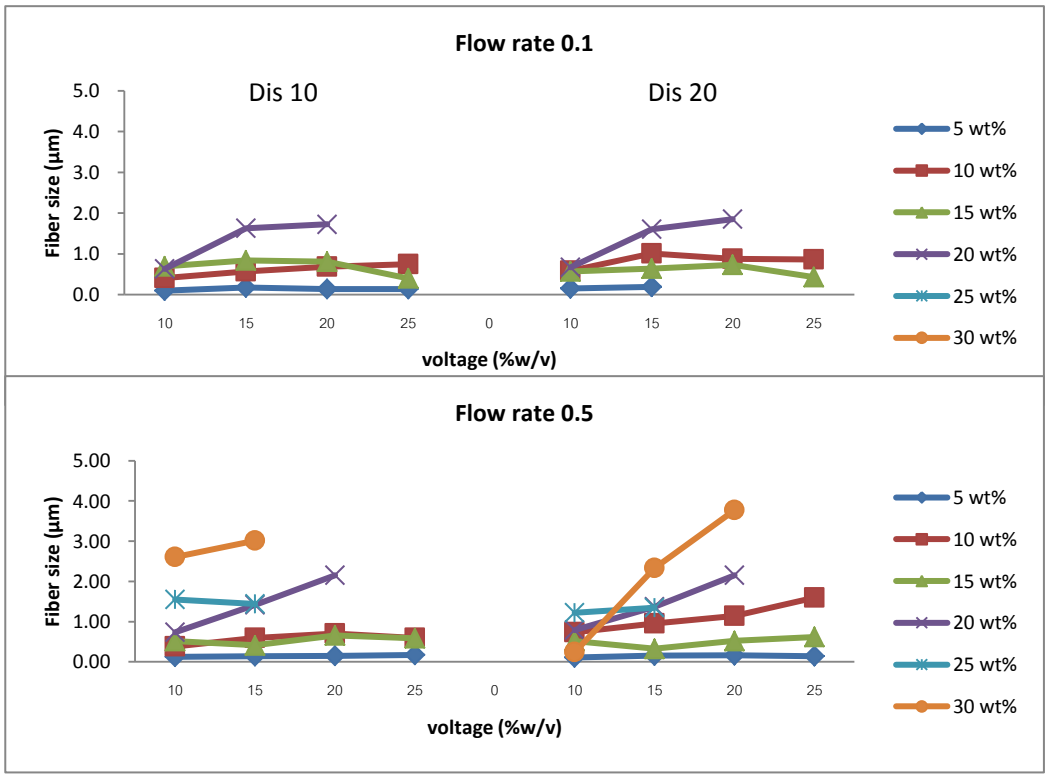

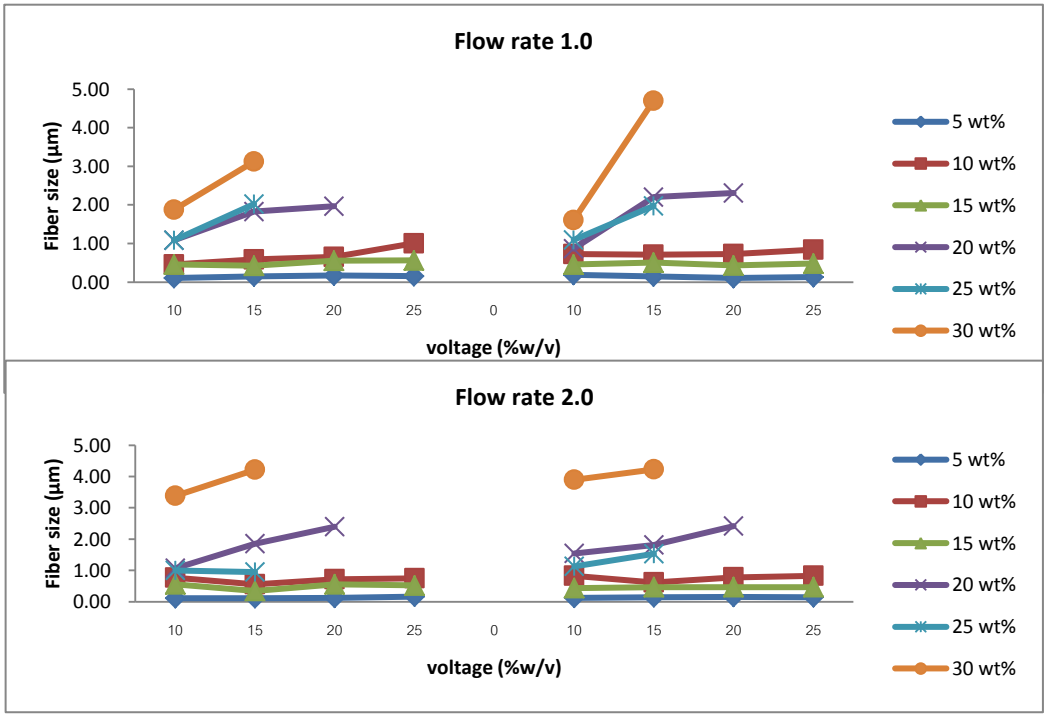

Figure a. fiber diameter size of PCL electrospun fiber mats (2D) at various processing parameters

Appendix C: Protocol of cell culture

Preparation of cell culture

Mouse fibroblastic cells (L929) were used to investigate the cellular activity on nano fiber both of mat and sponge structures. The subculture ratio is between 1:8 to 1:12, the confluence time is 3-4 days.

(1). Preparation liquid medium

DMEM liquid medium

Firstly, 1% Penicillin-Streptomycin antibiotic and 1% of L-glutamine (10 ml in 1000 ml medium) were filter using the sterilized filter system (0.22 μm). After that the FBS was dissolved in the mixed liquid (10%; 100 ml in 1000 ml medium). The system was stored in cool place at 4°C.

(2).Trypsinization

For cell preparation ,when the subconfluence of cells is about 80% of plate area, we must be trypsinized to move the divided cells into another plates. The procedures of cell trypsinization are as following,

The laminar flow hood must be sterilized before using, the medium and trypsin were warm up due to freezing in water bath at 37°C. The old medium was moved from plate then the remained medium with PBS was washed. After that the trypsin/EDTA solution was added to cover cell monolayer (1 ml for 10 cm tissue culture plate) and incubate at 37°C for 5 min (until cells detach). Then the cells were investigated using a microscope, the detached celled would show in round shape. Then the fresh medium was added to inhibit the trypsin activity. The detach cells from bottom of the plate using autopipette and homogenize the cell suspension. The cell suspension was transferred into 50 centrifugal tube and then centrifuged at temperature of 4°C, with rotor speed of 1200 rpm for 5 min. After that the supernatant was carefully removed out (to careful the cell might be also taken out), and then the fresh medium and homogenize the cell suspension were added to replace. The cell suspension was divided to proper subculture ratio (1:8), and transfer to the new plates which contains the fresh medium (10 ml for 10 cm tissue culture plate). It was orbitally shaked and incubated at temperature of 37 °C in 5% CO_2 atmosphere. (the medium and trypsinize must be changed every 3 days during subconfluent).

(3).Cell count & calculation (Hemocytometer)

A hemocytometer was cleaned with 70% ethanol and wiped with lint-free tissue paper. Those cells from plate (which described above) was trypsinized and homogenized to be cell suspension using autopipette. After that the cell suspension 5X was diluted by the mix of 40 µl of cell suspension and 160 µl of fresh. The dead cells were stained by the mixed 40 µl of cell suspension and 160 µl of fresh medium on a strip of paraffin film. Then 1-2 µl stained cells on hemocytomer were put and coved with glass slide, cell suspension will be sucked into hemocytometer with capillary force

Put 10-20 µl of stained cells on hemocytometer covered with glass slide, cell suspension will be sucked into hemocytometer with capillary force. The count 3 big squares as shown in figure and find an average of the counts to calculate cell density

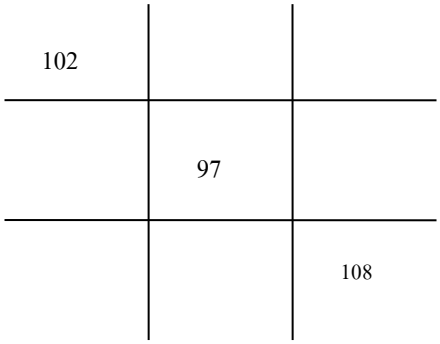

For example ;

Cell density = (average cell count) x (dilution factor of cell suspension) x 10^4

$$= \left(\frac{102+97+108}{3}\right) \times \left(\frac{5}{4}\right) \times (5) \times 10^4$$

$$= 640 \times 10^4 \, cells / ml$$

Appendix D : Measurement of the fiber diameter size

For example, to measure the fiber diameter size of fibers using SEM Afore 5.21.

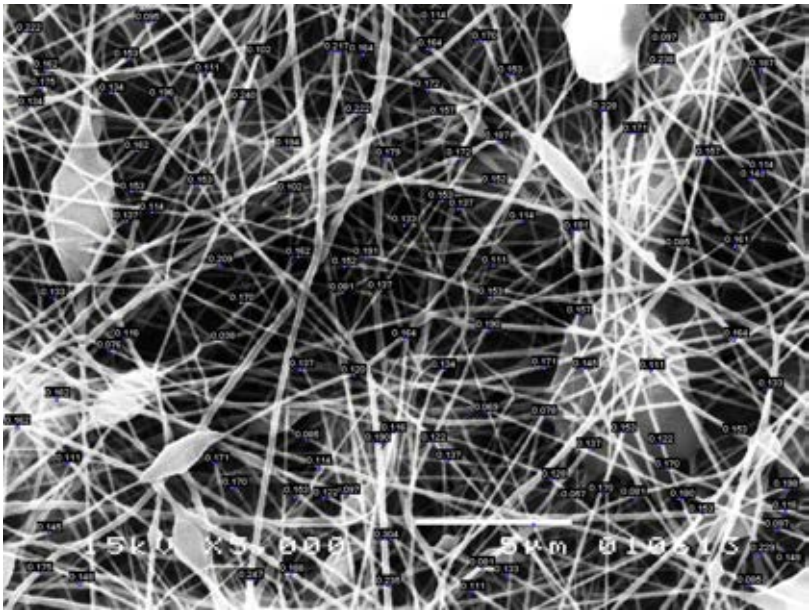

Figure a. Fiber obtained from the solution of PCL 5% wt. at applied voltage 15 kV, flow rate 1.0 ml/hr, and collecting distance 20 cm.

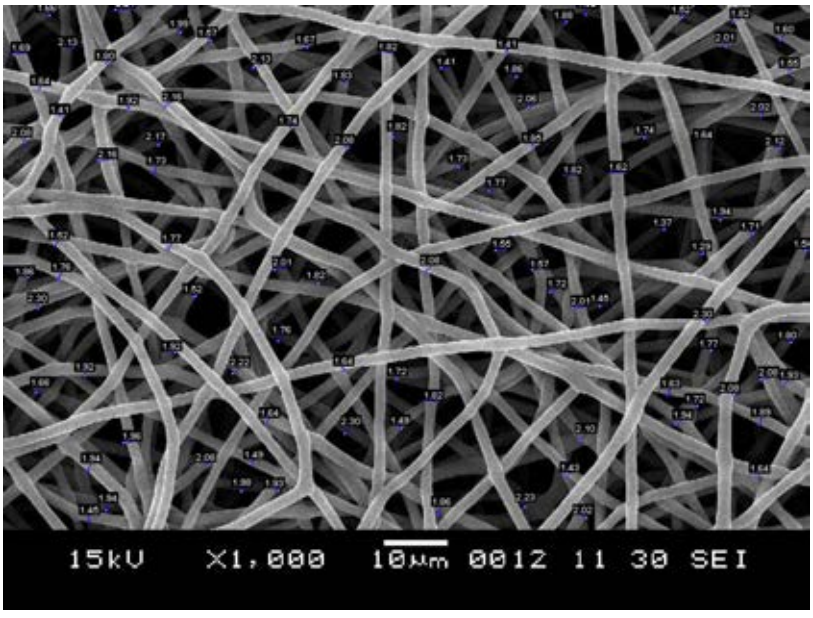

Figure b. Fiber obtained from the solution of PCL 25% wt . at applied voltage 15 kV, flow rate 1.0 ml/hr, and collecting distance 20 cm.

Appendix E: Measurement of the pore size of fibers

For example, to measure the pore size of fibers using SEM Afore 5.21.

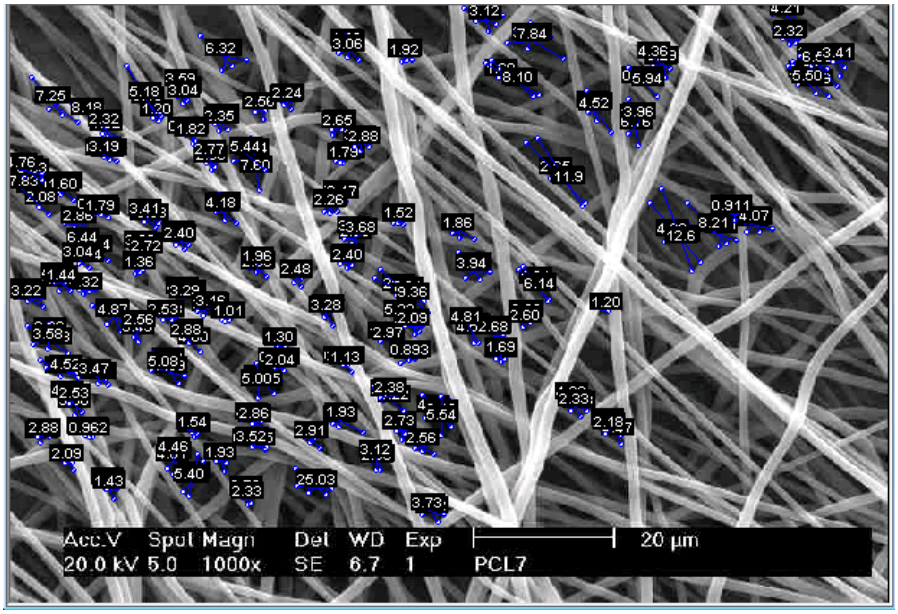

Figure a. The solution of PCL 20% wt . at applied voltage 15 kV, flow rate 1.0 ml/hr, and collecting distance 20 cm.

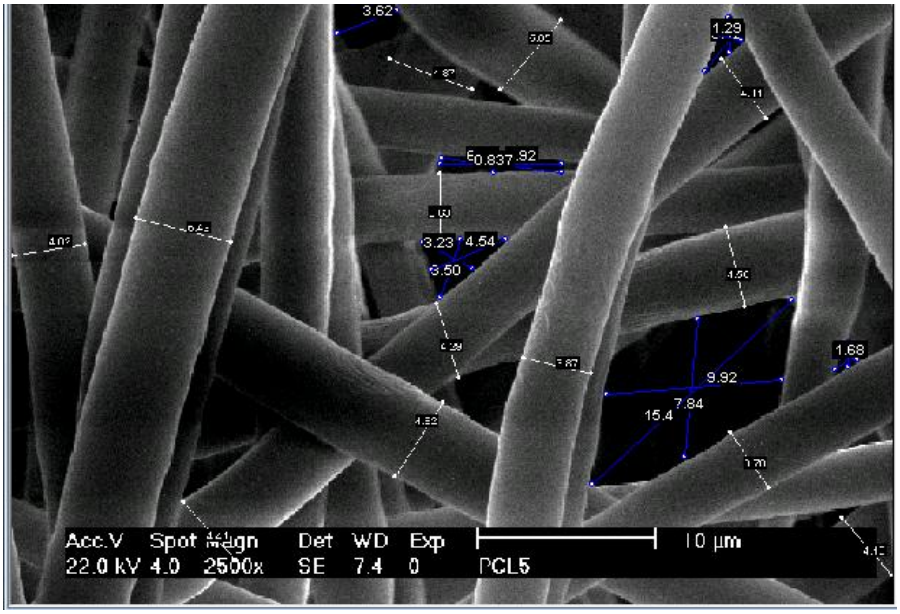

Figure b.The solution of PCL 30% wt . at applied voltage 15 kV, flow rate 1.0 ml/hr, and collecting distance 20 cm.

Appendix F : Standard of *in vitro* in cell culture test

Table a. Absobance at 570 nm. From MTT assays for standard curve of electrospun mats

Cell number (cells/well)	5000	10000	20000	40000	80000
0	0.05	0.07	0.144	0.282	0.514
0	0.044	0.081	0.131	0.276	0.51
0	0.052	0.07	0.159	0.283	0.526
0	0.047	0.074	0.166	0.302	0.559
Mean	**0.048**	**0.073**	**0.150**	**0.285**	**0.527**

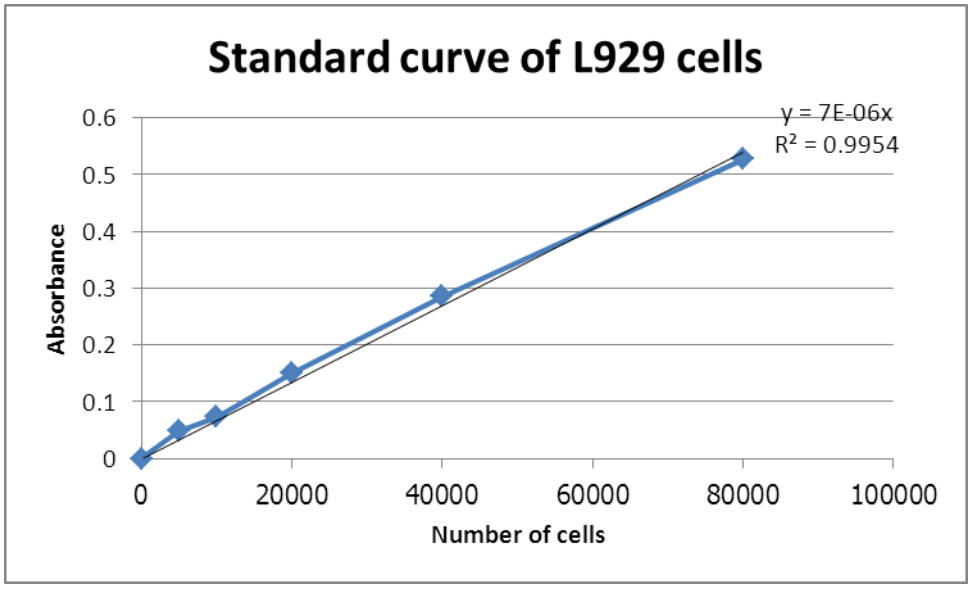

Figure a. Standard curve of L929 fibroblast

Table b. Absobance at 570 nm. from MTT assays for standard curve of 3D structure.

Cell number (cells/well)	20000	40000	80000	160000	320000	640000
0	0.13	0.217	0.368	0.554	0.75	0.984
0	0.134	0.22	0.36	0.504	0.603	0.976
0	0.135	0.221	0.361	0.533	0.677	0.954
0	0.14	0.224	0.373	0.564	0.739	1.064

	0.13475	0.2205	0.3655	0.53875	0.69225	0.9945
Mean	**20000**	**40000**	**80000**	**160000**	**320000**	**640000**
SD	**0.134**	**0.220**	**0.365**	**0.538**	**0.692**	**0.994**

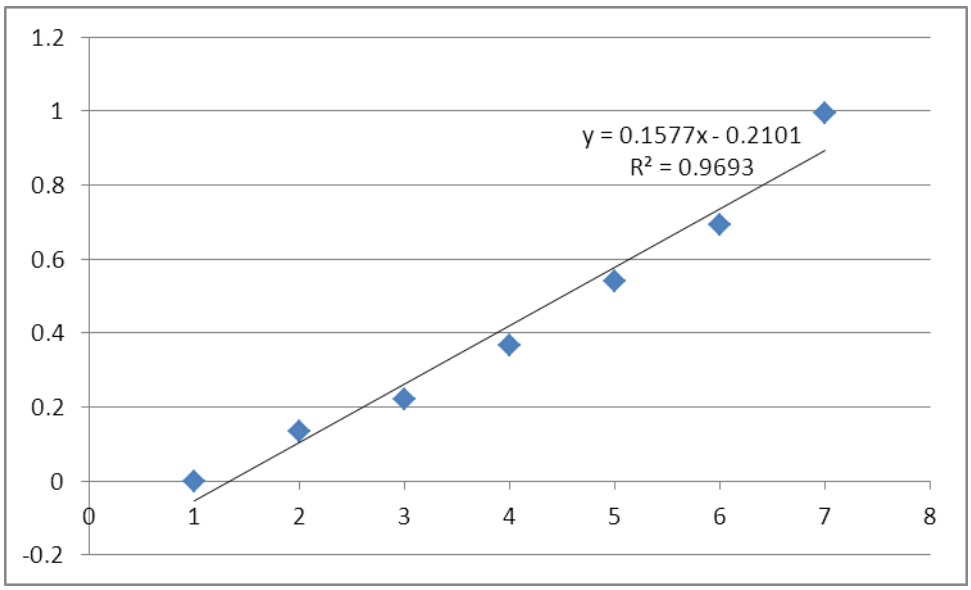

Figure b. Standard curve of L929 fibroblast for 3D structure

Table c. Raw data of absorbance at 570 nm in *vitro* culture test

6 h	**Control (TCP)**	**PCL1**	**PCL2**	**PCL3**	**PCL4**
Blank (DMSO)	0.042				
#1	0.102	0.103	0.107	0.088	0.139
#2	0.114	0.121	0.125	0.075	0.115
#3	0.106	0.116	0.128	0.088	0.116
#4	0.106	0.12	0.121	0.106	0.134
#5 (no cell)		0.059	0.058	0.072	0.07
no cell-DMSO		0.017	0.016	0.03	0.028
Day1	**Control (TCP)**	**PCL1**	**PCL2**	**PCL3**	**PCL4**
Blank (DMSO)	0.042				
#1	0.109	0.142	0.121	0.093	0.134
#2	0.111	0.124	0.138	0.105	0.117
#3	0.113	0.109	0.13	0.102	0.131
#4	0.108	0.148	0.14	0.099	0.137
#5 (no cell)		0.092	0.087	0.079	0.095

		0.05	0.045	0.037	0.053
Day3	**Control (TCP)**	**PCL1**	**PCL2**	**PCL3**	**PCL4**
Blank (DMSO)	0.042				
#1	0.331	0.189	0.216	0.181	0.214
#2	0.296	0.21	0.245	0.151	0.283
#3	0.312	0.206	0.265	0.208	0.229
#4	0.352	0.218	0.255	0.239	0.221
#5 (no cell)		0.072	0.08	0.066	0.069
Day5	**Control (TCP)**	**PCL1**	**PCL2**	**PCL3**	**PCL4**
Blank (DMSO)	0.042				
#1	0.515	0.404	0.416	0.143	0.638
#2	0.461	0.44	0.691	0.231	0.41
#3	0.462	0.43	0.546	0.445	0.523
#4	0.469	0.415	0.558	0.157	0.589
#5 (no cell)		0.09	0.08	0.075	0.091

Appendix G : Calculation of porosity

The porosimetry was referring to S.Soliman et al (2009). The porosity **(ε)** was calculated as

$$\%\varepsilon = V_{EtOH}/(V_{EtOH} + V_{PCL}) \times 100$$

By dividing ;

V_{EtOH} = Mass change after intrusion/ρEtOH

V_{PCL} = Mass of initial scaffold before intrusion /ρPCL)

For example, Calculated porosity of PCL electrospun mats from 20% PCL solution.

When ; $V_{EtOH} = 0.26$ g/ml

$V_{PCL} = 1.24$ g/ml

$$\%\varepsilon = V_{EtOH}/(V_{EtOH} + V_{PCL}) \times 100$$

VITAE

Miss Narissara Kulpreechanan was born in Ang-Thong, Thailand on August 8, 1982. She finish the high school education in 1999 from Singburi School. In 2003, she received her Bachelor Degree of Science with major of Materials Science and Textile Tecnology from Chulalongkorn University. In 2005, she received her Master Degree of Science with major of Materials Science and Advance Textile Tecnology from Chulalongkorn University. After gtraduation, studied in Doctoral Degree of Nanoscience and Technology, Chulalongkorn University

Some part of this work was presented at the conferences as follow;

- Narissara Kulpreechanan, Tanom Bunaprasert, Siriporn Damrongsakkul, Sorada Kanokpanont, and Ratthapol Rangkupan Effect of polycaprolactone electrospun fiber size on L929 cell behavior. Oral presentation.
- Paper paper has been published in Advanced Materials Research Vol. 701 (2013) pp 420-424, © (2013) Trans Tech Publications, Switzerland

doi:10.4028/www.scientific.net/AMR.701.420